Causes and consequences of Aspergillus niger pelleting behavior in industrial cultivation

Hagemann, Robert Timo

Publication date:
2018

Document Version
Publisher's PDF, also known as Version of record

DTU Chemical Engineering
Department of Chemical and Biochemical Engineering

Causes and consequences of *Aspergillus niger* pelleting behavior in industrial cultivation

Robert Timo Hagemann
PhD thesis
August 2018

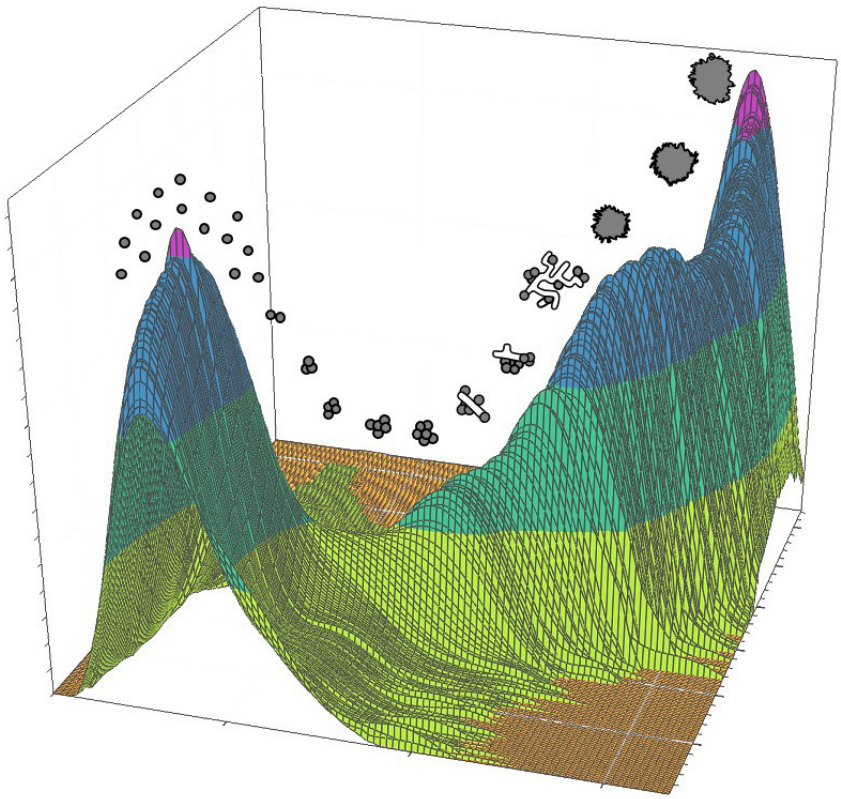

Causes and consequences of *Aspergillus niger* pelleting behavior in industrial cultivation

PhD thesis

Robert Timo Hagemann

Process and Systems Engineering Centre
Department of Chemical and Biochemical Engineering
Technical University of Denmark

August 2018

Supervision:
Krist V. Gernaey
Ulrich Krühne
Kim Hansen

DTU

novozymes®
Rethink Tomorrow

Address: Process and Systems Engineering Center (PROSYS)

Department of Chemical and Biochemical Engineering

Technical University of Denmark

Building 229

Dk-2800 Kgs. Lyngby

Denmark

Phone: +45 4525 2800

Web: www.kt.dtu.dk/forskning/prosys

Print: STEP PRINT POWER

DTU Chemical Engineering
Department of Chemical and Biochemical Engineering

Contents

I Summary & resumé (på dansk)

The greater goal of this thesis is to understand the growth patterns of the filamentous fungus *Aspergillus niger* in submerged cultivations. The resulting morphology is reported to have impact on productivity of the diverse products that are manufactured by *A. niger*.

Existing mechanistic growth models and knowledge had to be consolidated and expanded with confirming trials and testing of various parameters to influence the morphology to create the ideal morphology for the specific production process. The topics included in this thesis cover morphology altering by pH, power input by agitation, presence and concentration of particles, initial conidia concentration and ion concentration.

The outstanding feature of this thesis is the tracking of morphology with particle size analysis by laser diffraction. Assuming spherical particles, first conidia and in the later course of the fermentation pellets, the Fraunhofer approximation was deemed to suffice in precision detail for displaying a volume based density function. To follow development of conidia aggregation, germination and pellet formation, the bimodal distribution could be split into modes of conidia and pellets to differentiate their respective particle size development.

Using the lab strain *Aspergillus niger* AB1.13, several growth conditions were evaluated in terms of influence on morphology engineering towards either freely dispersed mycelia or pelleted growth with defined diameter to prevent particle internal gradients. A conception is presented with the core control handle to determine when pellet formation takes place being pH. Initial cultivation at a pH of 3 prevented the first conidia aggregation step and the following aggregation could be controlled by shifting pH upwards to 5.5. The particle size could be tuned by adjusting parameters like power input and initial conidia concentration which possess inferior influence on particle size and biomass development compared to pH.

The resulting model was applied onto an industrial glucoamylase producing strain in courtesy of Novozymes A/S. The media was as close to the production environment as the settings of the model allowed. The result was that this strain behaved very differently from the suggested model, and all settings that were evaluated experimentally resulted in mixed morphology with

both freely dispersed mycelia and pellets being present. In most cases, the pellets were also fragmenting before cultivation end thus making particle size engineering meaningless.

The model was then applied to the *Aspergillus niger* wildtype BO-1 strain to validate its general usefulness. Being the third strain to be tested, a third growth pattern could be detected. This indicates that morphology engineering probably must be evaluated for each strain separately.

The question arose if morphology matters to produce enzymes, in this case production of glucoamylase with BO-1. With introduction of different concentration of cellulose particles, the respective morphologies could be tailored. Employing the achieved morphologies as inoculum for cultivations, it was shown that freely dispersed BO-1 mycelia morphology is superior in producing glucoamylase despite oxygen limitation.

In conclusion, production processes should be checked for their morphology and the respective strain preference of producing enzymes.

Resumé

Det overordnede formål med denne afhandling er at forstå filamentøs svampen *Aspergillus nigers* vækstmønster. De forskellige morfologier kan påvirke produktiviteten af forskellige produkter fremstillet med *A. niger*.

De eksisterende mekanistiske vækstmodeller og viden skal konsolideres eksperimentelt for at undersøge indflydelsen af forskellige parametre på morfologien, således at den ideelle morfologifor den specifikke proces kan bestemmes. Emnerne i denne afhandling dækker over modificeringer i morfologien ved hjælp af pH værdien, power input fra omrøring, tilstedeværelse og koncentration af partikler samt de oprindelige konidier - og ionkoncentrationer.

Det enestående særkende ved denne afhandling er sporingen af morfologi med partikel størrelse analyse ved laser diffraktion. Antagelsen er, at der foreligger sfæriske partikler, først konidier og i løbet af den senere gæring pellets. Derfor er kriteriet for Fraunhofer approximation vurderet tilstrækkeligt i præcision for at vise en volumenbaseret densitetsfunktion. For at følge udviklingen af konidie-aggregation, spiring og pellet dannelse, bliver den bimodale fordeling opdelt i modi for konidier og pellets for at differentiere deres respektive partikelstørrelsesudvikling.

Med lab stammen *Aspergillus niger* AB1.13 blev flere vækstbetingelser evalueret mht. indflydelse på morfologiens design mod enten frit spredte mycelier eller pelletvækst med defineret diameter for at forhindre partikelinterne gradienter. En vækstmodel blev skabt, hvori det vigtigste justeringsparameter for at bestemme hvornår pellet dannelsen finder sted, er pH værdien. En indledende pH på 3 forhindrer det første konidie-aggregationstrin og i det følgende kunne sammenlægning af biomassen kontrolleres ved at flytte pH opad fra 3 til 5.5. Partikelstørrelsen kan indstilles præcist ved at justere parametre som power input og konidiestartkoncentration, som har en mindre indflydelse på udviklingen af partikelstørrelsen og biomassen i forhold til pH.

Den resulterende model blev anvendt på en industriel glucoamylase producerende stamme stillet til rådighed af Novozymes A/S. Kultiveringsmedierne var så tæt på produktionsmiljøet som modellens indstillinger tillod. Resultatet var, at denne stamme opførte sig meget anderledes end

den antagende model. Alle indstillinger, der blev evalueret eksperimentelt, resulterede i blandet morfologi med både frit spredte mycelier og pellets. I de fleste tilfælde fragmenterede biomassen før afslutning af gæring. Det gør partikelstørrelsesdesign meningsløst for denne stamme.

Modellen blev derefter anvendt på vildtypen *Aspergillus niger* BO-1 for at validere modellens generelle anvendelighed. Med denne tredje stamme blev et tredje vækstmønster påvist. Dette indikerer, at morfologi design sandsynligvis skal vurderes separat for hver stamme.

Spørgsmålet opstod hvorvidt morfologien er afgørende for at producere enzymer, i dette tilfælde produktion af glucoamylase med BO-1. Med indførelsen af forskellige koncentrationer af cellulose partikler kunne de respektive morfologier skræddersys. De opnåede morfologier blev brugt som inokulum for en gæring med "ren" morfologi. Det blev påvist, at de frit spredte BO-1 mycelierer bedre egnet til at producere glucoamylase på trods af iltbegrænsningen.

Den ultimative konklusion er, at hver produktionsproces med filamentøse svampe skal analyseres separat med hensyn til morfologidesign og stammens præference for at producere det ønskede produkt.

II Preface

The final stages of the thesis were a collaboration between the department of Fermentation Optimization of Novozymes A/S and the department of Chemical and Biochemical Engineering of the Technical University of Denmark. Alone for the re-initiation of the PhD-project in 2013 am I very grateful, especially to Stuart Stocks. Our discussions made me realize that finalizing the PhD actually would be possible. To Jens Dynesen who as my Novozymes manager supported commencing it professionally. To Krist Gernaey for having me as PhD student and for always providing productive feedback and moving mountains.

To Kim Hansen for being my Novozymes supervisor and for encouraging out-of-box experiments.

To Ulrich Krühne who is co-supervisor for my thesis. And, of course, to Gitte Læssøe whom I could ask anything except for how to do a thesis.

Over the span, plenty of people helped along. To every feedback that was given am I thankful. I would like to say thank you to Ingo Kampen for training me in particle size analysis, Friederike Schädel for raising my spirits, Carsten Thun for moral support, Guido Melzer for discussions about the morphology model, Morten Carlsen for reading my publication release requests as well as for general support.

To Anne K. Ringel, Anders Nielsen and Josephine F. Roien who were MSc. students willing to accept my advice and who collaborated fantastically in the laboratory. To Daniela Quintanilla for the literature discussions we had.

To Louise Johansson, for encouragement and motivation. She wouldn't have liked me to give up. To Erik, Katrina, Ingmar for love and support.

III Nomenclature

Abbreviations

A. niger	*Aspergillus niger*
AGU	Glucoamylase Activity Units
BDM	Bio Dry Matter
DLVO	Theory explaining aggregation in aqueous solution; named after Derjaguin, Landau, Verwey and Overbeek
DOT	Dissolved oxygen tension
FBRM	Focussed Beam Reflectance Measurement
FDA	Food and Drug Administration (US)
GRAS	Generally regarded as safe
HPLC	High performance liquid chromatography
ISO	International Organization for Standardization
NAD(P)	Nicotinamide adenine dinucleotide phosphate
OTR	Oxygen Transfer Rate
PDA	Potato dextrose agar
PCR	Polymerase Chain Reaction
PNPG	4-Nitrophenyl α-D-Glycopyranoside
RFLP	Restriction Fragment Length Polymorphism
UV	Ultra violet (light)

Greek letters

δ	Density [g L^{-1}]
ζ	Zeta potential [mV]
Θ	Scatter angle of laser
λ	Wavelength of light [nm]
μ	Biomass growth speed [h^{-1}]
μ_{max}	Maximal biomass growth speed [h^{-1}]
ω	Thickness of active layer [m]

Roman letters

C_x	Concentration of biomass
Kg	Kilogram
k	Growth constant
L	Litre
m	meter
M	Molar concentration [mol L^{-1}]
osmol	Osmotic concentration
$Q_r(x)$	Cumulative particle size sum
$q_r(x)$	The particle size density distribution
R	Radius
pH	Negative of the base 10 logarithm of the molar concentration of hydrogen ions
pK_a	Negative of the base 10 logarithm of the acid dissociation constant
RPM	Revolutions per minute [min^{-1}]
T	Temperature
VVM	Aeration rate in volume [gas] per volume [liquid, reactor] per time [minute]
W	Watt [kg m^2 s^{-3}]

Chapter 1: Introduction to the project

The overall aim of this project is to understand the growth patterns of the fungus *Aspergillus niger* in submerged cultivations leading to different morphologies that might impact the productivity in industrial processes at Novozymes A/S. Existing mechanistic growth models and knowledge must be consolidated and expanded with additional experiments for generating the data confirming these models, and which also aim at identifying the parameters that could describe the morphological development of the fungus. Therefore, the topics covered by this thesis include designing a certain morphology type by altering cultivation conditions as well as particle size development to obtain advanced fermentation strategies of industrial relevance.

1.1 Structure of the thesis

Work on this thesis was done over a period of around 10 years and there are various traceable reasons for this elongated time frame. This is reflected in the structure of the thesis: The methods and a growth control model were developed with the lab strain *Aspergillus niger* AB1.13 at the institute of biochemical engineering of the Technische Universtität Braunschweig, Germany. The findings of this work were applied to an amylase producing production strain in courtesy of Novozymes A/S at different scales. Based on the contradicting results, the wild type BO-1 strain was introduced as a third strain, with the aim of finding out whether the lab or production strain differed compared to "normal" behaviour.

1.1.1 The introductory part

The chapters "Introduction to the project", "About *Aspergillus niger*", "Particle size analysis", "Conceptions about *A. niger* morphogenesis" and "Conceptions about *A. niger* morphogenesis" belong to the introductory part. The latter is included based on supplemental information about the applied particle size measurement systems and cultivation environments.

1.1.2 The results and conclusions sections

The chapter "Results & discussion" is split into a of three sections, one for each strain. Each strain section contains sections about biomass growth, particle size development and/or enzyme activity trends, respectively.

The chapter "Conclusions" is organised similarly, which is per strain, and this chapter is followed by a subchapter providing the overall conclusions of the thesis.

1.2 Introduction to Biotechnology

The utilization of microorganisms by mankind is millennia old, especially in the nutritional sector. The first written rules about how to produce a starch based alcoholic beverage date back to Sumerian times, about 4000 BC. The deeper understanding of the underlying processes has not been unveiled for a long time, though. The structured and scientific approach to microbial processes was decisively initiated by the construction of capable microscopes by Antonius van Leeuwenhoek (1632 – 1723). By using microscopy, microorganisms were described for the first time[1]. Van Leeuwenhoek's results were first verified 200 years later by the work of Louis Pasteur who also brought this topic to the scientific community[2]. Already in the beginning of the 20th century, industrial production processes based on fungal cultivation were thriving and were also the subject of scientific investigations: In 1917, for example, Currie described "The Citric Acid Fermentation of *Aspergillus niger*"[3]. Nowadays, the market volume for this product, citric acid, is around 1.75 million tons per year[4] and still, research is ongoing[5,6].

Citric acid has numerous application possibilities, and its producers are similarly versatile: Filamentous fungi. The application spectrum of filamentous fungi ranges from recombinant protein production[7], bio-catalysis of fatty acid esterification[8], production of nitriles[9], production of pharmaceutical products through stereo-selective biotransformation of steroids[10] and up to production of enantiomer purified epoxides[11]. The industrial production of enzymes by filamentous fungi is a major focus point on its own: With enzyme products, the human carbon footprint can be reduced by e.g. enabling low temperature laundry cleaning[12] or the manufacturing of ethanol out of lignocellulosic feedstock for usage as biofuel[13].

1.3 Challenges in submerged cultivation of filamentous fungi

Use of enzymes as catalyst in production processes has several production advantages, like stereo-selectivity (stereospecific pure L-malic acid production[14]) or the ability of combining several catalytic steps in one enzymatically catalysed reaction step[15,16] under relatively mild conditions (processing of biorenewables[17]). However, it is also important to mention that the management of an enzyme producing process relying on filamentous fungi can be challenging: The polarised growth of the filamentous fungi, e.g. *Aspergillus niger*, can cause the development of differentiated macroscopic morphologies.

The morphological extrema are growth as freely dispersed mycelia on the one hand, and the development of tightly entangled hyphae that form spherical particles known as pellets on the other hand. The morphology potentially influences the production yield: It has been described in the literature that penicillin is produced by the fungus found as dispersed mycelia[18] while the model protein glucoamylase of the lab strain *Aspergillus niger* AB1.13 is secreted with highest productivity when the strain is in a pellet state [6,19].

From a process point of view, the main disadvantage of the freely dispersed mycelia is the increased viscosity of the broth which might hamper bulk mixing behaviour inside the bioreactor[20]. In contrast, growth as pellets leads to almost Newtonian flow behaviour of the media which excels in terms of mixing characteristics. In consequence, gradients in the bulk phase are reduced under conditions promoting pellet formation.

The gradients might however appear inside the bio-particle because oxygen and substrate must be transported towards the centre. The diffusion of nutrients into the core of the pellet becomes limiting when the nutrient consumption rate increases. On top of the potential starvation metabolic products like e.g. carbon dioxide cannot adequately be transported towards the bulk phase[6].

The most effective method of controlling the potential diffusion limitation is to take control over the particle size development: A maximum threshold of particle size must not be exceeded. As secondary factor, particle density could be employed. Both methods rely on controlling particle

size development from the onset of secondary particle formation, which in the case of *Aspergillus niger* is represented by aggregating conidia, and later growth in particle size as function of growing biomass[21].

1.4 Origins of the project

The origin of this work lies in the special research area (in German: **S**onder**f**orschungs**b**ereich) SFB 578 by the German Research Foundation and its subproject B3 which focussed on controlling the morphology of a filamentous production host[22]. This host is *Aspergillus niger*, a fungus which is classified as a coagulating organism that forms conidia with the potential to attach to each other as conidial aggregates[23].

During the B3 project, the aggregation behaviour of the *A. niger* conidia and the growth of the pelleted biomass were studied and described by e.g. Grimm[24–26] and Kelly[27–29]. The main conclusions from their work affect cultivation parameters like initial conidia concentration[26], power input by agitation[28,30] and aeration[31] as well as the pH value.

Their respective models are based on different particle size measurement techniques and are separated by process time. There is a 15 h gap between Grimm's conidia aggregation model and the start of Kelly's pellet growth model. The lack of overlap is based on conidia aggregation kinetics, which are very fast, and pellet growth, which includes big particles with coarse surfaces.

Because optical methods are too slow to follow the conidial aggregation, it is tracked *in situ* and online by focussed beam reflectance measurement (FBRM). The FBRM method is mostly limited by the coarse surface structure with hyphae sticking out: Particles with sizes above 50 µm were detected as several smaller ones. Therefore, and depending on the cultivation conditions, FBRM could just be used to characterize the first 15 – 20 h of the cultivation.

The opposite problem was faced when employing (manual) picture analysis to cultivations younger than 24 h. The particles were simply too small for the chosen setup during the initial cultivation phase. Additionally, sampling is required which introduces a new source of variation

as the particles tend to aggregate and representative sampling is not possible. An example of how biomass looks in the early stages of fermentation is given in Figure 1.

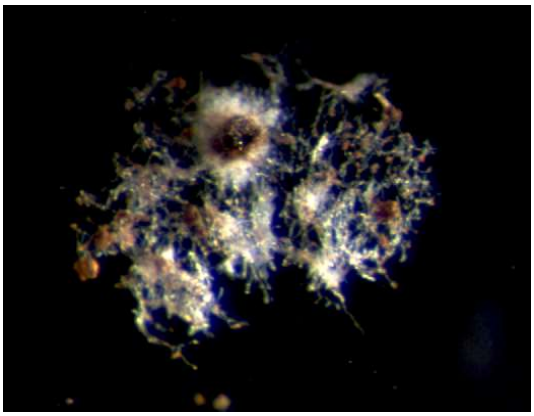

Figure 1: Early stages of Aspergillus niger *AB1.13 cultivation contains conidia, conidia aggregates and biomass with the tendency to aggregate when agitation is not available (e.g. sampling)*

1.5 Goal definition

The original purpose of this thesis is to unify Grimm and Kelly's models of aggregation and growth. Required is therefore a particle size measuring technique that covers a particle size span from 3 µm (conidia) to 2 mm (pellets). Ideally, the measurement takes place in situ as sampling would alter the aggregation of the biomass. At the same time, the sensor should be cleansable/removable from the system to counter the frequent issue of fouling in fungal fermentations [21].

1.5.1 Particle size analysis

Laser diffraction is a method that fulfils the requirements. It is well-established in areas with inorganic particles and comes therefore with a lot of know-how. The usual spectrum of usage ranges from characterising concrete particles[32] up to pharmaceutical aerosols[33] and calcium carbonate particles for bone glue[34]. Lartiges was one of the first to use the Malvern MasterSizer

laser diffraction spectrometer for biological studies in 2001 for analysis of microorganism populations from river Rhine sediments[35]. Apart from the above-mentioned size range, the Malvern MasterSizer 2000 can be connected to a bioreactor via a by-pass which enables online measurement and potential cleansing. Its usage has not been described before for this kind of application.

1.5.2 Modelling the growth

A Grimm and Kelly unifying approach must start by investigating which factors are decisive at which point in time for the aggregation of conidia and biomass. It is stated that aggregation of conidia does not take place at a fermentation pH of 3 while it is very pronounced at a pH of 5.5[36]. Step changes from non-aggregating to aggregating conditions should enable insights about the different kinds of interactions: conidia – conidia, conidia – hyphae and hyphae – hyphae. These are the cornerstones of the later pellet regarding size and density. Ideally, and depending on the production purpose, a defined biomass dry matter concentration can be created with a determined particle diameter which does not exceed a certain maximum.

This means the development of a morphology control model for controlling the development of the biomass during the cultivation beginning with conidia and up to fully mature biomass. Metabolic activity should be tracked for the fungal reactions towards manipulations of its cultivation environment like e.g ionic strength, pH value, presence of particles and mechanical power input by agitation as well as aeration and head space pressure. The aim is to provide the best morphology for high productivity in an industrial strain.

For the industrial setup, pre-cultures are common[37] and thus investigations about pushing the fungus into a certain morphology has to start there. For economic reasons[38] or to stimulate the specific enzyme production[39], the cultures often contain complex raw materials which is a difference towards academic laboratory conditions. Thus, the potential influence of the state of the substrate must be evaluated. Key is to keep the broth's rheology in control for an optimised oxygen transfer rate (OTR) from aeration into the bulk phase of the fermentation.

With different viscosities and particle diameters, it could be determined whether gradients in the bulk phase or the particle internal are limiting. Ideally, a preference of morphology for production of enzymes could be identified.

For verification of the model achieved with the lab strain, an internally well characterized amylase production strain of *A. niger* is chosen. This strain is known to be able to form both pellets as well as freely dispersed mycelia. The knowledge gain could directly merge into the current production process. The improved productivity would increase production capacity and would lead to beneficial economics. Therefore, the experiments will be conducted at several scales ranging from shake flasks, 20 L reactors up to pilot scale of 400 L.

Chapter 2: About *Aspergillus niger*

The genus *Aspergillus* is a member of the family of ascomycetes and belongs to the order of eumycetes, i.e. higher fungi. The genus includes about 350 species[40]. In contrast to other sac fungi, *Aspergillus niger* does not develop a sexual stadium. The reproduction is solely done by asexual formation of conidia. In this specific case, the terms spores and conidia are synonym. Therefore, *A. niger* is also classified as deuteromyces, fungi imperfecti[41].

Traditionally, the different species in this genus were identified by their morphological characters and sorted into subgenera mainly based on the phenotype[42]. The most recent approach to taxonomically classify the fungus is based on its phylogeny and follows the "one fungus – one name" principle[43]. Accordingly, there are now four subgenera, *Aspergillus*, *Circumdati*, *Fumigati*, and *Nidulantes*) and 20 sections proposed[44]. The classification is justified by the finding that these fungi built a monophyletic group[45]. With these newer findings, some traditional names were replaced with correct ones. This also means that e.g. a company's strain library must be updated to display the correct taxonomy, avoid confusion and improve communications[46].

The monophyly is based on sequencing technology that allows analysing the internal transcribed spacer region of the ribosomal RNA gene cluster which is used as official DNA barcoding region for fungi. This method might be insufficient to distinguish between different species though[47]. As a secondary marker, the DNA structure for the fungus' b-tubulin can be employed[48]. The Restriction Fragment Length Polymorphism (RFLP) method[49] has recently been updated with additional PCR analysis to quickly differentiate between species inside a subgenus[50].

As saprophytes, the natural role of these filamentous fungi is the digestion of dead biomass like e.g. trees and other solid and complex substrates which makes the filamentous fungi a good source for discovery of e.g. cellulose digesting enzymes. To be able to make nutrients available, an efficient secretion system is required which is also advantageous for exploitation of the fungal productions capabilities: If the target protein could be secreted, downstream processing can omit unit operations required for treatment of the biomass[51].

As eukaryotic organism, *A. niger* can do posttranslational protein modifications which resemble the products of cell cultures to some extent. These include proper folding of bigger protein molecules, methylation and glycosylation which could be of immense importance for pharmaceutical products, especially considering production of heterologous and eukaryotic proteins[7].

Obtaining the GRAS status is advantageous for industrial purposes– **g**enerally **r**egarded **a**s **s**afe. The American Food and Drug Administration (FDA) approved *A. niger* as a GRAS organism in 1994. With this approval of the strain, the approval of processes by the authorities becomes less of a hassle as well despite the fact that the production organisms are still able to build up mycotoxins depending on the applied process parameters[52,53].

2.1 Tip growth of hyphae

The vegetative form of *Aspergillus* is characterized by a septate and branched polynuclear mycelia. When reaching suitable conditions, asexual conidia will be developed by cell division of a hyphal segment into a specialized sporogenous cell. Figure 2 showcases the overall development of conidia from *A. nidulans*, a close relative to *A. niger*: One hyphae starts growing aerial into a stem and becomes a vesicle by swelling (A & B). In a budding-like process, metulae are formed (C) which produces up to three phialides (D). The phialides are continuously sectioned into single-nucleus conidia (E).

Sensing substrates, the first biomass as such is a thallus extending the conidia[54]. After swelling, the conidia develop a germ tube which becomes the later hyphae. The growth of the developing hyphae is polarized and highly directed towards substrates[55]. Prolongation of the hyphae exclusively takes place in a narrowly defined area at the hyphal tip, the apical cell, which is separated by a septum from the sub-apical cells. Several cell nuclei could be present in the apical cell[41].

The germ tube's growth speed is exponential at first and becomes linear with increasing hyphal length. Growth speed is determined by the micro tubules based vesicle velocity which provides

the apical cell with cell wall synthesis building blocks produced in the entire hyphal volume. An additional factor is also the exo-/endo-cytosis equilibrium which interacts with flexible actin stabilization of the tubules[56].

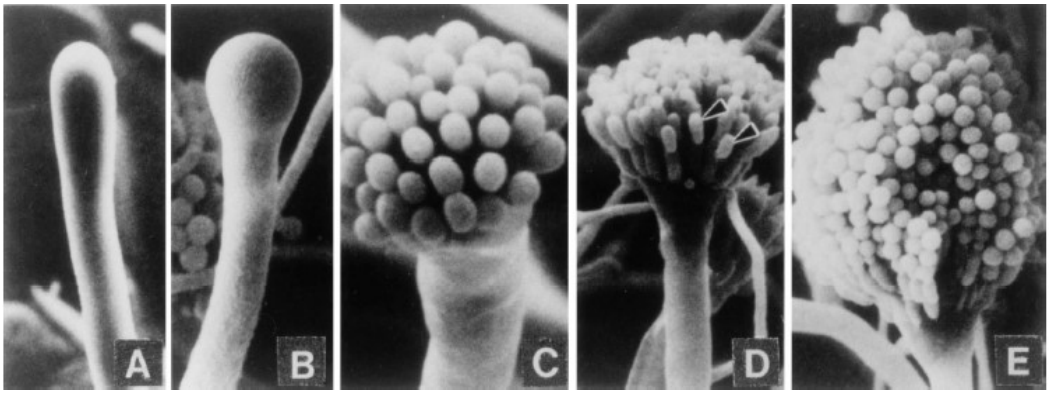

Figure 2: Morphological changes during conidiophore formation. Shown are scanning electron micrographs of the stages of conidiation. (A) Early conidiophore stalk. (B) Vesicle formation from the tip of the stalk. (C) Developing metulae. (D) Developing phialides. (E) Mature conidiophores bearing chains of conidia [57,58].

The transition from exponential to linear growth speed also reflects the point in time when branching of hyphal elements out of the sub-apical cells starts to occur[59]. Further branching happens when the content of bio-synthesis material exceeds the consumption of this material by the apical cell. Theoretically, the amount of hyphal mass can develop exponentially thus leading to an overall quasi exponential growth similar to that of a unicellular organism[6].

It is believed that the hyphae could be separated into three sections: An extension zone representing the tips of the hyphae, an active region which is responsible for growth and product formation and an inactive hyphal region[60].

2.2 Morphologic appearance

The natural habitat of *A. niger* supplies the fungus with solid substrates. While polarized growth and branching of hyphae is well suited here, it leads to a range of morphological appearances in

submerged cultures. Figure 3 illustrates the two extrema: a) Growth as distinct spherical aggregates which are called pellets & b) growth as freely dispersed hyphae or mycelial clumps[6,61].

The freely dispersed growth is characterized by mycelial trees which are found distributed in the cultivation medium. Because of freely dispersed growth, the apparent viscosity of the suspension could be drastically increased. The extreme situation could be reaching pseudo-plastic flow behaviour[62]. To ensure a sufficient mass and heat transfer therefore requires (relatively) high power input which also could be problematic from an economical point of view for large scale cultivations.

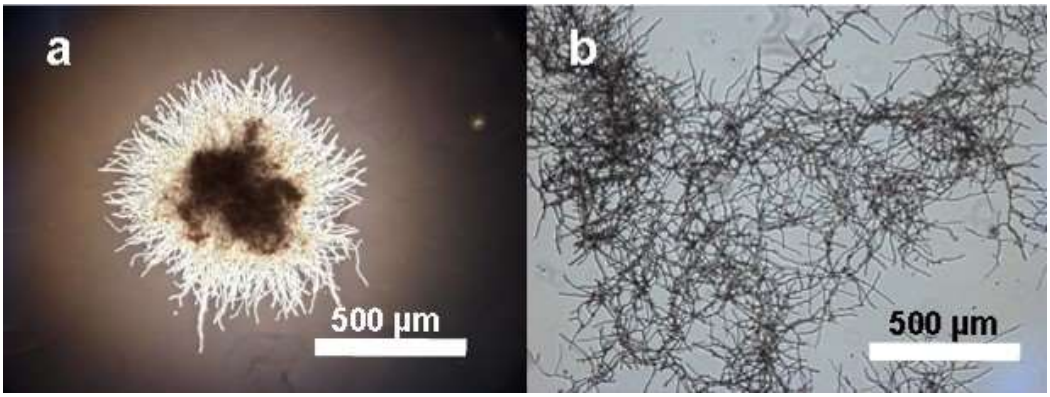

Figure 3: Types of morphology typically found in submerged cultures of filamentous fungi a) pellet; b) freely dispersed mycelia.

Despite the higher power input, inhomogeneity can still occur in terms of pH, oxygen and nutrient supply and carbon dioxide and heat removal, respectively. Moreover, intensive power input might hamper the growth/development of the biomass due to excessive shear which in turn might have a negative effect on the synthesis of heterologous proteins[63]. When shear is not an issue with the selected strain or the chosen setup, freely dispersed mycelia seems to allow enhanced production based on the fact that the morphology at the microscopic level has an influence on the production kinetics and on the secretion of enzymes[64].

In contrast, pellets consist of highly entangled hyphae and can reach particle sizes of several millimetres. The pelleted morphology type can be preferred because there are no free hyphae to

increase the viscosity. The resulting Newtonian fluid behaviour of the bulk phase is marked by superior mixing characteristics with lower required power input[65]: Bulk gradients can mainly be avoided. However, nutrient concentration gradients might occur in the pellet[66].

The mass transport inside of particles might be diffusion limited above a particle size of 1 mm[6,67]. The limitation will be enhanced by consumption of oxygen and substrates by the growing biomass. From a process point of view, smaller pellets are thus preferred over bigger ones[68], mainly because of the lower diffusion distances. The diffusion is also dependent on the density and porosity of the pellet which stands for the overall surface being in contact with the liquid phase[69].

Depending on the desired product, the optimal morphology for a given bioprocess might vary and cannot be generalized. In some cases both types of morphology are present in one process[70]. Penicillin G produced with *Penicillium chrysogenum*, for example, is produced with highest productivity when grown as freely dispersed mycelia[18,71]. In contrast, citric acid is produced with optimal space-time-yield when *Aspergillus niger* is cultivated as pelleted suspension[5,72].

In the case of the production of the enzyme glucoamylase, it seems like *A. niger* prefers the pelleted state. The assumed reason for this is that catabolite repression is not activated in the inner regions of the pellet due to the gradient inside the pellet. Since there also is an oxygen gradient, the oxidative inactivation of protein synthesis could be prevented[73]. The morphological development towards pellets can therefore be seen as differentiation which, induced by cell-cell interaction, could lead to specialization of single segments and thus to an improved production capability[6].

The morphology of filamentous fungi is double edged: The productivity as well as the fermentation conditions can be affected by the outer appearance of the fungus. The challenge is to separate these effects to be able to connect observed productivity gains to the correct phenomenon causing it.

2.3 *A. niger* growth in submerged culture

In analogy to the growth characteristics of single cell organisms, the biomass development of a filamentous fungus in a batch cultivation can be divided into different phases. After inoculation with conidia, there is a lag-phase. The lag-phase represents adaption of the organism to the new environment. Before swelling and germination take place (see 2.1 Tip growth of hyphae), the surface charge and structure of the conidia might be altered. Non-covalent proteins could be detached and the conidia's UV-protection substance, melanin, dissolves. These two phenomena could be decisive for later stages of the cultivation and will have a major influence on the model of aggregation of conidia described by Grimm[30].

Taking up water marks the beginning of metabolic activity. The conidia swell and germ tubes are formed. For *A. niger*, the lag phase of conidia varies between 6 – 10 h[26]. Following the lag phase, an exponential biomass growth phase takes place which transforms into linear growth (see 2.1 Tip growth of hyphae).

There are two major types of models describing the fungal growth. The first assumes that the dispersed mycelia follow similar growth characteristics as single cell organisms. The dynamics of the biomass concentration can therefore be considered as exponential and the law of Maltus can be applied with C_x as concentration of biomass, t as time and μ as growth rate:

Equation 1: Law of Maltus describing growth

$$\frac{dC_x}{dt} = \mu \ C_x$$

With the growth rate being constant in the exponential phase (no limiting substrate), the differential equation can be integrated

Equation 2: Law of Maltus integrated with constant μ

$$\mu = \frac{ln\frac{C_x(t_2)}{C_x(t_1)}}{t_1 - t_2}$$

The maximal specific growth rate μ_{max} of *Aspergillus niger* is usually between 0.1 and 0.3 h^{-1} [6].

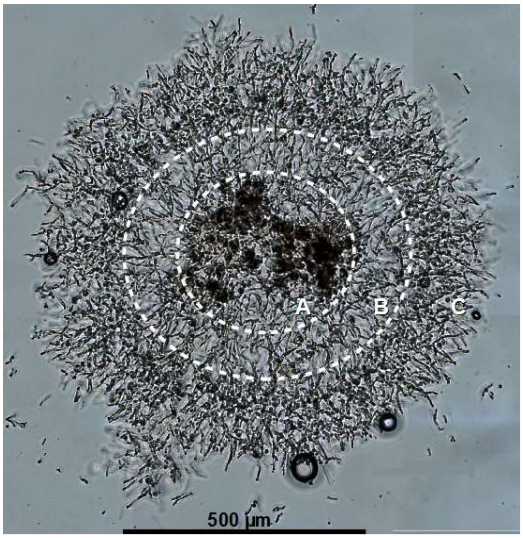

Figure 4: Pellet structure of Aspergillus niger AB1.13. The inner circle A marks the core of the pellet which also contains aggregated spores attached to each other and hyphae. The middle layer B is characterized by hyphae with relatively low density. The outward layer C shows active growth and appears denser than the middle layer[74].

The second approach to describe fungal growth rate takes pellets and their structure into account. Figure 4 displays how the interior of the pellet can look like. It is assumed that just the outer layer (C) is active. If the number of hyphal tips is now increasing exponentially, the pellet radius R increases with a constant rate based on the initial radius R_0, assuming no (diffusion) limitations. Equation 3 describes this relation in dependency of the thickness ω of the active layer, the growth rate of the biomass μ and time t.

Equation 3: Mathematical description of pellet radius in dependency of time, growth rate and thickness of the active layer

$$R = R_0 + \omega \mu t$$

This mathematical description also forms the basis of the cube root law which was developed in the 1950s by Emerson[75]:

Equation 4: cube root law describing pelleted growth

$$C_x(t)^{\frac{1}{3}} = C_x t_0^{\frac{1}{3}} + k\, t$$

During the exponential phase of the outer and active layer, the factor k is a constant which was determined to be in the range $0.035 \leq k \leq 0.07\ kg^{\frac{1}{3}}\ L^{-\frac{1}{3}}\ h^{-1}$ for the strain *Aspergillus niger* AB1.13[28] which was employed for the experiments.

2.4 Fermentation parameters influencing morphological development

The cultivation media represents the direct environment of the fungus which naturally makes it a parameter with substantial influence on future growth and morphology. Lack of nitrogen, for example, is described to induce pelleted growth while excessive phosphate as growth enhancer suppresses it[6]. The ion composition of the media is also important: Manganese ions (Mn^{2+}) can induce aggregation of biomass to pellets in an else dispersed cultivation[72].

A lack of Mn^{2+} ions in turn is reported to reduce the activity of an oxalo-acetate-acetal-hydrolase which in a cascaded effect increases production rate of citric acid[11]. This emphasizes the fragile balance between direct effects of media on the productivity and its effects on morphology.

The pH value of the media influences the transport and the solubility of nutrients and it might affect extracellular enzyme activity. From the morphological point of view, the pH value is decisive in terms of surface charge of the conidia. In general, it has been reported that *Aspergillus niger* tends to grow as freely dispersed mycelia at pH values of 2 while growth at pH 5.5 mainly is pelleted[76,77].

Aspergilli in general are known for their resilience over high sodium chloride concentrations up to 20 %[78]. High salinity affects morphology and production of e.g. enzymes though[79]. Osmolality in the range of 0.2 to 4.9 osmol kg^{-1} was tested on two different academic *Aspergillus niger* strains with the results that lag phase increases with higher osmolality while the overall biomass development was hampered. The morphology changed from spherical pellets towards elongated particles in a more mycelia like growth pattern. Intriguingly, the productivity increased[80].

A different approach for control of the morphological development was introduced by addition of microparticles consisting of silicate or aluminium oxide to the cultivation [81,82]: The presence of

microparticles during cultivation strongly influenced the morphology, and by varying both size and the concentration of the particles, distinctive morphologies were achieved. It is believed that the addition of inert microparticles causes a disturbance of the initial spore aggregation (see chapter 4.1)[81]. Based on these observations, the addition of inert microparticles looks promising as a tool for morphology engineering of filamentous fungi.

The concentration and type of inoculum (conidia or vegetative forms) are described to affect the morphological development[30]. A start concentration of conidia above 10^8 mL^{-1} usually leads to dispersed growth, or, in turn, pelleted growth can just be achieved by applying a start concentration below 10^8 mL^{-1} [6]. It seems, though, that pellet formation follows an optimum function: Employing a lower conidia inoculum concentration like e.g. 10^4 mL^{-1} leads to formation of bigger pellets in lower concentration while more pellets with smaller diameter develop with higher conidia concentration[26].

Apart from the desired effects of improved dispersion of the gas phase and an enhanced bulk mixing with higher mass and heat transport, mechanical power input also influences the morphology: Shear can damage the cell structure. Changes in morphology, growth rate and production rate might be the consequences[6,65,67,83]. With a variation of the power input, the fluid dynamics inside the reactor are altered. With higher power input, the intensified interactions between pellets and eddies lead to shaving off hyphae that stick out of pellets, thus leading to a smoother pellet surface and thus a denser outer active layer[28].

In summary, the above-mentioned parameters have an influence on the morphological development of *A. niger*. Given sufficient knowledge about the leverage of these parameters on the fungal behaviour, they could actively be employed as handles to design and steer the cultivation towards a specific outcome in terms of morphology.

Chapter 3: Particle size analysis

3.1 Particle Size properties – dispersion

The system that should be measured consists of a liquid phase (cultivation media) which as continuous phase resembles the dispersion agent, and a solid phase (the biomass). The dispersion value characterizes the system. It consists of a numerical value and a unit and could be geometrical (e.g. sectional area for a digital image analysis) or physical (e.g. the mass for gravimetrical measurements). It is important to realize that particles usually do not appear in a unified shape or size and that a collective of particles usually exists as a mixture which complicates the collectives' characterization.

The dispersion value is determined with particle size dependent characteristics. The particle size measuring technique serves to register this dispersion value. In many cases, the dispersion value is converted into the diameter of an equivalent sphere (spherical equivalent diameter). Alternatively, the system could be calibrated with spherical particles to relate the measured value with spherical particles. First then will it be possible to present the composition of a particle collective as a particle size distribution.

Particle size distributions are usually presented in two ways. The first way is as a cumulative sum of the distribution $Q_r(x)$. It resembles a representation of the distribution which for each point x on the X-axis adds up the relative subsets of particle sizes smaller than the specific particle size x. All particle classes together or all measured particles together converge to a cumulative sum of 1. Figure 5 displays the cumulative sum function.

In this context, the index r describes the type of distribution, e.g. if this is a volume or a number distribution. Because r resembles the exponent of the equivalent diameter, it has a significant effect on the shape of the curve: Number, length, area and volume are displayed as 0, 1, 2 and 3, respectively. With index r increasing, the greater is the influence of larger particles on the shape of the distribution. This means that smaller particles have less influence on the shape of a volume distribution than in a number distribution[34]. This concept is graphically explained in Figure 6.

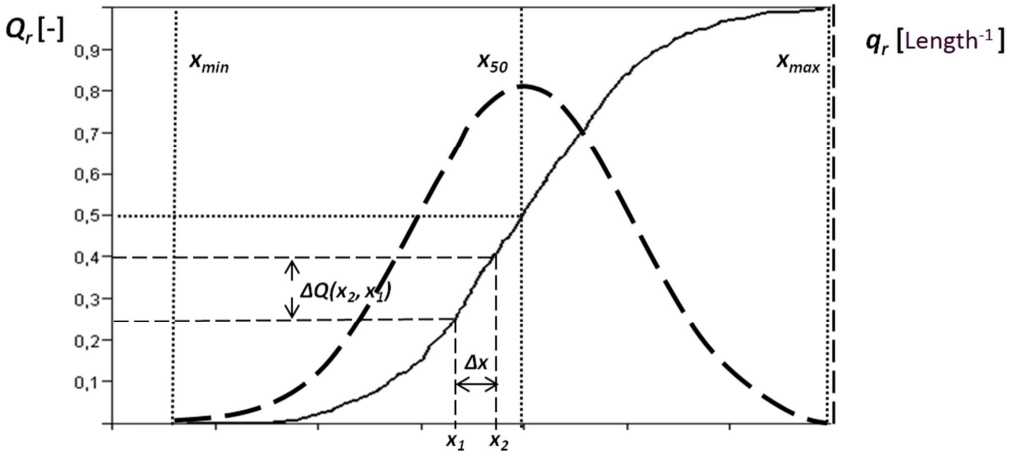

Figure 5: Display of the cumulative particle size sum and the particle size density distribution

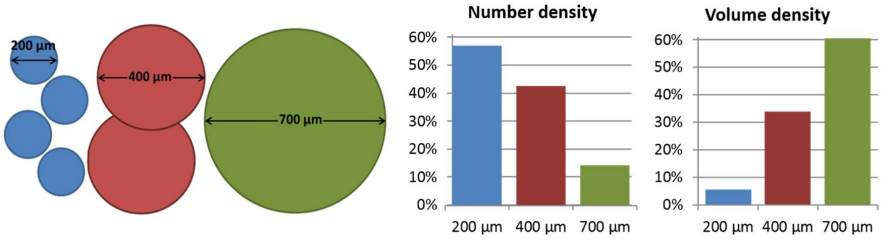

Figure 6: Graphical explanation of the two types of output from particle size distribution measurements. The bar charts represent the two outputs when a sample is measured with the 7 particles to the left.

As described before, the value of the cumulative sum of the distribution for the maximal particle size equals 1. This means that the value of the cumulative sum is zero for any size below the minimum particle size in the distribution. If the relative number of particles at a certain particle

size x (alternatively the infinitesimally small interval Δx) is of interest and if the sum function is continuously differentiable, the distribution density q_r can be derived as displayed in Equation 5.

Equation 5: particle size density distribution is the derived version of the distribution sum

$$q_r(x) = \frac{dQ_r(x)}{dx} \leftrightarrow Q(x) = \int_{x_{min}}^{x} q_r(x)dx$$

To characterize a particle size distribution with the lowest number of parameters possible, different location parameters can be defined. The most common is the median:

- Beside the arithmetic mean value of the number weighted particle diameter, the median value $x_{med,r}$ is of importance. At this particle size, 50 % of all measured particles are of smaller equivalent size. In the cumulative sum of the distribution $Q_r(x_{med,r})$ hence takes the value 0.5. The median is heavily dependent on the type of distribution. Usually, the median should just be used for mono-modal distributions.
- When encountering bi- or multi-modal distributions, it could make sense to employ the mode $x_{mod,r}$ instead of median $x_{med,r}$[84]. $X_{max,r}$ resembles in this context the highest value of $q_r(x)$. The mode is defined as the particle equivalent diameter which is present at the local maximum in the density distribution (see Figure 25 on page 78).

The location parameters are easily available and are standard output of modern particle size measurement systems. When the laser diffraction system solves the spectra via the Fraunhofer analysis, it makes sense to weigh the distributions as sectional area as the assumption is that the light is bent towards a circular projection plane[34,84].

3.2 Definition of agglomeration and aggregation

The terms agglomeration and aggregation have a different meaning outside the particle technology area. Inside particle technology, however, both terms describe a collection of primary particles. During the work presented in this thesis, the primary particles are *Aspergillus niger* conidia. A precise definition at the beginning of this work is necessary though because even

specialists in the field of the particle technology area are not always following the conventions[85], and different international organisations suggest deviating terminology (British Standard Institution). In the powder processing field it was even suggested to solely use the term agglomeration[85]. The following definitions justify the usage of the terms agglomeration and aggregation for this thesis:

- The word agglomeration derives from the Latin verb *aglomerare* which translates as to bundle or to clump together to a ball or assembly[86]. Agglomerates consist of primary particles that are loosely connected with each other. The connection is not due to surfaces but on edges and angles. The surface of an agglomerate equals the sum of the surfaces of all single particles. Due to low coherence, an agglomerate can be easily disintegrated.
- The term aggregation is not used in the biological sense in this work, where the term stands for the fact that cells form collections of cells without losing their individuality. Instead and despite of this, the definition from the particle technology area will be employed. According to the Oxford English Dictionary, an aggregate is a mass which consists of a collection of individual particles[86]. The origin of the term derives from the Latin verb *agregare*, which means to merge. Following this description, an aggregate is defined as a more tightly bonded collective of particles compared to an agglomerate. Further, it was stated by Gerstner (as mentioned in [87]) that an aggregate consists of primary particles attached to each other via surfaces. In consequence and in contrast to the agglomerate, the surface of the aggregate is smaller than the sum of the surfaces of the individual particles, and the inner surface of the aggregate is inaccessible. Due to the tight bonds, this particle assembly cannot be easily broken up by e.g. intensified hydrodynamic energy provided by agitation.

The definitions and the mechanism describing conidia attaching to each other during the primary aggregation would allow the characterization as agglomeration process because spherical particles cannot attach to each other via surfaces. It cannot be excluded though that there are interactions between molecules, e.g. proteins or melanin, because the definition of agglomeration is not sufficiently precise. Further on, Grimm describes that aggregation and de-aggregation of

conidia reach an equilibrium until the secondary aggregation step[25]. The particle size distribution of conidia and the aggregates, respectively, show that the aggregates do not entirely break up into their primary particles. This supports using the term aggregate and aggregation henceforth.

3.3 Principles of laser diffraction

Laser diffraction will be used to follow the particle size development. The instrument of choice is a Malvern MasterSizer 2000. The measuring principle is based on scattering of a laser beam when dispersed particles are obstructing the optical path of the light beam. Diffraction is the phenomenon that occurs when interferences arise in the geometrical shadow of the particle where absence of light would normally be expected. Interference describes the interaction of two harmonic waves with identical wavelength which either leads to amplification or cancellation.

In the shadow of a spherical particle, scatter of monochromatic and coherent light (laser) causes several diffraction maxima as positive interference and minima as destructive interference. The distances between the maxima and minima are dependent on the particle size and the wavelength of the light. Employing a laser with known wavelength makes it possible to use the diffraction pattern to analyse the particle sizes of the obscuring particles.

Figure 7 schematically displays the optical bench of the laser diffraction analyser. The arrangement is set up to detect as many scatter signals as possible. Ensuring the correct concentration of particles is important such that the light can reach each individual particle independently. Assuming now that all particles harbour the same size, all will scatter the light in the same angle.

The minima and maxima can be focused onto the focal plane with a lens. The result is an intensity distribution with the absolute maximum in the middle (all not deflected or scattered beams of the laser which are also used to determine the overall obscuration). Perpendicular to the direction of the light beam, the intensity follows a wave-like pattern in which the intensity of the maxima decreases with increasing distance to the center[88].

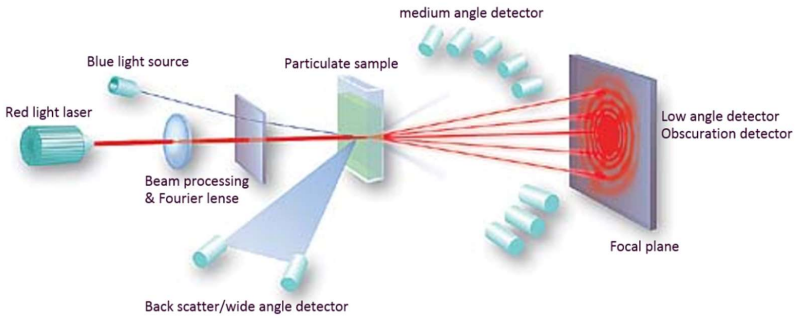

Figure 7: Schematic structure of a laser diffraction analyzer with the typical, circular symmetric intensity distribution caused by scattering of light on spherical particles (picture from Malvern online course).

Assuming now that the dispersed particles form a grid and that the dispersant acts like slits, the following relation for determination of the location of the maxima can be used:

Equation 6: Basic relation between wave length λ, location of the first maximum z, the particle size x and the angle the light will be scattered at (Fraunhofer approximation on multiple slit).

$$sin\theta \approx \frac{z\,\lambda}{x}$$

The location of the first maximum z = 1 is dependent on the size of the projection area of the particle given the wave length λ of the employed laser is constant. With increasing particle diameter x, the scatter angle Θ decreases. Apart from the setup of the instrument, for example in terms of light intensity or distance from the particle, the intensity of light detected at the sensor is dependent on the number of particles[89].

If an ensemble consists of particles with different sizes, all signals from particles with the same size will be bundled. It also means that there is an overlay of signals from particles with different sizes as all particles receive the incoming light beam at the same time. To solve that challenge, ring-like detectors (diode-detectors) are installed with fixed angles in the focal plane of the Fourier lens. Knowing the intensity of the first maximum allows for concluding how big the fraction of this specific particle size is.

There are different methods to solve the scatter patterns of a known particle size distribution. There is as the first approach the Mie-theory which is the exact solution to Maxwell's wave equation for spherical symmetrical particles. For calculation of scatter patterns, the optical parameters must be known. The Mie- theory is valid for all size ranges, wavelengths and scatter angles.

The second approach is the Fraunhofer approximation. It is part of the Mie-theory and is only valid for particle sizes above the Mie-range: $\lambda * 10^{-1} \leq d \leq 10 * \lambda$. The here employed helium-neon laser generates a wavelength of $\lambda = 0.632$ µm which corresponds to reliable measurements down to particles with the smallest particle diameter of 6.3 µm. Required optical parameters are that particles are spherical and that these are impervious to light so that these can be treated like discs which only cause forward scatter of the light with rather low angles (≤ 10 µm)[90].

The optical properties refractive index and absorption coefficient change during the cultivation and are hence not known for most of the experiments. It is therefore advised to solve the scatter pattern with the Fraunhofer approximation (ISO 13320[91]).

The smallest particles encountered in this work are the conidia: These are spherical and light impervious, and have a diameter of around 3 – 5 µm. Microscopic control proved that the Malvern MasterSizer 2000 is capable of determination of the correct size of spores using just the Fraunhofer approximation, and hence this method will be employed in the following. It has to be kept in mind that results might deviate from reality if the given assumptions are not (longer) valid[91].

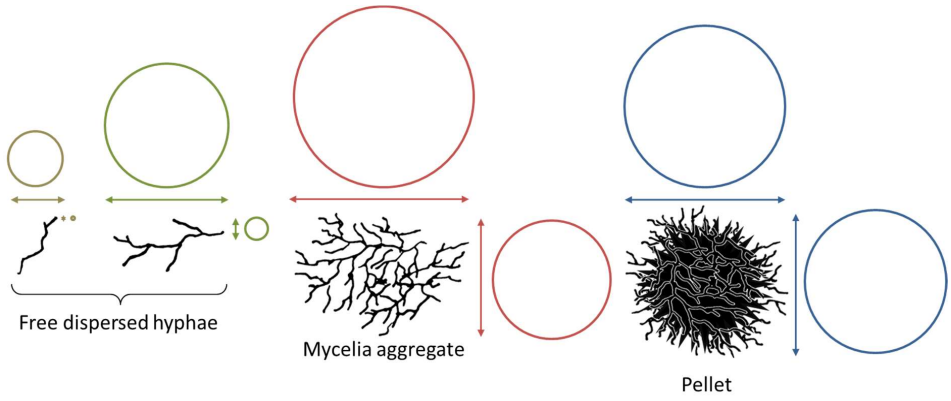

Figure 8: Two-dimensional illustration of how the particle size is determined for three different types of morphology typically seen in this study of A. niger. To the left: an example of freely dispersed hyphae, in the middle: mycelia aggregate, to the right: pellet. The coloured arrows indicate examples of lengths which the MasterSizer could detect, dependent on the direction of the particle as it passes through the measuring chamber. The coloured circles illustrate the volume of the particle which the software would calculate based on this measured length [92–94]

That means that the method is only applicable when a submerged *A. niger* culture consists only of conidia or pellets. When the morphology includes dispersed mycelia and free hyphal elements, this method it not very suitable. Figure 8 illustrates examples of how laser diffraction would detect particles when measuring a submerged culture of filamentous fungi with different types of morphology [94,95]. The arrows on the figure indicate examples of particle lengths which would be detected. The circles indicate the respective volume (presented in 2D) corresponding to the detected lengths if the result is given as volume distribution. The figure illustrates the two major problems related to measuring particle size distribution of different morphologies:

1. A single hyphal element can be measured to several different lengths, meaning it would be almost impossible to distinguish between orientation of particles and the distribution in particle size.
2. It is difficult, if not impossible, to distinguish between pellets and large agglomerates of mycelia. As experienced from this study, loose agglomerates can grow very big, and when results are analysed as a volume distribution, all small particles become insignificant.

Calculating now the particle size distribution of a particle ensemble of unknown composition requires a complex process. In the case of the Malvern approach, solving the spectra is an iterative process. Out of the scatter pattern the software derives a particle size distribution (using Fraunhofer approximation). That distribution is then used to predict the scatter pattern. If now the calculated scatter pattern is not congruent to the measured one, the calculation process will be repeated. When reaching the pre-defined precision, the calculation process will be terminated. The particle size distributions based on laser diffraction are heavily dependent on the employed algorithm[84,89].

Major advantages of laser diffraction in the context of this work are the large number of particles that are constantly measured which gives some statistical certainty, and the ease of handling compared to the (not automated) image analysis. The most important advantage though is the possibility to connect the Malvern MasterSizer 2000 to the bioreactor via a bypass as a quasi-online measurement for the particle size distribution with a short sampling interval (frequent measurement points).

A drawback of the method might be the inability to track the concentration of the measured particles even though the number of particles is inherently influencing the intensity signal of each scatter maximum. The information about number of particles contained in the scattering pattern cannot be quantified, though[84].

The user must be aware about the sources of systemic errors. If the above stated requirements for the method are not matched, there could be major deviations in the calculated distributions compared to the real ones. Therefore, it is recommended to employ microscopy for controlling and documenting the laser scattering results.

Chapter 4: Conceptions about *A. niger* morphogenesis

4.1 Concept of conidia aggregation by Grimm

According to Metz and Kossens[62], most filamentous organisms could be classified as either coagulating or non-coagulating. Examples of the latter are some *Streptomyces* species which develop one pellet per spore – the hyphae forms the core of the pellet[76]. For the coagulating organism type, like the here investigated *A. niger*, the conidia possess the potential to attach to each other during the early stages of the cultivation. The core pellet could thus consist of aggregated conidia which are surrounded by the hyphal network developed out of one or more but not necessarily all conidia.

Grimm developed a two-staged model of conidial and biomass aggregation[26]. The model is based on population balances which handle the entity of particles inside the reactor. The first step is the adaptation phase of the cultivation: Just moments after inoculation, conidia attach to each other – aggregation! The relative particle concentration drops to about 90 % of the original value. Figure 9 illustrates this concentration drop at the very beginning of the graph. For the remaining part of the lag phase, the particle concentrations appear to be stable. It is described as a dynamic equilibrium between aggregation of conidia and aggregates and the respective disintegration.

The second stage is initiated with the beginning of germination and active biomass growth. With biomass growth, new surfaces are built up exponentially and non-germinated conidia or smaller aggregates could attach to it. This leads to the second decrease in particle concentration between 7 and 13 h in Figure 9 which correlates to the growth rate. A dynamic equilibrium is reached again at a lower concentration of particles. The secondary aggregation stage can be considered terminated after about 15 h when all conidia have germinated or are attached to/incorporated into other particles. Using the software PARSIVAL by CiT GmbH[96] for modelling the aggregation via population balances enables to calculate the kinetics of the aggregations.

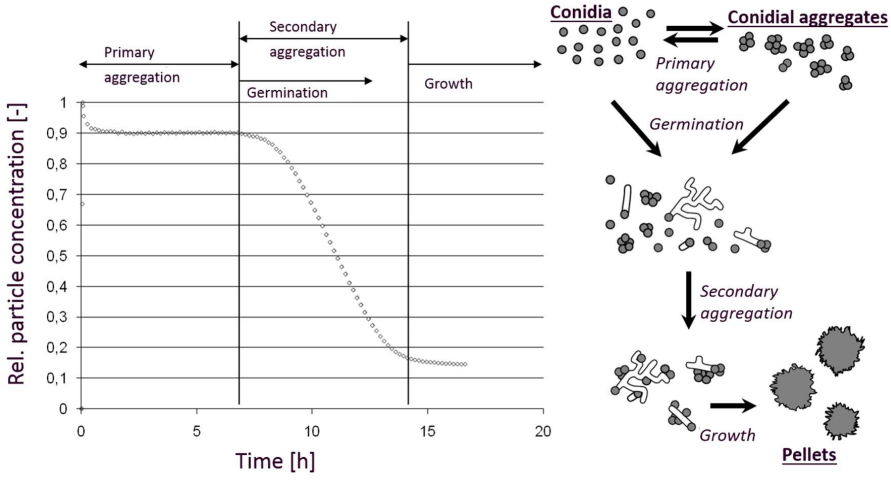

Figure 9: Kinetic model of aggregation of A. niger conidia consisting of two stages. First, there is a conidia-conidia interaction which happens at the onset of the cultivation. Secondly, conidia attach to growing biomass/hyphae after germination[30].

For balancing, the aggregation and the biological growth are formulated as growth, source and sink functions. The primary aggregation is based on two counteracting processes. The first is the formation of conidia packages with the velocity constant k_{+1}. The second resembles the disintegration of packages into conidia (or particles of a smaller size class) and is characterized by the disintegration constant k_{-1}. Both aggregation and disintegration lead to genesis and disappearance of particles with a chord length of L.

Primary aggregates with a specific chord length of L, a parameter which resembles the spherical equivalent diameter, could develop by attachment of smaller aggregates ($b_{agg}(L)$, aggregation source function) as well as by disintegration of bigger aggregates ($b_{break}(L)$, disintegration source function). As equilibrium, there also is a loss of aggregates with the chord length L which could happen by recombination with other aggregates to form larger particles ($d_{agg}(L)$, aggregate sink function) or disintegration into smaller particles ($d_{break}(L)$, disintegration sink function).

For the secondary aggregation it is further assumed that the decline in conidia concentration is proportional to the average length increase of the hyphae and that conidia can attach anywhere

on the newly built surface[97]. Growth of the biomass can be both source and sink for a distinct chord length. It is though integrated in the model as provider of surfaces for attachment. Equation 7 summarizes the descriptions in the above paragraphs:

Equation 7: Mathematical description of the population balance model

$$\frac{\partial n_0(L,t)}{\partial t} = b_{agg}(L) - d_{agg}(L) + b_{break}(L) - d_{break}(L)$$

Both mechanical power input and the pH value of the media can influence the kinetics of the two aggregation stages. The particles existing during the first stage are too small to be affected much by the power input, though one known exception are reactors with high aeration rate and thus high energy input. In general, the influence of power input increases with progressing growth and particle size, mostly on the secondary aggregates.

It was investigated how the pH value of the media influences the surface charge of the conidia, which is described by the ζ-(zeta-)potential, and how this is related to the rate of aggregation during the primary stage. Lowering the pH leads to a lower drop in particle concentration during both stages of aggregation. According to the DLVO theory[98], the pH value stabilizes the aggregates. Furthermore, the quantification of interaction forces can be used for linking the fluid dynamic load description on the aggregates as it incorporates the local maxima in load intensities.

4.2 Pellet growth model by Kelly

In 2006, Kelly described the pellet growth of *Aspergillus niger* AB1.13[29]. The pellet population is regarded as a collective of particles that differ in dispersion characteristics like diameter, concentration and morphology (see section 2.2). The dispersion characteristics are influenced by the growth process and change during the cultivation.

For this model, it is assumed that mature pellets occur after 20 h of cultivation and that successive growth happens as pellet growth (of the active biomass layer). Pellet growth is

characterized by increasing median values $d_{P,50,1}$, especially until cultivation time reaches 30 h. Afterwards and in dependency of the mechanical power input, Kelly calculated the pellet growth speed to be a constant velocity of $u_{P,max}$ = 0.043 mm h^{-1}.

Because of accumulation of growth inhibiting factors, the pellet growth decreases after around 50 h into the cultivation despite sufficient nutrients being available. An equilibrium between positive growth-related processes and the negative processes like erosion of the outer hyphae because of mechanical influences like shear as well as decreasing stability/tensile strength of hyphae is then assumed to be established. At the same time, the pellet density decreases. Caution is advised by the author because the calculation of particle volume is proportional to the diameter to the power of 3 ($V_{particle} \sim d_{particle}^3$) which makes the measurement error prone.

Just as the model for the aggregation, the software PARSIVAL was used to model the growth via population balance. The model relies on the measurement of the dispersion characteristics which become terms for particle growth and erosion as well as metabolic rate. Because the cultivation experiments are batch processes, there are no sources or sinks in terms of volume. For the model, the particles do not disintegrate completely. Instead, it assumes that exposed hyphal branches are eroded. In principle, these sheared off hyphae can form new pellets of their own. The absolute number of these sheared off hyphae though is sufficiently low to be neglected[99]. These assumptions allow the simplified version of the population balance which describes the time dependent changes in the pellet population only with the particle growth velocity u_P:

Equation 8: population balance as growth model with time changes and growth/erosion as summands

$$\frac{\partial q_0(L,t)}{\partial t} + \frac{\partial}{\partial t}\left(u_P\, q_0(L,t)\right) = 0$$

The particle growth velocity is defined by the fraction of active biomass of the pellet as well as damping of growth by inhibitors. Because diffusion limitations might occur inside the particles when particle diameter increases, it is assumed that keeping the hyphae at the core of the particle alive is not prioritized, or they might even be completely lysed (→ decreasing particle

density)[100]. Consequently, this means that there is just the outer layer of biomass contributing to growth. The model offers the possibility to adjust the density and the substrate limitation inside of the pellet manually accordingly to experimental findings, without the necessity to add additional terms to the population balance.

4.3 Control of the morphology

The previous chapters "Concept of conidia aggregation by Grimm" and "Pellet growth model by Kelly" describe the interaction of conidia with conidia, conidia with hyphae as well as the particle size expansion by biomass growth of an active layer as a function of time and the mechanical power input. Both models are based on population balances, though Kelly's pellet growth model is not a balance as such because it does not include neither sources nor sinks for the overall number of particles. Hence it is "just" a growth model. Based on the difference in particle concentration at the end of the aggregation model and the beginning of the pellet growth model, it is assumed that there might be a tertiary aggregation step.

The time point of this hypothetical step after the outgrowth of conidia and before mature pellets occur leads to the assumption that this aggregation is based on hyphae-hyphae interaction. Per the description of secondary aggregation, single and not germinated spores could link hyphae together but these would be affected by the pH of the cultivation media, the power input and the general physiological conditions of *A. niger*. These parameters are hence the biggest sources of influence and therefore also the most potent handles for controlling the morphology. Ideally, the conditions inside the bioreactor can be switched from aggregation promoting to aggregation preventing conditions.

The schematic overview over control possibilities to direct the morphology to specific particle sizes in Figure 10 is based on the following ideas: Conidia at the onset of the cultivation (as well as in the inoculum) at a pH 3 remain as single particles and maybe as smaller aggregates. The by Grimm observed aggregation does not happen. The conidia swell, germinate and are present in

higher concentration by skipping aggregation compared to cultivation at pH 5.5 (condition applied for the derivation of Grimm's model).

If a pH of 3 is maintained, both the biomass and the degree of branching increase during the exponential phase. If this phase at a pH of 3 is continued further, the fungus continues to grow as freely dispersed mycelia, which is also why the pH was rated with 100 in the index of control potential at the start-up of cultivation – it is decisive. The control potential declines after germination as the number of conidia present and being able to aggregate decreases, and there might be a lack of suitable aggregation candidates.

Conidia in cultivations started with a pH value of 3 do not aggregate. This means that the conidia concentration after inoculation resembles the later concentration of vegetative biomass particles after outgrowth. Increasing initial conidia concentrations might lead to a higher biomass content.

The initial concentration of conidia only shows control potential when the start pH is 5.5 which is due to the primary aggregation. With germination, the control potential of the conidia concentration diminishes until the end of the secondary aggregation phase. Changing the pH after germination does thus not have any influence on further aggregation behaviour.

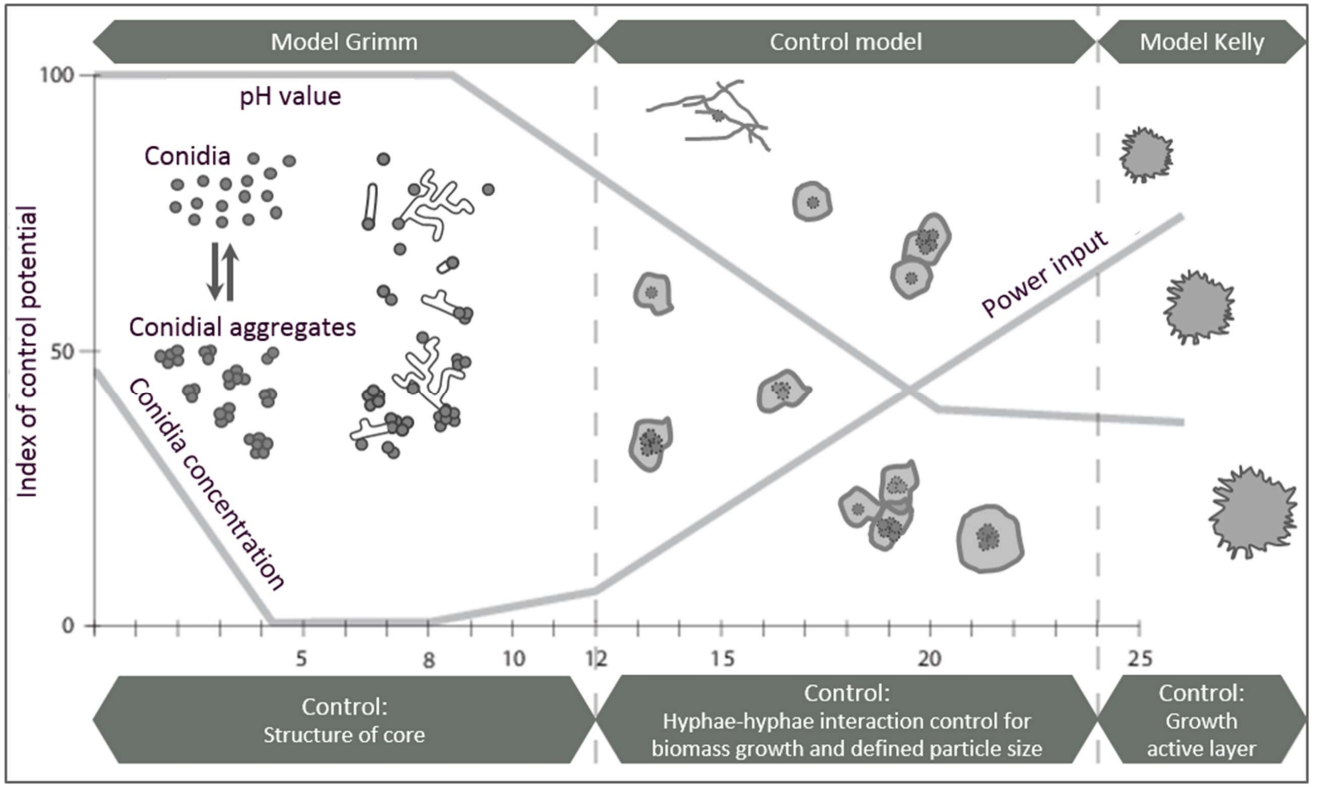

Figure 10: Schematic presentation of the model for controlling A. niger *particle development with process parameters as levers*

Like the initial conidia concentration, the power input is supposed not to be a major factor when the cultivation shows a pH of 3. The effect of power input on the primary aggregation is limited, which is also prevented due to pH. Instead, the power input is an excellent parameter to control the growth of the particles with bigger sizes like after 15 h cultivation.

Based on the description above, it could be stated that it should be possible to control the potential hyphae-hyphae interaction and therefore also the final appearance/shape of the biomass with the parameters initial conidia concentration, volumetric power input and pH value of the media. Except for the initial conidia concentration, the parameters can be changed actively while running the cultivation for forcing freely dispersed growing mycelia into the shape of pellets.

The underlying model approach includes Grimm's description of the two-staged conidia aggregation, Kelly's pellet growth model as well as influences on the potential tertiary aggregation. It is very unlikely that the formation of pellets could be reverted with the presented means. This reflects the definition as aggregates which cannot easily be divided into the primary particles. There also is the probability that the primary particles, conidia, do not exist anymore because of germination which also implies interlocked hyphae. The latter means two things: The pellets are aggregates and there must be a hyphal aggregation interaction.

Chapter 5: Materials & methods

5.1 The strains

Based on the structure of this project, several strains were investigated: *Aspergillus niger* lab strain AB1.13 to develop the control model, a glucoamylase producing production *Aspergillus niger* strain for testing the model in an industrial setup, and a naturally high producer of glucoamylase wildtype *A. niger* strain for concluding on productivity experiments in a setup that yields publishable results:

- *Aspergillus niger* AB1.13 is a protease deficient, uridine auxotrophic and glucoamylase producing strain[23]. It was derived by UV-irradiation from *A. niger* AB4.1[101].
- The glucoamylase producing strain was provided by Novozymes A/S; information on the provided strain is confidential, apart from the fact that the strain has been optimized in the classical sense.
- *Aspergillus niger* BO-1 (DSM 12665) was also provided by Novozymes A/S. The strain is known as a natural high producer of glucoamylase[102,103] and is used for both verification of the previous findings as well as to determine how much the physiology of the fungus contributes to differences in the productivity.

5.2 Media

5.2.1 Solid media (propagation)

All strains were kept as glycerol stabilized cryo-cultures in vials at – 80 °C.

5.2.1.1 Academic media for AB1.13

A defrosted conidia solution aliquot was inoculated on PDA plates containing (in g L^{-1}) potato-dextrose-agar (30.0), agar (10.0) and uridine (1.0). After 5 days of growth at 30 °C, conidia were harvested with 0.9 % NaCl-solution (w/v). The obtained solution was clarified with Miracloth (Merck KGaA; typical pore size about 22–25 µm) and yielded a conidia concentration of about 10^{11} L^{-1} which was verified with a spectrophotometer at 640 nm. The suspension was used to inoculate the medium of the bioreactor obtaining a final spore concentration of 5 10^{8} L^{-1} in the bioreactor.

5.2.1.2 Industrial strain and wildtype BO-1

Spore propagation medium was inspired by the collaboration with Novozymes A/S and work published by Vongsangnak[104]: 218 g L^{-1} sorbitol, 10 g L^{-1} glycerol 99.5 %, 2.02 g L^{-1} KNO_3, 25 g L^{-1} agar, and 50 mL L^{-1} salt solution (26 g L^{-1} KC l, 26 g L^{-1} $MgSO_4 * 7\ H_2O$, 76 g L^{-1} KH_2PO_4 and 50 mL L^{-1} trace element solution (40 mg L^{-1} $Na_2B_4O_7 * 10\ H_2O$, 400 mg L^{-1} $CuSO_4 * 5\ H_2O$, 1.2 g L^{-1} $FeSO_4 * 7\ H_2O$, 700 mg L^{-1} $MnSO_4 * H_2O$, 800 mg L^{-1} $Na_2MoO_4 * 2\ H_2O$, 10 g L^{-1} $ZnSO_4 * 7\ H_2O$)).

The cultures were inoculated with 5 mL of spore solution harvested from mycelium grown on this agar at 30 °C for 12 days. Spores were harvested with Tween 80 0.1%

5.2.2 Liquid media

5.2.2.1 Academic media

The composition of the medium for batch cultivation experiments consisted of (in g L^{-1}) glucose (20.0), uridine (0.24), 50 mL L^{-1} salt solution containing (in g L^{-1}) $(NH_4)_2SO_4$ (33.0), KH_2PO_4 (50.0), $MgSO_4 * 7\ H_2O$ (4.0), $CaCl_2 * 2\ H_2O$ (2.0) and 0.1 mL L^{-1} trace element solution. The trace element solution consisted of (in g L^{-1}) $C_6H_8O_7 * H_2O$ (50.0), $ZnSO_4 * 7\ H_2O$ (50.0), $Fe(NH_4)_2(SO_4)_2 * 6\ H_2O$ (10.0), $CuSO_4$ (1.6), H_3BO_3 (0.5), $Na_2MoO_4 * H_2O$ (0.5) and $MnSO_4 * H_2O$ (0.5). The salt solution and the trace element solution were sterilized separately and added aseptically to the sterilized bioreactor with the remainder of the medium. This medium is based on a modified Vogel's medium as described in Emmler's work[19].

5.2.2.2 Production strain

The employed medium was inspired by production cultivation broth and consisted of: 63 g L^{-1} sucrose, 76.8 g L^{-1} soy grits, 1.1 ml L^{-1} antifoam and tap water adjusted to a total weight of 11 kg before sterilisation.

For a high osmolality trial to test an additional effect on conidial aggregation[80], medium was enriched with 63.6 g L^{-1} sodium chloride dissolved in 2.5 L tap water. The required concentration of sodium chloride was determined from the theoretically calculated osmolality for the soy grits and sucrose added, see Table 1.

Table 1: Overview of the numbers and concentrations used, and calculated for estimating the osmolality and required amount of sodium chloride. Soy bean meal was assumed to have a water content of 8 %[105].

	g/mol	g/kg	g in SBM	Molar	g (DM)	Osmol/kg
Calcium	40.08	2.71	2.30	0.057		
Magnesium	24.31	2.27	1.93	0.079		
Phosphorus	30.97	5.14	4.36	0.141		
Available phosphorus	-	-	-	-		
Potassium	39.10	6.66	5.65	0.145		
Sodium	22.99	0.3	0.25	0.011		
Sodium Chloride	58.44				764	2.18
Soybean meal					848.42	0.04
Sucrose	342.30				756.60	0.18
Total Osmolality						2.40

5.2.2.3 BO-1 media

Two different media were used for cultivation: ½ MU-1 and MLC. The media compositions are as following:

½ MU-1: 130 g L^{-1} Maltodextrin 01, 3 g L^{-1} $MgSO_4$, 6 g L^{-1} KH_2SO_4, 5 g L^{-1} KH_2PO_4, 0.5 ml L^{-1} antifoam, 0.5 ml L^{-1} trace metals described for solid media in section 5.2.1.2 and 20 ml L^{-1} 50 % sterile urea compound. Urea compound is added after autoclavation.

MLC: 40 g L^{-1} glucose, 50 g L^{-1} soy meal, 4 g L^{-1} citric acid, 0.1 ml L^{-1} antifoam.

5.3 Cultivation conditions

5.3.1 Cultivations with *Aspergillus niger* AB1.13

The standard conditions for this strain are pH 5.5, 0.5 VVM, 107.5 W m^{-3} (≙ 300 RPM) and an initial conidia concentration of 5 * 10^6 L^{-1}. The core of the experiments is to shift the pH from 3 (non-aggregating) to 5.5 (aggregating conditions) to provoke a dynamic reaction to conclude on the type of aggregation (conidial, hyphal or a mixed form) and the importance of different factors.

5.3.1.1 pH and pH shifting experiments

Table 2: Overview over pH shifting experiments

Experiment type	**Initial pH**	**Shift after**	**Final pH**	**Duration of shift**
pH 5.5	5.5	–	5.5	–
pH 3.0	3.0	–	3.0	–
pH shift in 0.5 h	3.0	8 h	5.5	0.5 h
pH shift in 1 h	3.0	8 h	5.5	1 h
pH shift in 2 h	3.0	8 h	5.5	2 h
pH shift in 4 h	3.0	8 h	5.5	4 h
pH shift after 6 h	3.0	6 h	5.5	2 h
pH shift after 10 h	3.0	10 h	5.5	2 h
pH shift after 12 h	3.0	12 h	5.5	2 h

The basis of the experiments is at constant pH of 5.5 and 3, respectively, which resembles aggregating and non-aggregating conditions. Shifting the pH happened by manual pH regulation with 2 M NaOH which was added drop-wise to prevent biomass from being damaged. A more diluted caustic soda solution would have influenced the reactor volume too much. Table 2 provides an overview over the conducted experiments and their respective timing.

5.3.1.2 Power input and power input shifting experiments

Much attention was paid to the influence of power input on the cultivations when reviewing literature[6]. With testing the AB1.13 at different power input levels and shifting, like with pH, from non-aggregating to aggregating conditions could aid in designing the proper biomass particle. Table 3 provides an overview over the conducted experiments and their respective timing.

Table 3: Overview over power input experiments

Experiment type	**Initial W m^{-3}**	**Shift after**	**Final W m^{-3}**
300 RPM	107.5	–	107.5
150 RPM	25	–	25
shift after 8 h	107.5	8 h	25
shift after 12 h	107.5	12 h	25
400 RPM	212	–	212
500 RPM	430	–	430

5.3.1.3 Initial conidia concentration

It is described that the initial particle/conidia concentration influences the aggregation[26]. Hence the extent of influence of conidia concentrations must be tested in terms of usage as levers for altering the resulting morphology. Apart from the standard conidia concentration of $5 * 10^6$ L^{-1}, concentrations of $2.5 * 10^6$ L^{-1}, $4 * 10^7$ L^{-1} and $5 * 10^7$ L^{-1} are tested.

5.3.1.4 Bioreactor system

The employed bioreactor is an Applikon glass reactor with 2 L working volume. As depicted in Figure 11, the reactor featured agitation with Rushton impellers on two levels with one extra impeller as foam crusher. The standard setting is 300 RPM which resembles 107.5 W m^{-3}.

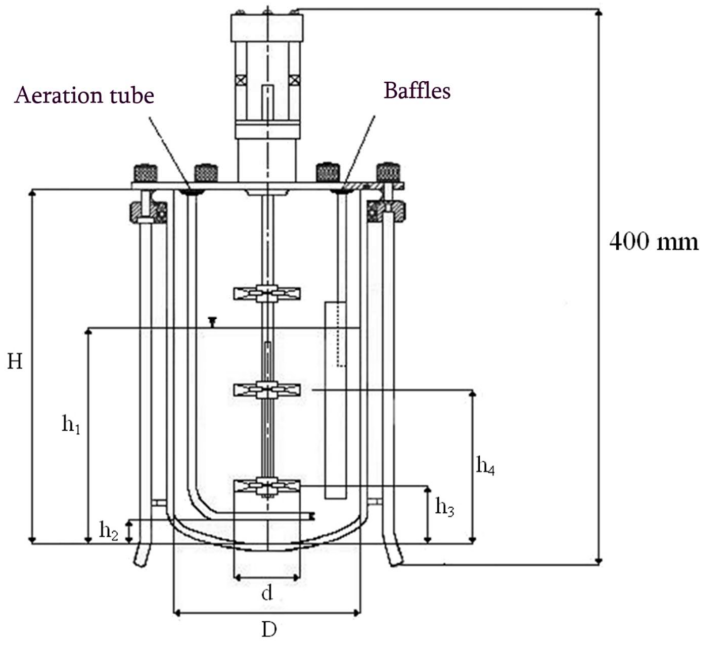

Figure 11: Schematic drawing of the employed bioreactor system; more features than aeration and baffles are installed and are illustrated in the following Figure 12

For improved mixing, 3 baffles are installed and the reactor can be aerated. Air flow rate was controlled with a Vögtlin gas flow meter while off-gas analysis is conducted with a BC preferm system (Bluesens). Additional features are depicted in the schematic drawing of the on-top view of the reactor lid in Figure 12. Per standard, temperature and pH are measured and controlled.

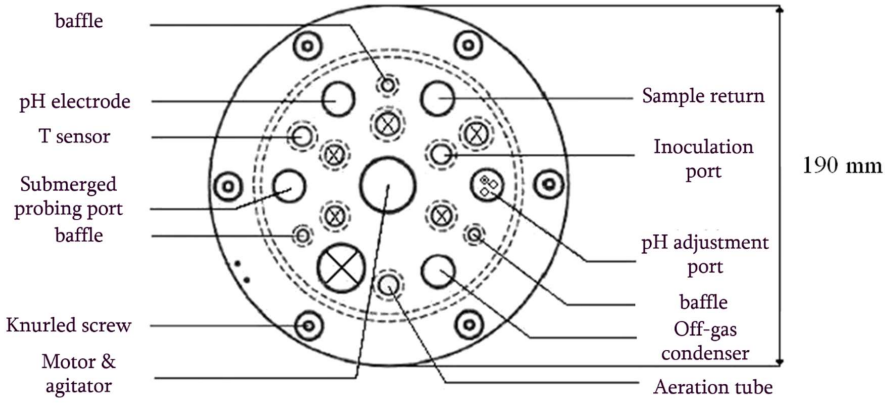

Figure 12: Lid of the employed bioreactor system; all installed features are illustrated

Uncommon features are the submerged sample port and the sample return for the in-line particle size analysis which is explained in the subchapter further down in this section on page 51. The technical details of the reactor are summarized in Table 4.

Table 4: Technical details of the bioreactor system

Reactor part	**Description**	**Symbol**	**Value**	**Unit**
Reactor Vessel	Total volume	V_G	3	[L]
	Total height	H	250	[mm]
	Working volume	V_A	2	[L]
	Filling height	h_l	170	[mm]
	Inner diameter	D	130	[mm]
	Ratio H/D	H_l/D	1.3	
Aeration system	Installation height	h_2	35	[mm]
	Number of holes	-	7	

Reactor part	Description	Symbol	Value	Unit
Rushton	Number of discs	-	2 (3)	
	Diameter	D	45	[mm]
	Height impeller 1	h_3	50	[mm]
	Height impeller 2	h_4	12	[mm]
	Blades per disc	-	6	
Baffles	Number	-	3	
	Width	d_B	14	[mm]
	Distance to wall	d_A	10	[mm]

In-line laser diffraction analyser

*Figure 13: Bioreactor system with in-line laser diffraction analysis; **A** Malvern MasterSizer 2000, **B** bypass, **C** peristaltic pump for bypass, **D** 3 L bioreactor, **E** off-gas analysis, **F** pH regulator, **G** temperature regulator, **H** stirrer regulator, **I** rotameter for air flow control, **J** thermal mass flow meter for air flow check-up, **K** dosing pumps for pH adjustment*

The outstanding feature for the cultivations with *A. niger* AB1.13 is the bypass from the 3 L Applikon reactor to the laser diffraction analyser Malvern MasterSizer 2000. The effect of the tube pump was verified with manual image analysis control and deemed negligible for the employed pump rate of 0.28 L min^{-1}. The setup is displayed in detail in Figure 13.

5.3.2 Conditions for the industrial strain

The standard conditions for this strain in 20 L reactors is pH 5.5, 0.6 VVM (higher air flow needed due to gas analysis minimum flow), 600 RPM and initial conidia concentrations in the order of 10^4 L^{-1}. These experiments are carried out to validate or falsify the derived AB1.13 model. Factors which are part of the model are variations in pH, initial conidia concentration, power input and salt content (see section 5.2.1.1 for media composition, Table 1).

The following pH set-points without shifting pH are used: pH 3, 4, 5, 5.5, 6 and 7. The standard initial conidia concentration is 7 * 10^2 L^{-1} and high concentration inoculums of 2* 10^3 and 1 * 10^5 conidia L^{-1} are tested for confirming the findings of Grimm[26] and the potential role for the morphology control model. The last parameter, salt concentration and molality, is introduced to extend the underlying model. Wucherpfenning did some work in 2011 describing the morphology engineering this way[80] which should be replicated with the industrial strain to investigate the practical usefulness.

5.3.2.1 A. niger *industrial strain trials*

The work with the lab strain *Aspergillus niger* AB1.13 resulted in ideas of how to control the morphology of *A. niger* in industrial cultivations. With this work, these ideas could directly be applied to a process like a production process with an actual industrial strain. Novozymes A/S provided both the setup, the lab equipment and the strain for this rare occasion of hypothesis testing and direct comparison of strains.

The concrete task is the evaluation of the main findings from the academic AB1.13 strain about the influence of pH on the macro morphology. Different pH levels which remain constant for the

duration of the fermentation should be screened to find out if either mycelial growth, ideally at pH 3, or pelleted growth, ideally at 5.5, is promoted. Besides these two pH values, pH 4, 5 and 6 were tested as well to investigate possible deviations with the industrial strain from the earlier academic findings.

5.3.3 *Aspergillus niger* BO-1 conditions for provoking different morphologies

The reasoning for performing additional experiments with the wild type was to find the cause for the outcome of the experiments with the industrial strain. The soy included in the MLC resulted for the most part in mixed morphology and was hence not further in the focus of the experimental work to be conducted. Table 5 gives the overview about the basic settings which were also chosen for MLC cultivations. Apart from that, a VVM of 1 was employed in the reactors.

Table 5: Growth conditions for BO-1 to create distinct pelletised growth or distinct dispersed growth.

	Basis pelletised growth conditions	Basis dispersed growth conditions
Medium	½ MU-1	½ MU-1
Temperature	30°C	30°C
Inculcation conc.	$5 \cdot 10^7$ conidia l^{-1}	$5 \cdot 10^7$ conidia l^{-1}
pH	3.5	4.2
Agitation (reactor)	150 RPM	600 RPM

5.4 Analytics

5.4.1 Laser diffraction

Most of the particle size analysis was done using the Malvern Mastersizer software 5.40. For the Fraunhofer approximation for size distribution calculation (see section 3.3), the optical properties of water are selected and the particles are considered to be spherical, non-reflective

and non-transparent. The approximation model was set to general purpose following the manufacturer's guideline for "samples from nature"[90]. This model reflects that the spherical particles are not smooth.

Table 6: properties of laser diffraction analysis

Refractive index biomass n(BM)	0
Absorption coefficient biomass α(BM)	0
Refractive index medium n(H_2O)	1.33
Density medium ρ(H_2O)	1 kg L^{-1}
Interval between measurements	285 s
Duration of one measurement	15 s
Snaps per measurement	150000
Total number of measurements per cultivation	≥ 380

5.4.1.1 MasterSizer 3000 measurements for BO-1 indications

The BO-1 cultivations were monitored off-line by quantifying the particle size distribution with the newer (compared to the Malvern MasterSizer 2000 which was used for the AB1.13 strain) Malvern MasterSizer 3000. Unlike the previous description of the on-line Mastersizer, it was connected to a manual wet dispersion unit (Hydro SM) which was flushed with demineralised water between the measurements. Water, added to the dispenser before the sample, was kept in a container over night to reduce the presence of air bubbles. The sample was added directly to the water in the dispenser until a certain obscuration was reached.

For samples with dispersed mycelia and mixed morphology the obscuration was 15-20 % and for distinct pelletised growth it was 19-24%. Stirring speed in the dispersion unit was 1400-1500 RPM. Samples were measured three times with a duration of 10 seconds for each measurement. All data used from the particle size distribution is in the form of an average of two or more measurements.

The MasterSizer 3000 software provided the result of a particle size distribution as the percentage of particles divided in 101 size classes ranging from 0.01 µm to 3300 µm. The sizes represented the different particle lengths/diameters detected by the analyser. The percentage values corresponding to the 101 size classes can be analysed with different methods. The data analysis reported here was based on graphical representation of the data in plots, and then as Dv(10), Dv(50) and Dv(90) values. Dv(90) is the 90 % percentile, meaning that 90 % of the particles in the sample are equal to this size or smaller, and Dv(10) and Dv(50) then correspond to the 10 % percentile and the median (50 % of the particles equal to this size or smaller) of the sample [106].

5.4.2 Measurement of ζ-potential

AB1.13 Conidia were harvested as described in section 5.2.1 , and then rigorously dispersed before filling them in a cuvette together with liquid cultivation media (section 5.2.2.1) at pH 2.3 for measurement in a Malvern zeta-sizer nano. The ζ-potential measurement is micro-electrophoretic, and the pH was continuously titrated towards pH 6.2 with 0.1 M NaOH. The series of measurements consisted of five runs. Already at this point it should be emphasized that the measurement of the ζ-potential is heavily dependent on the presence of salts and especially biomass. The latter has not been quantified in the samples, and therefore it cannot be taken into account, which means that the results should be interpreted with great care and with a critical attitude towards the final results[107].

5.4.3 Statistical Analysis

The statistical analysis of the achieved data and the derivation of the control model in terms of biomass and particle size growth were done using the software SAS jmp. The data basis here consisted of data from all *A. niger* AB1.13 cultivations. The factors looked at are power input, initial conidia concentration, pH value as well as time point and duration of the pH shift from non-aggregating to aggregating conditions. A regression analysis via least square methods was performed on the data cloud.

5.4.4 Bio dry matter (BDM)

Bio Dry Matter (BDM) was analysed with two different approaches explained in the following. All BO-1 cultivations were analysed following centrifugation except for the experiments with addition of cellulose. It was decided to shift to the filtration approach for the latter set of cultivations based on the higher precision that was needed for the specific calculation of biomass to activity ratio.

5.4.4.1 BDM by centrifugation

BDM was analysed by determining the weight of empty glass tubes, adding a certain weight of sample and then centrifuging the glass tube containing the sample at 3000 RPM for 10 minutes. The supernatant was discarded, followed by 2 washing steps with demineralised water and centrifugation while applying the same centrifuge settings. The tubes with washed samples were dried at 110°C overnight and weighed afterwards. BDM was calculated by means of the following equation:

Equation 9: Calculation of bio dry matter using centrifugation

$$bio\ dry\ matter\ \left[\frac{g}{kg}\right] = \frac{(weight\ after - weight\ before) \cdot 1000}{weight\ sample}$$

5.4.4.2 BDM by filtration

BDM was analysed by determining the weight of filters dried for 20 minutes at 110°C. A 5 ml sample was filtered and washed thoroughly with demineralised water. Filters were dried at 110 °C overnight and weighed afterwards. In a situation where the filter was used to determine BDM in a preculture to ensure inoculation of equal amounts of biomass (for parallel cultivations in the cellulose experiments), the filters were dried in the microwave oven for 15 minutes.

BDM was calculated by means of the following equation:

Equation 10: Calculation of bio dry matter using filtration

$$bio\ dry\ matter\ \left[\frac{g}{l}\right] = \frac{(weight\ after - weight\ before) \cdot 1000}{ml\ sample}$$

5.4.5 BO-1 morphology scale

A scale from 1-6 has been employed to evaluate the observed morphology during experiments. Later discussion will refer to this scale to provide a quick overview over the achieved morphology in a simplified way. It also makes it possible to plot morphology in graphs along with other data like BDM and enzyme activity.

The morphology scale is presented in Figure 14 with illustrations of the morphology corresponding to three different points on the scale. Point 1 on the scale indicates distinct dispersed growth and point 6 distinct pelletised growth.

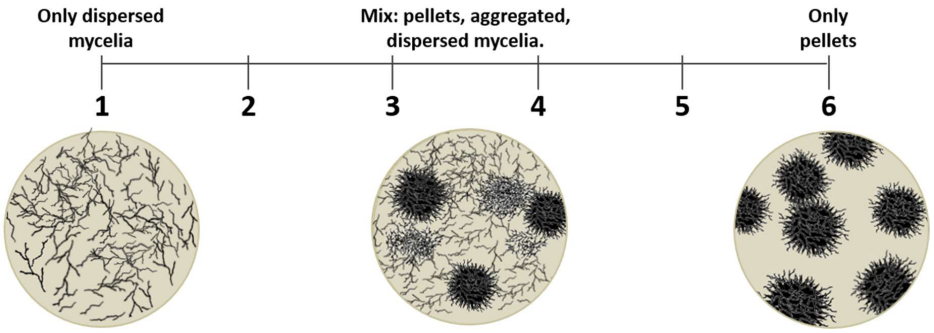

Figure 14: Morphology scale used to simplify the explanation of morphology throughout the report. Three illustrations are indicating approximately how morphology would look like in a microscope for three points on the scale. At point 1 morphology consists of entirely dispersed mycelia, point 3 – 4 is a situation with half mycelia, half pellets or aggregates of various size and shapes. At point 3, the morphology is dominated by dispersed growth, at point 4 it is dominated by pelletized growth. At point 6 the morphology is distinct pelletized.

5.4.6 BO-1 enzyme assay

Enzyme activity was determined by use of 4-Nitrophenyl α-D-Glycopyranoside (PNPG) (Sigma-Aldrich N1377). Under reaction with AMG, 4-nitrophenol will be released from PNPG which appears yellow under alkaline conditions. By spectrophotometric analysis the intensity of the yellow can be measured which indicates how much 4-nitrophenol has been released, i.e. a measure of enzyme activity.

For determination of AMG activity, samples were centrifuged at 3000 RPM for 10 minutes and the supernatant was stored at -20 °C for 1-3 weeks until enzyme assays were performed. The standard used for activity analysis was prepared from a cultivation with the known activity of 307 AGU g L^{-1}. For each series of measurements, 10 µl of standard and the respective samples were each mixed with 100 µl PNPG and incubated for 30 minutes at room temperature. The reaction was quenched by addition of 50 µl stop reagent (0.5 M Na_2CO_3). The absorbance was measured at 405 nm and the AMG activity was calculated based on comparison of the standard to the calibration curve which was created with the standard concentration series.

5.4.7 BO-1 pellet concentration

The pellet concentration could be determined in cultivations with ½ MU-1 medium with distinct pelletised growth. 1 ml of sample was dispersed on a Petri dish from which pellets were counted, without magnification. Pellets were counted for 6 ml of each sample.

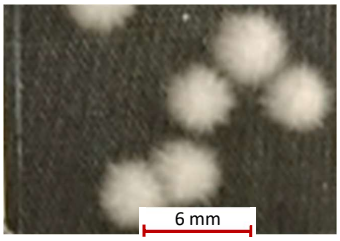

Figure 15: Picture taken from a Petri dish during pellet count after 60 hours of cultivation, for the determination of the pellet concentration

Chapter 6: Results & discussion

6.1 *Aspergillus niger* AB1.13 as model strain for control of morphology

6.1.1 Development of AB1.13 biomass under different experimental conditions

6.1.1.1 pH value and shifting pH from non-aggregating to aggregating conditions

To exclude a variation of the bio dry matter concentration (BDM) based on a deviation of the actual initial conidia compared to the target concentration, Equation 11 is used to determine the corrected biomass concentration. The correction factor is based on the ratio between the target and the actual concentration of conidia. All AB1.13 bio dry matter concentration values reported below in the figures are corrected in this way.

Equation 11: correction factor for bio dry matter concentration

$$c_{X,corrected} = c_X \frac{c(conidia)_{target}}{c(conidia)_{actual}}$$

For providing a better overview, the pH-shift experiments are divided into groups: Different shift speeds (0.5 h, 1 h, 2 h & 4 h) and different time points (6 h, 8 h, 10 h & 12 h). Table 2 (section 5.3.1.1), summarizes the grouping. Both groups refer to the same references at a constant pH of 3 (non-aggregating conditions) and 5.5 (aggregating conditions).

First, the influence of the shift speed should be determined. The pH was shifted with caustic soda from the non-aggregating conditions, pH 3, to aggregating conditions, pH 5.5, at different speeds/durations of the shifts. Shifting too fast could potentially harm the initial biological development while shifting slowly, i.e. a gradual shift over a longer period of time, might overlap with the above described growth and aggregation phases.

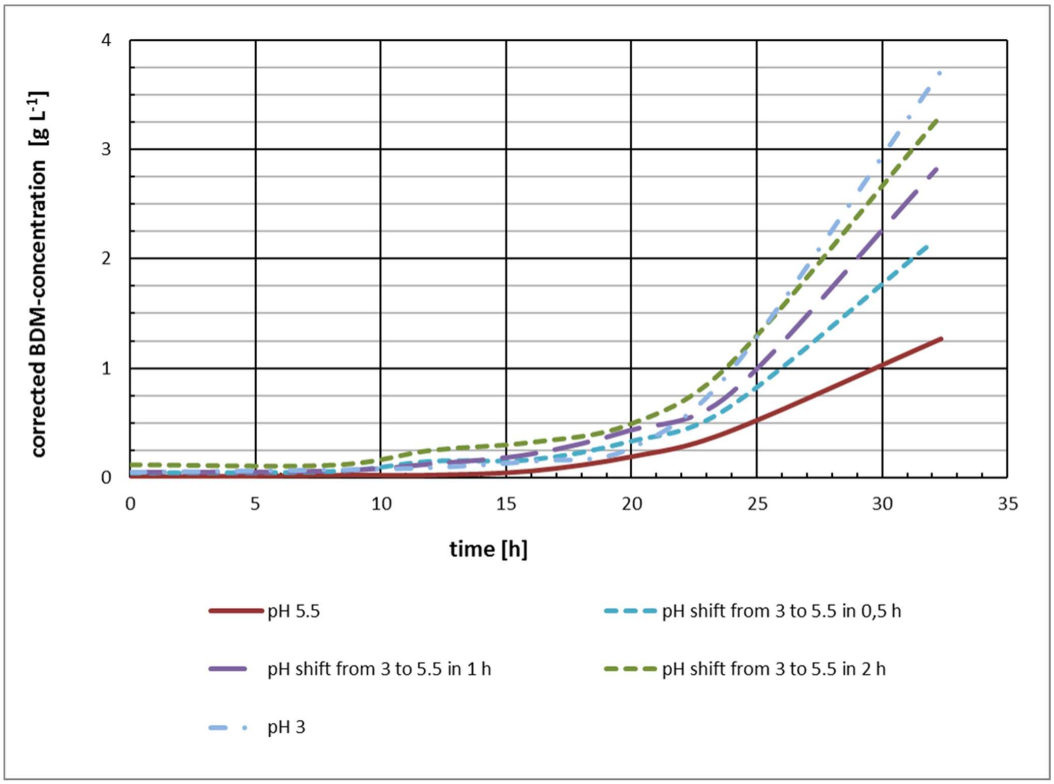

Figure 16: The bio dry matter is drawn as a function of the cultivation time for the different durations of the shift from non-aggregating pH 3 to aggregating pH 5.5 conditions. For better comparison, the corrected biomass (see Equation 11) was plotted.

Figure 16 displays the achieved bio dry matter concentrations for the shift-duration experiments. Low initial values of BDM are expected during the lag-phase. After 6-8 h of growth, differences in BDM due to the applied pH conditions become visible: The basic aggregating conditions with a constant pH of 5.5 show the lowest BDM values during the whole course of the cultivation and result in slightly more than 1 g L^{-1} of BDM after 32 h of cultivation. Consequently, the slope is lowest and the derived maximum growth rate is only about $\mu_{max} = 0.15\ h^{-1}$.

Cultivations with a starting pH of 3 showed higher BDM concentrations throughout the cultivation and especially at the final measurement after 32 h. The results in Figure 16 can be

summarized as follows: the slower the shift from pH 3 to 5.5 is executed, the less severe are its effects on the growing biomass. The shift with 2 h duration reaches almost the same maximal growth speed of μ_{max} ~0.20 compared to 0.22 h^{-1} and almost the same BDM, 3.25 compared 3.75 g L^{-1}) as the top-performing cultivation at constant pH 3.

It must be emphasized that the pH shift from 3 to 5.5 is executed starting at 8 h cultivation time while the real consequences take effect 24 h later at the end of the cultivation. Therefore, the time lag between the environment change and the appearance of the consequences should be incorporated into the model for controlling growth (see section 4.3).

It confirms that the biomass adapts to the altered cultivation conditions. Changing pH influences the surface charge of the cytoplasm membrane, which in consequence could alter transport processes through the membrane like for example the proton dependent trans-membrane synport process of importing glucose[108]. The slower the conditions are changed, the more time is available to the organism to adapt to the changes.

Figure 17 is built the same way as Figure 16 and represents the respective bio dry matter concentrations for cultivations with pH shifted at different cultivation time points. Like before, cultivations at constant pH 5.5 performed worst in terms of BDM development. The question is if this inferior behavior is due to the fermentation parameters or the pelleted growth from swelling of the conidia.

The second lowest BDM values were observed for the fermentation with the earliest shift of pH from 3 to 5.5 after 6 h which relates to the question posed in the previous paragraph. At 6 h, the conidia already are swollen but have not developed germ tubes. This links to the primary aggregation described by Grimm. The achieved BDM is though doubled up compared to cultivations at constant pH of 5.5.

The BDM developments of cultivations with pH shift after 12 h and after 6 h result in the third lowest final BDM concentration. Consequently, this means that point in time of the pH shift and its consequences on bio dry matter development (and particle size) follow a maximum/optimum curve. After the shifting pH at 12 h, the BDM development is characterized by a lower μ which

could represent a re-adaptation of the biomass to the new environment that happened at a moment when the growth speed was accelerating to reach μ_{max}.

The pH shift after 8 h resulted in BDM of 3.25 g L^{-1} which means 2.7-fold increase in biomass compared to cultivations with constant pH 5.5. Only cultivations with a constant pH of 3 and a shift after 10 h yielded a higher BDM value.

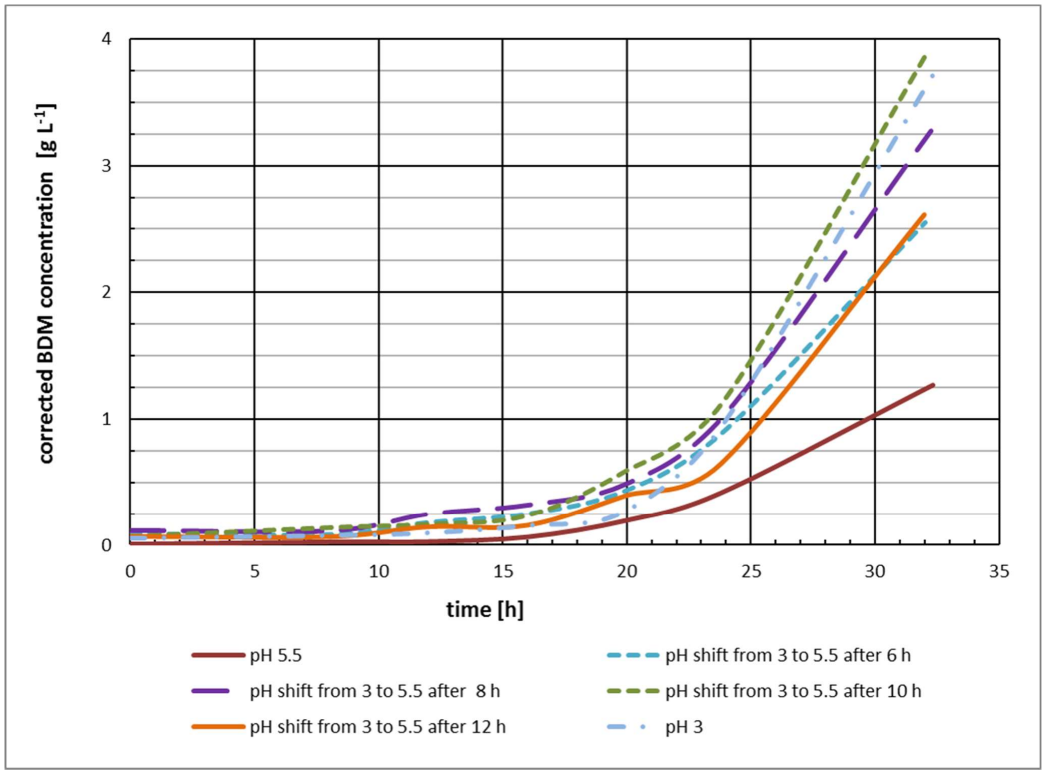

Figure 17: The bio dry matter is drawn as a function of the cultivation time for the different time points of the shift from non-aggregating pH 3 conditions to aggregating pH 5.5 conditions. For easier comparison, the corrected biomass concentration values (see Equation 11) were plotted.

In summary, it could be stated: Obviously, high BDM is achieved with higher μ_{max}. There is a time point around 12 h though which is prone to interruptions of growth. For the control model, this

could be used as a lever to control/limit the biomass concentration and thus the formation of particles/pellets with too large diameter.

6.1.1.2 Power input with shift towards aggregation promoting conditions

Figure 18 displays the biomass concentration development when shifting the cultivation conditions to more aggregating conditions in terms of mechanical power input by stirring analogous to the previously discussed pH experiments.

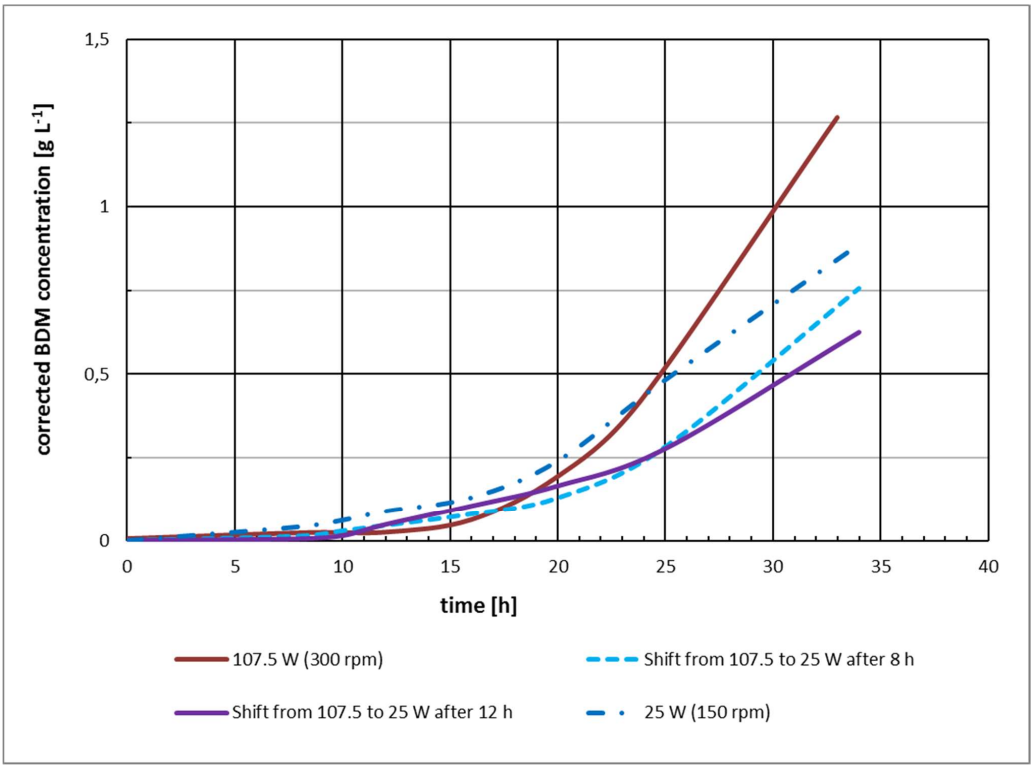

Figure 18: The bio dry matter concentration is plotted as a function of the cultivation time for the different time points of the shift from less aggregating 107.5 W m^{-3} condition to aggregating 25 W m^{-3} conditions. For better comparison, the corrected biomass concentration values (see Equation 11) were plotted. Because of the lower BDM values, the Y-scale differs from the previous two plots.

The standard power input is 107.5 W m^{-3} at 300 RPM (which also is used for the experiments with the pH shifts). This was reduced to 25 W m^{-3} (150 RPM) after 8 and 12 h, respectively to create more aggregating conditions. With BDM concentrations below 1 g L^{-1} after 32 h, the most important result is that inferior oxygen transfer or other bulk transfer rates hamper the biomass development and should not be employed as a handle to limit biomass growth at any point of the cultivation.

6.1.1.3 Power input and initial spore concentration

During the development of the control model for biomass and particle size, power input was investigated and considered to be a potential factor influencing the formation of a specific biomass morphology. A power input of 212 W m^{-3} (400 RPM) and 430 W m^{-3} (500 RPM) was tested, apart from the standard value of 107.5 W m^{-3} (300 RPM).

Similarly, initial conidia concentrations were tested: Apart from the standard of 2.5 * 10^6 L^{-1}, concentrations of 4 * 10^7 L^{-1} and 5 * 10^7 L^{-1} were tested.

All experiments deviating from standard conditions described in section 5.3.1 resulted in BDM concentrations below 1 g L^{-1} and are thus considered out of the question for potential industrial use[102].

The superior mass transfer with higher power input apparently is balanced by more damage to the biomass than what was expected based on Kelly's descriptions[27]. It could be that the power input has a higher damaging potential on growing biomass (used here) than on mature pellets that were used in the studies of Kelly. Similarly, Grimm described that there might be growth inhibition for high inoculum concentrations[25] which can be confirmed here, and more conidia do not necessarily result in a higher biomass concentration.

That also means that these two factors, power input and initial conidia concentration, are not of interest as single control parameters for the model. Still, these handles could be employed to balance the major levers.

6.1.2 Metabolic activity in dependency of environmental conditions

One of the main points of the pH-shift experiments was that the biomass thrived better when *A. niger* AB1.13 experienced lower pH conditions. It was thus investigated via HPLC analysis how the carbon conversion was affected by the environmental conditions.

Figure 19 displays the result of the HPLC and off-gas analysis from the pH-shift point in time experiments. Clearly, the supplied C-source has not been used up: The cultivations at a pH of 5.5 converted most of the provided carbon into gluconic acid (17 % glucose, 57 % gluconic acid). Gluconic acid also is bio-available and is known as early by-product in citric acid production[109]. The glucose to gluconic acid conversion does not involve a consumption of available carbon.

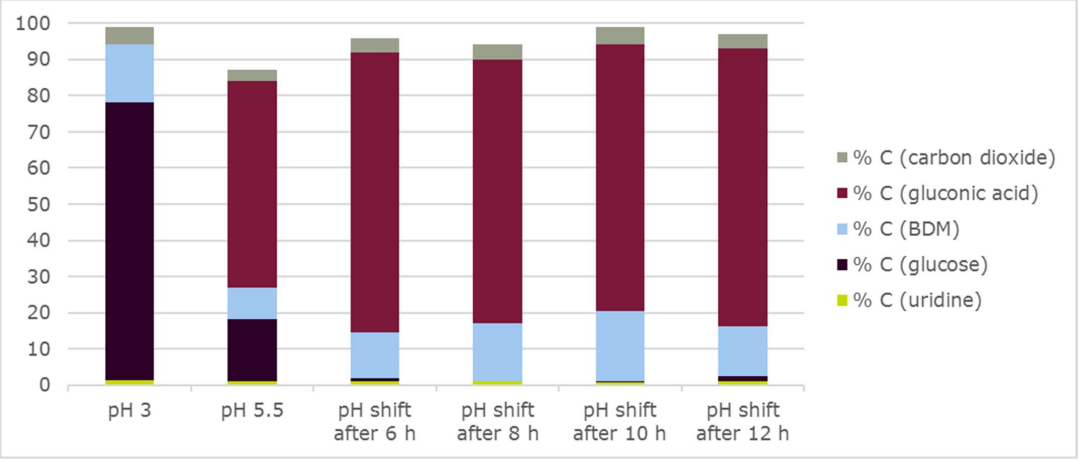

Figure 19: C-balance after 32 hours of cultivation; show case from the pH shift point in time experiments; the pH shift is from non-aggregating conditions of pH 3 to aggregating conditions of pH 5.5

Cultivations with a pH change from 3 to 5.5 converted almost all available carbon into gluconic acid (just around 1 % of the glucose left). With the enzyme glucose oxidase being inactive below pH 3.5[5], it is expected that no gluconic acid is formed and 77 % of the supplied glucose remained in the media. This also means that the average yield in biomass just reached $Y_{X/S} = 0.12\ g_{BDM}\ g_{substrate}^{-1}$ which is considered to be very low[110].

In combination with a low BDM concentration of less than 1 g L^{-1}, a yield $Y_{X/S}$ below 0.15 $g_{BDM}\ g_{substrate}^{-1}$ usually points towards an atypical biomass development as higher values are expected based on literature reports[6,111–113]. A major influencing factor for development of biomass concentration could be the peristaltic pump for the laser diffraction by-pass. With microscopic control, no deviating morphology was detected.

Also, the experiments with lower mechanical impact (lower power input) did not show an enhanced growth which would have been expected if shear was the major factor. In fact, it is reported that higher power input rates would not damage the cells, but instead aid growth because of the higher oxygen transfer rate that could be achieved[31,114].

Because of *A. niger*'s preference for low pH values[108], it is not unexpected that a triple BDM concentration is reached at pH 3 compared to 5.5. Changing the pH from 3 to 5.5 during the cultivation has, as expected, a negative effect on the biomass formation. Part of this could be the high concentration of gluconic acid as a marker for stress. The conversion usually takes place with (too) high glucose concentrations, at glucose oxidases pH optimum of 5.5 and high levels of dissolved oxygen[109]. All three factors are present and point out that the cultivation medium might be better suited for organic acid than for protein production. Energy consumption by the conversion is supposed to be too low to hamper growth processes.

In general, gluconic acid is a weak acid with a pK_a of 3.86 which reportedly is produced by *A. niger* to counter "high" pH environments[115]. The conversion of glucose is conducted by the exo-enzyme glucose oxidase which usually is either secreted into the media or acts as cell wall associated enzyme[116]. The regeneration of the enzyme after the reaction requires oxygen and results in formation of hydrogen peroxide. The latter is toxic to the fungus and induces the production of a catalase[117]. This reaction (mechanism) is also exploited for production of glucose oxidase and gluconic acid with the *Aspergillus* genus[118].

The efforts of the cells to reduce the pH cause a lower yield in both biomass as well as potential product. Other side products with the same effect are polyols which usually are formed by *A. niger* to regenerate the co-factor NAD(P)H when a lack of oxygen is encountered[119]. Since no

polyols were detected by HPLC, it can be concluded that no oxygen limitation is present which includes the core of the pellets. This was also expected as the pellet size remained below 1.2 mm[66,67,120,121] and the low BDM.

With 75 % of the initial carbon source left in the medium after 32 h and being able to exclude mechanical factors as well as oxygen limitations leads to the assumption that growth could be limited by the lack of an essential ingredient in the minimal medium[122]. HPLC analysis confirmed that the limiting factor is not uridine as it wasn't depleted at the end of the cultivations.

A potential cause for low bio dry matter concentrations could originate from the genealogy of the strain: It was derived by random chemical and UV mutagenesis (see section 5.1). As a consequence, the metabolism could be disturbed by deficits in regulatory functions[123]. This kind of effect can also be observed with undirected integration of heterologous genes into the genome of microorganisms in general[124].

6.1.3 Particle size analysis

Particle size distributions were analyzed with the laser diffraction analyzer Malvern MasterSizer 2000. The native output of the device is the disperse function of $Q_2(x)$ (see section 3.1) based on the Fraunhofer approximation of the cross-sectional area. This sum function is converted into the density function with the assumption of equivalently sized spherical particles.

The particle volume density distributions of the fermenter content are recorded every 5 minutes. They can be stacked behind each other using time as the Z-axis to create a 3-dimensional graph like Figure 20.

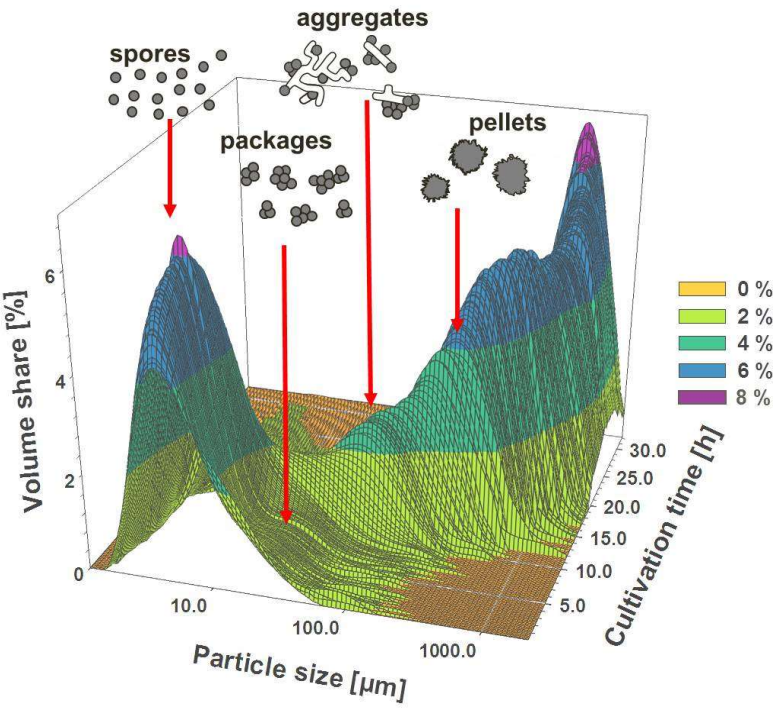

Figure 20: Display of relative particle volume distribution in percent (Y-Axis) over size range in µm (X-Axis) and the cultivation time in hours (Z-Axis); Aspergillus conidia and conidial aggregates with which the cultivation was inoculated can be seen in the size band around 2.5 µm throughout the cultivation. This cultivation experienced a shift in pH after 6 h.

At the onset of the cultivation, only the seeding material consisting of conidia/spores is detected at sizes about 2-5 µm at 0 h. A large fraction appeared to be aggregated at sizes around 50 µm – this can be considered an artefact of the volumetric evaluation: The diameter is incorporated to the power of three and few big particles can skew the distribution.

The three-dimensional presentation of the data in Figure 20 can be confusing at first. Guidance to read it starts with the volume share of the conidia increased directly after inoculation which could resemble the aggregation process described by Grimm[25]. In this case, the initial pH is 3 and therefore represents non-aggregating conditions. The equilibrium of aggregation and

decomposition is tilted towards the latter. The average size converges towards 6 µm with most conidia/particles not being aggregated.

The “shoulder” in the size range of around 20 µm could be identified by microscopic analysis as mostly conidial aggregates and some agar fragments and conidiophores from the solid propagation that slipped through the Miracloth filtration (average pore size of 22–25 µm). This reflects the necessity of the filtration step to avoid skewing the particle size density distribution with unwanted particles.

Until around 5 hours of cultivation, the distribution has been mono-modal and now develops into a bi-modal distribution. The “shoulder” of conidial aggregates at 20 µm develops into a second maximum. At the same time, the contribution of the conidia to the distribution decreased constantly.

The depicted cultivation in Figure 20 started with non-aggregating conditions at pH 3 and was shifted towards aggregating conditions to pH 5.5 after 6 h of cultivation. While conidia aggregation is mostly avoided, the secondary aggregation described by Grimm could take place to full extent.

Formation of hyphae is the basis for the secondary aggregation as additional surfaces are provided for conidial attachment. In consequence, the number of conidia is reduced leading to a lower conidial volume share and increased volume share of aggregates. The increase in particle size and volume share is though mostly based on the growth of biomass.

The secondary aggregation terminates after around 13 h of cultivation, which resembles particle sizes around 100 µm. This pre-Kelly growth theoretically follows the same principles as the later pelleted growth[29].

It is important to emphasize that volume based distributions are discussed. Higher volume shares could be based on few bigger particles. The volume based density distribution $q_3(x)$ was chosen because it enables both many small particles and fewer bigger particles being displayed satisfactorily in one graph.

The most important finding from the three-dimensional particle size distribution in Figure 20 is that the *Aspergillus* growth process does not follow a mono-modal distribution! Further analysis and characterization of growth and aggregation processes are therefore based on the mode $d_{max,3}$ with which the distribution could be divided into conidia/aggregates and (pre-mature) pellets.

The border between the modes is set at a size of 45 µm based on microscopic analysis, which confirmed that larger particles were more pellet type than conidial aggregates. These could be understood as pellet precursors with the potential to become a mature pellet in the sense of Kelly's model.

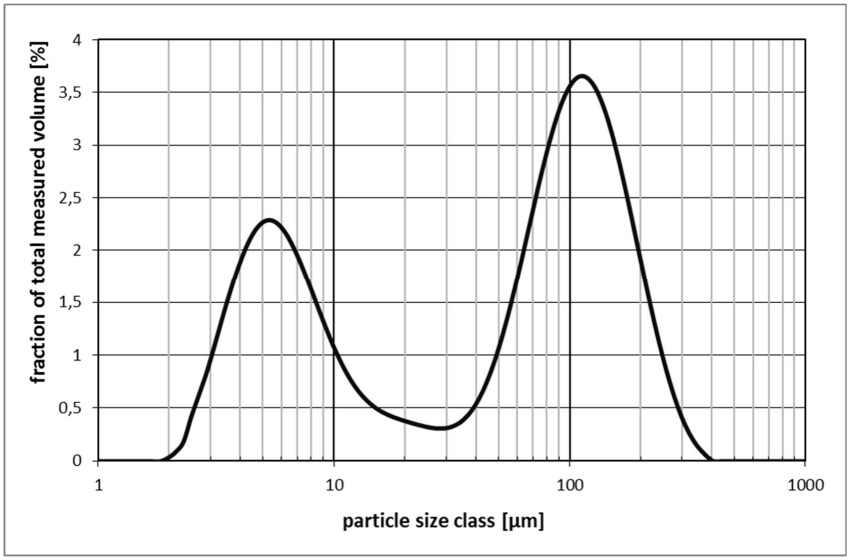

Figure 21: The particle size distribution (Figure 20) is split into two peaks: The first peak consists of conidia and conidial packages up to a size of 50 µm and the second is representative for the growing hyphae (above 50 µm). The maximum volume share of each peak is determined for each point in time.

Figure 21 is a snapshot from the particle volume density distribution (Figure 20) after 8 h. Approximately 2.4 % of the total measured volume is occupied by the spherical equivalent diameter of 5.5 µm – conidia. It resembles the highest value inside this conidial fraction and is hence the conidia mode $d_{max,3,conidia}$. The pellet fraction is treated the same way: About 3.6 % of

the total measured volume is within the size class of 100 µm (in spherical equivalence diameter). This is the pellet mode $d_{max,3,pellet}$.

The mode of the respective particle fraction, conidia or pellet, with the higher volume share will further on be called the leading particle class. In this specific case, the leading particle class is the pellet fraction and the size will be stated at 100 µm. The other fraction is still present and will also be displayed in later graphics.

Analyzing the results into more detail, and focusing only on the mode of conidia fraction, results in Figure 22. That figure displays the size trend of conidia for cultivations at pH 3 and 5.5, respectively. The initial particle size of conidia inoculated into pH 5.5 is with 3.8 µm 8 % smaller than the conidia at pH 3 with 4.1 µm. In the following, the conidia at both pH values swell and the average size of the conidia increases until 10 and 12 h, respectively. This resembles the swelling of conidia by taking up water for initiating growth processes. Formation of germ tubes moves the particle size even more.

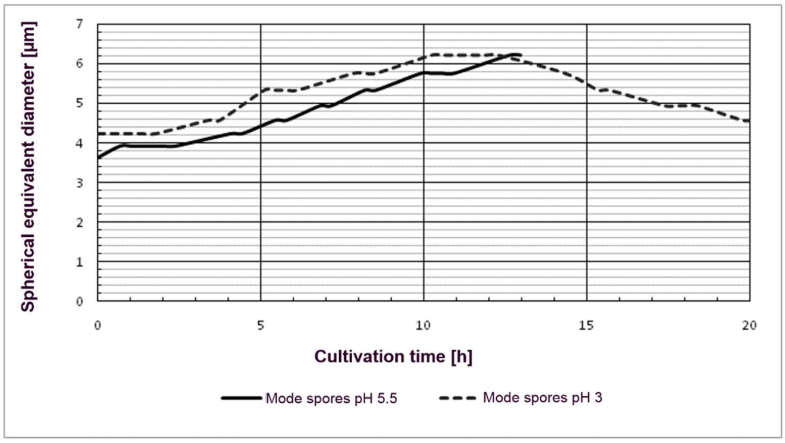

Figure 22: Detail of the conidia mode – following the swelling and outgrowth over time. A starting pH of 3 resulted in slightly larger values for the spherical equivalence diameter for spores which also could be tracked for almost the whole fermentation. A starting pH of 5.5 showed "smaller" spores which seem to disappear after 14 h.

The conidia at pH 5.5 remain smaller throughout the measurement period. A possible explanation could be desorption of melanin, proteins or other cell wall associated (macro-)

molecules which involves a change of surface charge[125]. This finding also leads to considerations and discussion in the following section 6.1.4 "ζ-potential & conidia surface structure".

The stagnating and after 13 h declining size of the pH conidia is an effect caused by the relative distribution. Most conidia swell, germinate and grow into bigger particle classes, and "leave" therefore the conidia mode and become part of the aggregate mode. The remaining spores do not grow or even swell and are supposedly dormant/inactive.

No more conidia could be detected at pH 5.5 after 13 h. In combination with the lower achieved BDM (see section 6.1.1.1), it can be concluded that the disappearance is probably not due to growth. It is rather an expression and indirect confirmation of the secondary aggregation described by Grimm[25]: Conidia attach on the newly provided surface by growing hyphae. The reverse conclusion is that choosing pH 3 at least partially circumvents the aggregation stages, which is important in terms of controlling the morphology (see section 4.3 "Control of the morphology").

6.1.3.1 pH and pH shift experiments

Aspergillus niger develops its morphological extrema of freely dispersed mycelia and pellets at pH values of 3 and 5.5, respectively. Shifting the pH from the first to the second conditions assumingly would result in a hybrid morphology. For characterization and evaluation of control possibilities towards achieving the goal of a maximum particle size ≤ 1 mm, factors such as duration and point in time of the conditions applied were tested.

Shift from pH 3 to 5.5: Duration

Figure 23 displays the result of using the above-described method of splitting the particle size distribution into the two modes of conidia and pellets, respectively. As particle size development of the conidia has been discussed, the focus now is on the aggregate/pellet mode and the respective leading particle class (conidia or pellets). The overview of the experiments considered here are presented in Table 2 in section 5.3.1.1 "pH and pH shifting experiments".

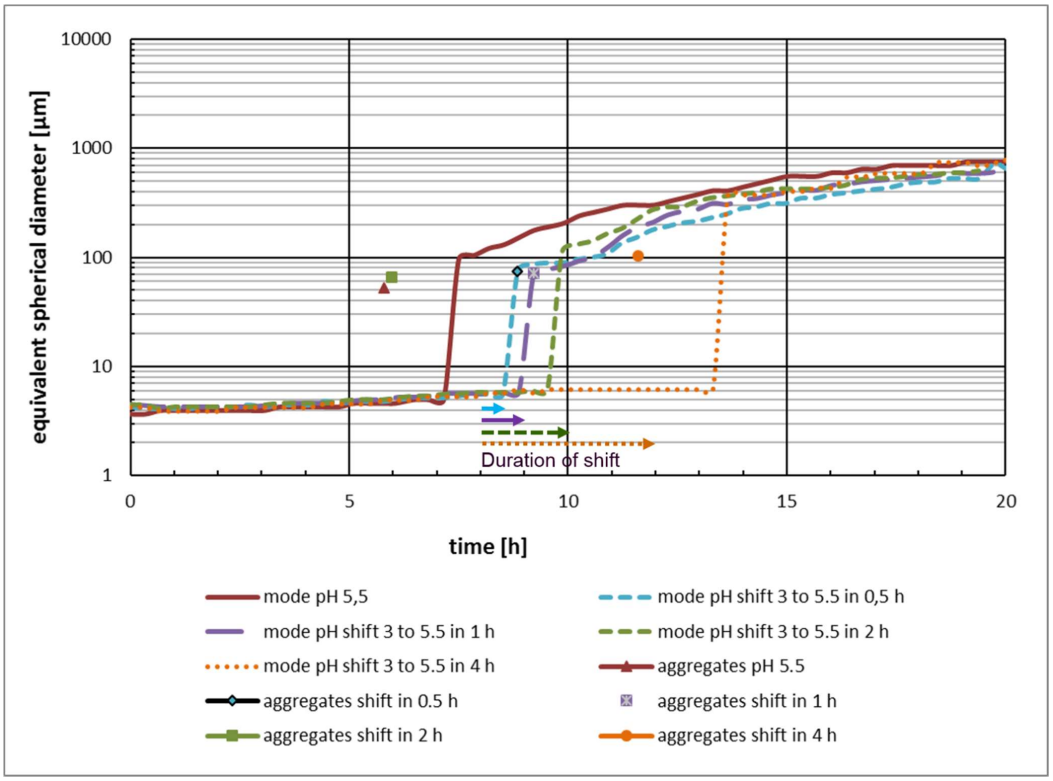

Figure 23: Display of the conidia and aggregate mode and the leading particle class determined with the method depicted above, and the dependency on the duration of shifting the pH from non-aggregating to aggregating conditions (from pH 3 to pH 5.5). The slowest shift leads to larger particle sizes at later time points; the single dots for each experiment setup reflects first appearance of aggregates.

Aggregates are defined to be of larger spherical equivalent diameter than 45 µm. At pH 5.5, aggregates could already be detected after 5.5 h of cultivation (the red triangle in Figure 23). After 7 h, the volume share of the aggregate mode is higher than the conidia mode, making it the leading particle class.

With an initial pH of 3 and therefore under non-aggregating conditions, aggregates are detected earliest after 8 h which corresponds to beginning biomass growth. The points in time are respectively marked in Figure 23. This observation points towards the circumvention of the conidia aggregation process.

The “jump” in the drawn curve in Figure 23 illustrates the point in time when the volume share of the pellet mode becomes the leading particle class when it increases above the volume share of the conidia mode. The faster shifts with durations of 0.5 and 1 h, respectively, have been completed before the pellet mode becomes leading. For the longer shift durations of 2 and 4 h, respectively, the change in leading particle class to pellets happens before the shift has been completed.

For the 2 h lasting shift, the leading particles switched to aggregates after 9.5 h cultivation time, corresponding to 75 % of the shift duration. Similarly, aggregates become leading particle class after 11 h during the 4 h duration shift which resembles the same 75 % shift completion ratio. The underlying cause could be longer time at lower pH which means better conditions for the conidia to germinate and grow. Consequently, these were not available any more for conidial aggregation. Instead, more biomass is present which could actively react towards the changes in the environment of the fungus.

Not presented in Figure 23 is the particle size analysis for cultivations at pH 3. It is because growth occurred as freely dispersed mycelia. No distinct particles were formed but long hyphae loosely entangled to flocs are registered as aggregates after around 17 h.

The particle size behavior and the course of the leading particle class for the cultivations at pH 5.5 are different compared to the experiments starting at pH 3. The aggregate mode became the leading particle class after 5.5 h of cultivation. This is about 2.5 h before the shift takes place in the other experiments. At this point, biomass growth has not started yet, and Grimm’s aggregation model can be corroborated in terms that there must be conidia–conidia based aggregation.

Cultivations featuring a starting pH of 5.5 are hence the only cultivations showing the primary aggregation as vegetative biomass is first present after 8 h. This also indicates that there is a secondary aggregation after 8 h.

Figure 24 shows the microscopic control after 16 h of a cultivation that was started at pH 3 and which has been shifted to pH 5.5 after 12 h in 2 h. Conidia, germinating conidia as well normally

grown hyphae are present. Some germinated conidia are associated with hyphae of other particles. This kind of interaction was expected but has not been described yet.

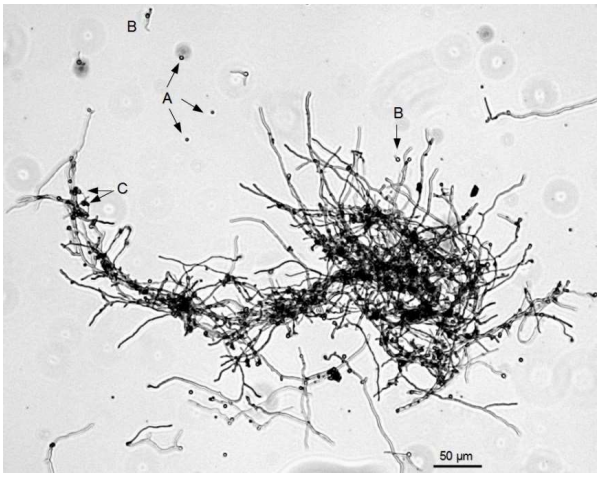

*Figure 24: Microscopic control after 16 h of cultivation with a start pH of 3 and a shift to pH 5.5 in 2 h after 12 h of cultivation: **A** single conidia present in the broth; **B** single conidia germinating without being part of an aggregate; **C** germinated spores attaching to hyphae of another particle → primary aggregation seemed to be partially circumvented*

Once the aggregates became the leading particle class in all cultivation types, apart from the shift in 4 h, their mode is at a size range of 90 – 100 µm (Figure 23). Compared to the start pH of 5.5, the shifted cultivations showed the "jump" in dependency of the duration of the shift. About 15 h into the cultivations though, the shifted ones caught up in size and all cultivations converged towards a particle size of 600 µm.

The higher particle size growth speed for the shifted cultivation could be explained by either aggregation of bigger particles than just conidia (e.g. biomass flocs) and a higher growth rate (see section 6.1.1.1), or potentially both phenomena occurring at the same time.

It is around a cultivation time of 13 h when the development of the aggregate mode for all cultivations begins to match each other and to follow a similar trend. This resembles the point of

transition of particle size control from the regime of pH towards an increased influence of power input (compare with Figure 10 in section 4.3 “Control of the morphology”).

This point marked the time when the growth dynamics in dependency of fluid dynamics follow the model described by Kelly. Apart of pH, other fermentation parameters are the same for all cultivations and a similar development and maybe a convergence to a specific size was expected. The converging size in Figure 23 is based on a power input of 107.5 W m^{-3} (300 RPM) and is about 900 µm after 32 h despite the differences in the environmental condition and the stress on the cells related to withstanding the differently changed pH conditions.

Larger particles potentially receive more time to interact with each other the longer *Aspergillus niger* cultivations are maintained at the non-aggregating conditions pH of 3. In the time frame of 12 – 13 h, it can be stated that the 2 h lasting shift results in aggregates of about 300 µm which are bigger than the 200 µm aggregates resulting from the 1 h lasting shift. The shortest shift duration of 0.5 h results in the smallest aggregates of below 200 µm.

The exception to this series of experiments is the 4 h long lasting shift which forms aggregates in sizes of around 500 µm at the point when aggregates become the leading particle class. Unlike the other experiments and in consideration of the achieved BDM development (see section 6.1.1.1), larger particles must have interacted with each other which again points towards the previously described hyphal interactions in addition to the two aggregation stages described by Grimm.

Circumventing the primary aggregation of conidia and bringing bigger biomass flocs to interact with each other by changing the pH comes with another consequence: The cores of these bio-particles do not consist of aggregated spores but of rather fluffy biomass which results from growth at a low pH of 3. In comparison to Figure 4 in section 2.3 “*A. niger* growth in submerged culture”, the density and size of the core and the fluffy layer around it (areas A and B) can be controlled via the pH handle of the cultivation. It is apparent that the physical properties of mechanical shear are more pronounced on the bigger and fluffier particles that originated from the longer shifts.

This is supported by the size of the aggregates in the beginning of pellet growth: Pellet formation and development occurs earliest of all experiments and like depicted in Figure 4 at pH 5.5. The biomass grows as an active outer layer (C). In theory, denser aggregates result in a constant slope of the particle size increase while the slope of the supposedly less dense aggregates/pellets, like the ones derived from the shifted pH, vary in slope as the cube root law (Equation 4 in section 2.3 "*A. niger* growth in submerged culture") is not necessarily followed.

Per the description in section 2.3 , the pellet growth is based on exponential tip growth which results in a linear increase of the particle diameter. Aging hyphae in combination with mechanical shear lead to denser pellets because hyphae sticking out of the pellets are removed by shear forces. Hyphae therefore grow into internal clearances and enforce the active layer of the pellet dependent on the power input.

Shift from pH 3 to 5.5: point in time

Like the previous chapter, the pH is shifted from non-aggregating to aggregating conditions, i.e. from pH 3 to 5.5. Different points in time of the pH shift during a cultivation are under investigation. The shift duration is set to 2 h as this appears to be the best compromise of obtaining the desired effect of aggregation in combination with higher than standard biomass concentrations. As references, cultivations with a single pH of 3 and 5.5, respectively, are employed.

Figure 25 displays the obtained results in the same manner as for the pH shift duration experiments. As expected, cultivations at pH 5.5 show the first aggregates earliest after 5.5 h. Aggregates also become the leading particle class earliest in that cultivation, after 7 h. In contrast, cultivations with a single pH of 3 do not show pellet formation though some loose flocs are observed.

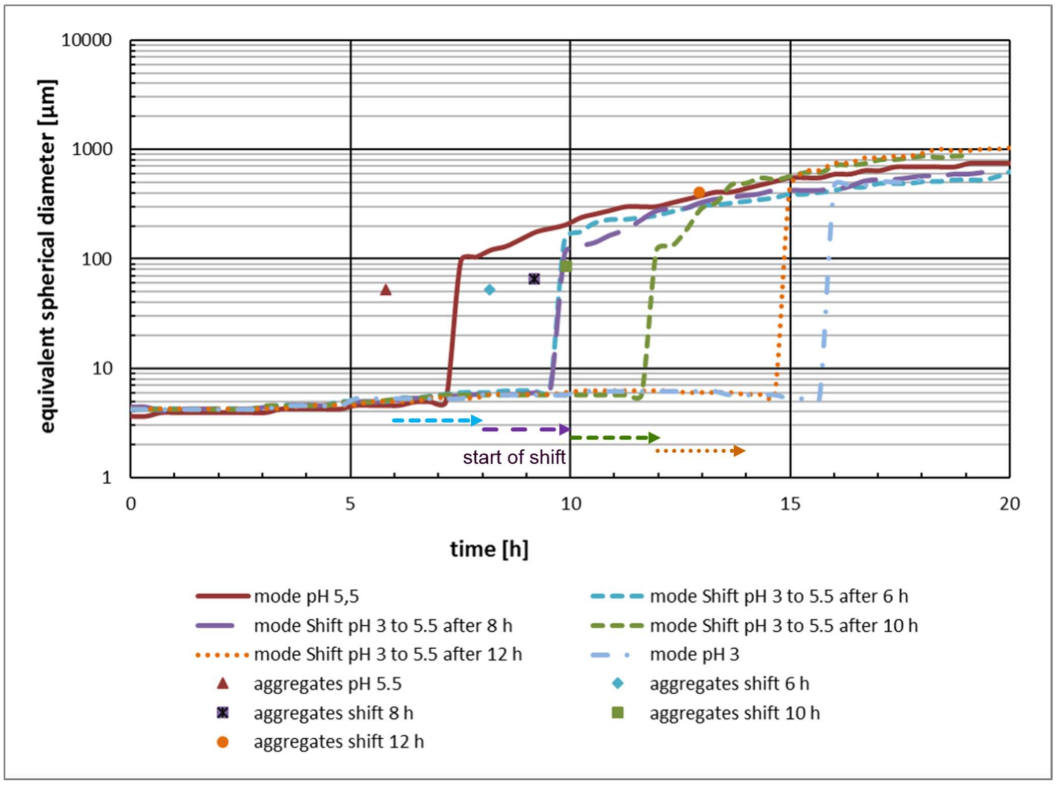

Figure 25: Leading particle class determined with the above depicted method of the modes over time for A. niger cultivations at pH 5.5, pH 3 and with a shift in pH from 3 to 5.5 over 2 h after 6, 8, 10 and 12 h; the later the shift is conducted, the later the aggregation of biomass occurs and the longer time it takes until the first aggregates can be observed; cultivations at a pH of 3 do not show aggregates at all despite the course of the experimentally determined curve – intensive biomass growth leads to high obscuration in the laser diffraction analyzer and therefore to unreliable measurements

Cultivations with pH shift from non-aggregating conditions (pH = 3) towards aggregating conditions of pH 5.5 after 6 and 8 h both have the aggregate mode becoming the leading particle class after 9.5 h. This is 4 h later than the cultivation at pH 5.5. This has been expected due to the findings of the experiments with pH shift duration (Figure 23) and the conclusion that primary conidia aggregation probably could be omitted.

The shift initiated at 6 h has been completed at 8 h (the light blue arrow indicator in Figure 25) with aggregates being present during the shift. It is 1.5 h after completion of the shift that the

aggregates become the leading particle class. The time frame would correspond to the lag-phase which means that the first aggregates are probably formed by a primary aggregation process.

The experiments with a shift beginning at 8 h have aggregates becoming the leading particle class at the same point in time (after 9.5 h) as after the shift at 6 h. This indicates the involvement of biomass growth which corresponds to Grimm's secondary aggregation with hyphal interaction.

Following the involvement of growing biomass, the cultivations with pH shifted at 10 and 12 h formed first respective aggregates after initiation of the pH shifting process. Aggregates become the leading particle class around completion of the shift. At this point in time, spores have been germinated or remained dormant (compare to Figure 22). While no primary aggregation could have taken place, the aggregates consist of hyphal flocs which aggregate with each other.

The mechanism can only be based on hyphal interactions and it is confirmed by microscopic control. Examples are shown in Figure 26. In consequence, the knowledge gap between the works of Grimm and Kelly now could be bridged with a "tertiary hyphal aggregation" mechanism.

The longer the cultivations remain at pH 3, the longer time the biomass can develop under growth enhancing conditions. Changing the environmental conditions and forcing an aggregation of these larger flocs leads to different particles. Figure 26 proves the "non-core" and this is also represented in the particle size of the mode: The aggregate mode of the two latest shifts after 10 and 12 h, respectively, showed larger particle/aggregate sizes towards the end of the cultivation compared to the aggregating condition of a cultivation at pH 5.5.

If the core of the pellet, or more the bio-particle, does not consist of conidia aggregates and if there is no core as such, the resulting density of the particle must be lower. Also, hyphae are sticking out of the particle in a higher degree compared to when grown as pellet at pH 5.5.

The fluffy structure of the particle allows for a higher particle internal biomass growth. This would correspond to the observed superior biomass development for the late shift cultivations compared to the earlier shifts considering the similar slope in particle size increase over time.

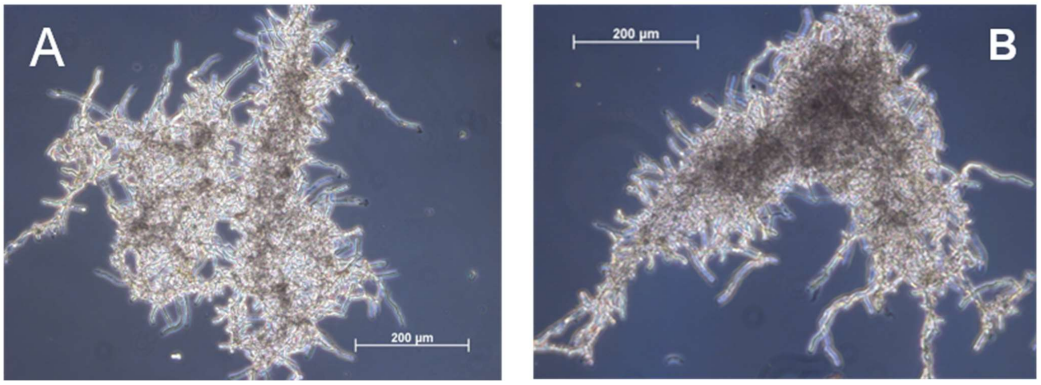

*Figure 26: Bio-particles formed during the experiments with shift of pH from 3 to 5.5 after **A** 10 h and **B** 12 h. The particles were derived from samples taken after 24 h of cultivation. No pellet core built of conidia was present, and instead, the particles were assemblies of rather loose biomass flocs.*

In conclusion, the point in time of changing the pH can be employed as lever for the morphology control and to design particles with sizes below 1 mm with earlier pH shifts resulting in smaller pellets compared to later pH shifts.

6.1.3.2 Power input and initial conidia concentration

The influence of mechanical power input and the initial conidia/particle concentration are levers for fine-tuning of the final particle size. The outcome of the experiments in terms of achieved biomass is not satisfying (see section 6.1.1.3). Therefore, this chapter summarizes the achieved particle size results for trials with a shift in power input from standard conditions of 107.5 W m^{-3} (300 RPM) to supposedly aggregation enhancing lower power input of 25 W m^{-3} (100 RPM) at time points of 8 and 12 h in Figure 27, increased permanent power input of 212 W m^{-3} (400 RPM) and 430 W m^{-3} (500 RPM) in Figure 28 and initial conidia concentration of 5 * 10^6 L^{-1} (standard), 2.5 * 10^6 L^{-1}, 4 * 10^7 L^{-1} and 5 * 10^7 L^{-1} in Figure 29.

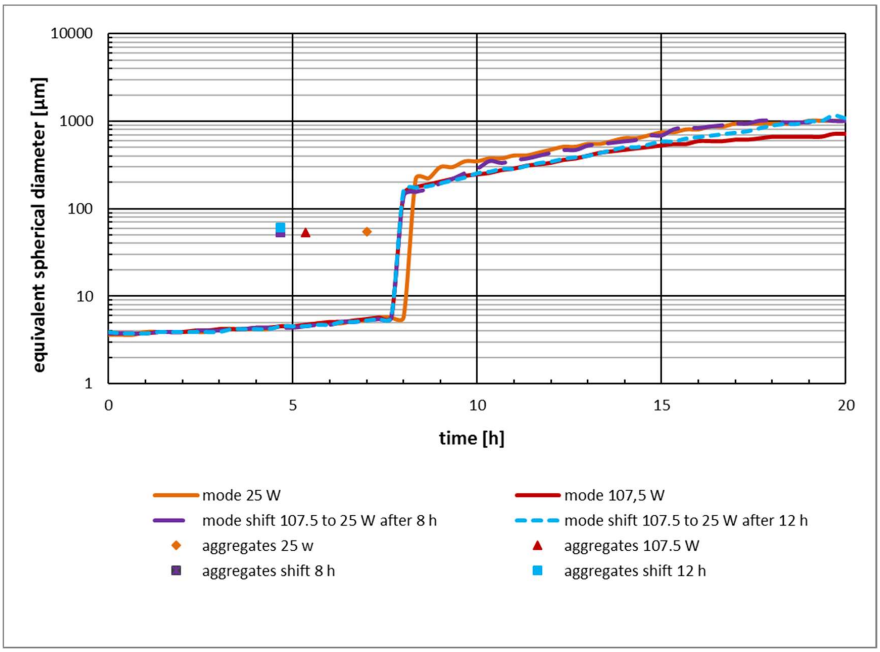

Figure 27: Mode and leading particle class in dependency of a shift in power input by agitation from standard conditions of 107.3 W m^{-3} (300 RPM) to 25 W m^{-3} (100 RPM).

The shift in power input towards aggregation promoting conditions is shown in Figure 27. The outcome is that lower power input from cultivation start leads to a delay of the moment where the aggregates become the leading particle class. This is not expected as low power input conditions are supposed to promote aggregation. In combination with the low biomass (section 6.1.1.3 "Power input and initial spore concentration") concentration, it can be concluded that suboptimal growth conditions, like e.g. lack of oxygen[126,127] lead to delayed germination which in turn delays the secondary aggregation.

The aggregates formed under the low power regime (low power from start as well as the shifted cultivations) develop particles with a diameter of 1100 µm. This is 46 % bigger than under standard conditions which resulted in 750 µm big pellets. The size difference is based on hyphae sticking out of the particle which are not being sheared off when lower power input is applied.

25 W m^{-3} power input was sufficient to avoid sedimentation of the bioparticles, but else the lack of mixing and the resulting lack of oxygen transfer, hampered the biomass too much in terms of the particle size and growth control model.

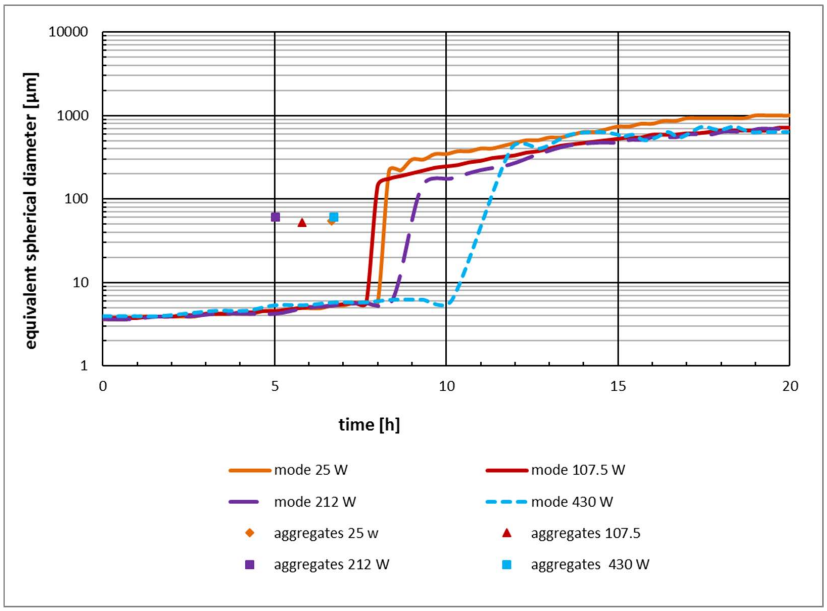

Figure 28: Mode and leading particle class in dependency of mechanical power input by agitation in standard conditions of 107.3 W m^{-3} (300 RPM), 25 W m^{-3} (100 RPM), 212 W m^{-3} (400 RPM) and 430 W m^{-3} (500 RPM).

Figure 28 displays the biomass' reaction on higher than standard power inputs. All the experiments presented were conducted at single stirrer speed. The result is that aggregates become the leading particle class in dependency of the power input: The higher the power input by agitation is, the later the aggregates became the leading particle class.

Exceptions are the experiments with low power input (25 W m^{-3} at 100 RPM) for reasons discussed above for the results presented in Figure 27. This is in line with Grimm's description of fluid dynamics and its influence on the secondary aggregation step.

The shift in stirrer speed was instant. The time needed for aggregates to become the leading particle class took longer the higher the power input was. It was most likely due to fluid dynamics which influence the previously claimed tertiary aggregation as interaction of hyphae.

The power input of 430 W m^{-3} resulted in the slowes rise in particle size from 10 to 12 h cultivation time. It could also be that hyphal aggregation was prevented and instead pellet growth was responsible for the observed gains in particle size.

The increased power input of 212 W m^{-3} & 430 W m^{-3} compared to the standard 107.5 W m^{-3} resulted in smaller pellets and all respective cultivations converged towards a final particle size of 700 µm. This means that the micro scale of eddies derived from the Kolmogorov scale of length and the respective production range of the dissipation spectrum[128] can be neglected in terms of particle size development. There is however a possibility that these were the cause for the deferred biomass development (compare to section 6.1.1.3).

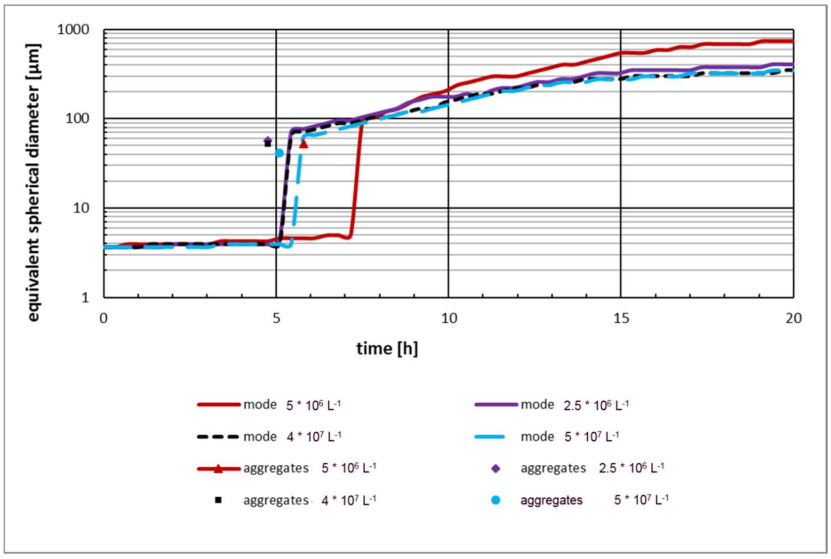

*Figure 29: Mode and leading particle class in dependency of initial conidia/particle concentration with standard conditions of 5 * 10^6 L^{-1} compared against 2.5 * 10^6 L^{-1}, 4 * 10^7 L^{-1} and 5 * 10^7 L^{-1}.*

The evaluation of the effect of initial particle concentration can be found in Figure 29. With initial conidia concentrations being higher than the standard 5 * 10^6 L^{-1} conidia concentration, enhanced primary aggregation led to aggregates becoming the leading particle class even before growth set in.

The first measured aggregates had a diameter of 60 µm – 40 % smaller than the first aggregates achieved with standard inoculation conditions of 5 * 10^6 L^{-1}. With increasing time, these aggregates slowly grew in particle size reaching just 400 µm final size compared to 750 µm for the standard cultivation.

Again, these experiments resulted in an unsatisfactorily low BDM. Like the power input, conidia concentration can therefore be a fine-tuning parameter for the particle size. The biomass growth could be hampered by particles consisting of too many conidia. There might be competition between the conidia in order to grow and a quorum sensing like behavior could limit the number of conidia that actually germinate[129] with lower biomass and particle growth as a consequence.

6.1.4 ζ-potential & conidia surface structure

In general, the ζ-(zeta-) potential is used to describe the surface of particles in terms of their isoelectric point. Despite being a potential of the not distinctively defined shear layer, the state of the electro-static double layer can be described given a sufficiently large particle ensemble.

Figure 30 displays the results of the ζ-potential measurements of *Aspergillus niger* AB1.13 conidia in cultivation medium in dependency of the pH value. The salt content of the media also contributes to the measurement, and compared to inorganic particles like silicon or titan dioxide, the measured range of -10 – 10 mV is considered very low[130]. The closer to zero the ζ-potential is the less electrostatic repulsion there is between particles. The lowest ζ-potential is measured at pH 5.5 which also resembles the premise for aggregating conditions.

At the same pH of 5.5, the cultivation media turned turbid when inoculated with conidia: Melanin desorbed from the surface of the conidia. Melanin is mainly known as a compound involved in providing UV protection for the spores[131], but also stabilizes the conidial surface by bridging

between surface proteins[54] which influences the vegetative phase[132] and it guards against chemicals[133].

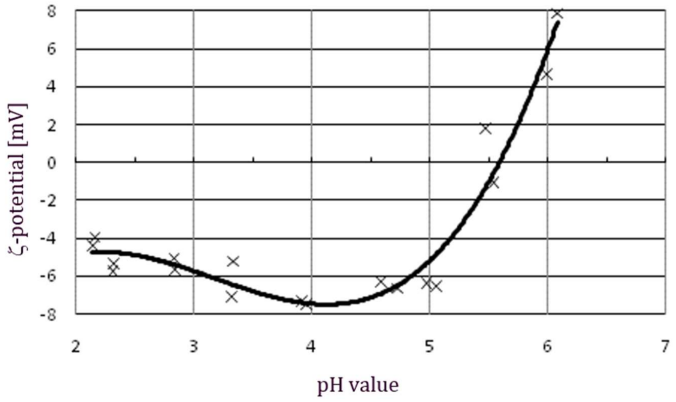

Figure 30: The ζ-(zeta-) potential for Aspergillus niger AB1.13 conidia in cultivation media was very low at all measured pH values; it was lowest (around 0 mV) at pH 5.5; the lower the ζ-potential, the less electrostatic repulsion is present, which could mean "improved" aggregation conditions.

The desorption could possibly scavenge harmful substances from the media but more importantly, it leaves the conidial surface, including the cell wall associated proteins and hydrophobins[134], exposed. Figure 31 displays the conceptual model of melanin desorption.

In the left part of Figure 31, conidia at a pH of 3 are depicted. The melanin layer is intact, covering both the chitin wall and the proteins stabilizing the bioparticle. Increasing the pH to 5.5, the melanin desorbs and dissolves in the media leaving the chitin wall and proteins, e.g. hydrophobins, exposed.

Hydrophobins could enable hydrophobic interaction for improved aggregation. The smaller particle diameter registered for conidia at pH 5.5 with the laser diffraction in section 6.1.3.1 supports this conceptual model and so does electron microscopy, imaging proving a thinner melanin layer[135].

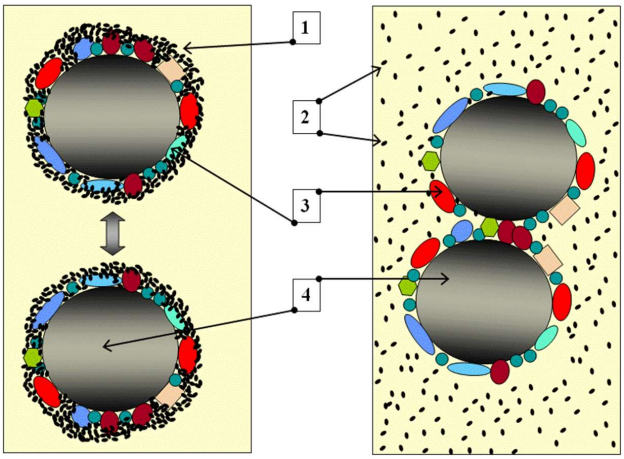

Figure 31: Conceptual model of melanin desorption with pH 3 applied for the left part of the figure, and pH 5.5 applied to the right; ***1*** *represents the melanin associated to the* ***4*** *conidia and* ***3*** *surface proteins; melanin desorbs at a pH of 5.5* ***2*** *leaving the proteins and the chitin wall of the conidia exposed for possible hydrophobic interaction, thus creating conditions for "better" aggregation.*

6.2 *A. niger* AB1.13 optimized parameters for particle size and biomass control

The introduction stated two major goals that should be achieved: Firstly, an optimized amount of biomass – too much biomass would mean spill of substrates for building up and maintaining biomass – and secondly, the particle (pellet) size should remain below 1 mm to avoid internal substrate limitations in the particle.

The null hypothesis for the statistical analysis is: The process parameters pH, power input and initial conidia concentration each had no significant influence on the development of the biomass. It is rejected only for the pH as high biomass concentrations could be reached employing pH 3 as start condition. With progressing time at pH 3, more and longer hyphae were formed which then remained freely dispersed. If pellet growth is preferred, a transition in morphology from freely dispersed to pelleted could only be achieved with a shift in pH.

Analogously, the significance is tested for particle size and all parameters are positive correlated. The analysis trend shows that the final particle size increased when both initial conidia

concentration as well as power input were decreased while the pH should be raised (to generate particles!). Focusing on the particle size, an example size of 800 µm could be reached with 6 * 10^8 conidia L^{-1}, a power input of 179.3 W m^{-3} (358 RPM) and a pH of 5.4.

Including the biomass in a combined model of BDM and particle size led to pH as single significant factor. By shifting pH from 3 to 5.5, dependent on the point in time and on the duration, both particle size and bio dry matter can be controlled in an appropriate way.

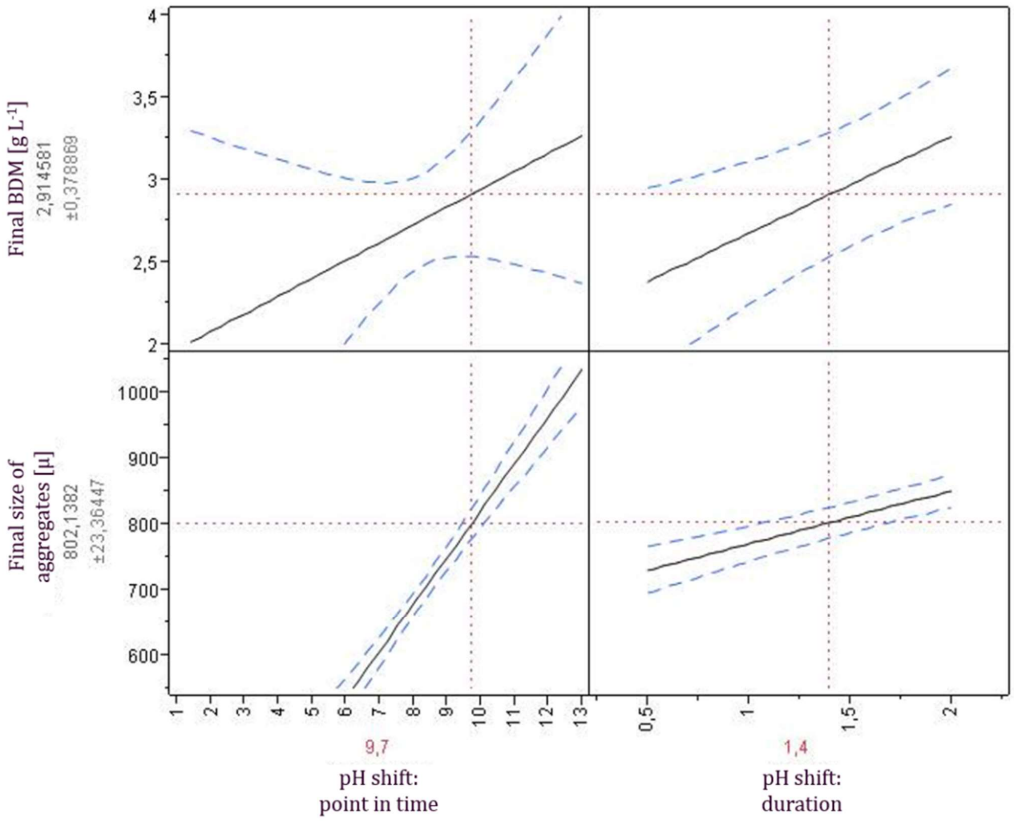

Figure 32: Statistical analysis shows that reaching an optimum concentration of bio dry matter of 2.9 g L^{-1} while keeping the maximum particle size at 800 µm could be achieved by shifting the pH from 3 to 5.5 after 9.7 h over a time span of 1.4 h.

Figure 32 displays the influence range achieved by varying the pH shift point in time and the duration of the shift in general as well as for the example case of a designated BDM of 2.9 g L^{-1} and a maximum particle size of 800 µm: The conclusion is that the shift should start after 9.7 h and should last 1.4 h.

Figure 32 is organized in the way that the target values are represented in the rows and the columns are built by the influencing parameters point in time of the shift and duration of the shift. The dotted straight lines in the graphs are an orientation help and resemble the above stated example. The plotted graphs show the trend for each parameter and its respective influence on the target variables and are covered by the confidence interval.

The regression analysis was based on two functions:

Equation 12: Function describing final BDM concentration of the cultivation

$$BDM = f_1(Duration_{shift}, Point\ in\ time_{shift})$$

Equation 13: Function describing the final particle size

$$final\ particle\ size = f_2(Duration_{shift}, Point\ in\ time_{shift})$$

For the example, the variables were set to 2.9 g L^{-1} and 800 µm. To calculate the parameters for other values of the variables, a family of curves can be derived for the parameter space of BTM = 1, 2, 3, 4 g L^{-1} with the Equation 12 & Equation 13. A pre-defined particle size could then be reached by reading the point in time and the duration of the shift:

Equation 14: function describing final particle size in dependency of BDM, pH shift duration and point in time of the pH shift

$$final\ particle\ size = f_1 + f_2 - BDM$$

In summary, it is possible to design a specific bio dry matter content as well as final particle size without introducing any further ingredients that might become problematic in further downstream processing[81], of course given that pH adjustment is part of the set-up anyway. The industrial scenario for application of this model could be industrial cultivations, specifically seed

tanks for growth of biomass. Ensuring the ideal format of the biomass morphology at the onset of the process could mean conditioning of the biomass for the intended production purposes.

6.3 *Aspergillus niger* production strain

The experiments with the production strain are conducted at 20 L scale under what resembles conditions close to production. The most important result of all attempted trials is that the strain behaves very differently compared to the results obtained with the *Aspergillus niger* AB1.13 strain: All experiments resulted in various degrees of pellet formation with freely dispersed mycelia present and with pellets disaggregating later in the fermentation. The data in this chapter serves more as proof that the model has been tested than to support any detailed scientific discussion.

6.3.1 Production strain growth at pH 5.5

The morphology was assessed for growth at pH 5.5, and results are displayed in Figure 33. Different from expectations, the biomass develops both large and small pellets next to soy grit particles up to 60 h fermentation time. Microscopic control also reveals pellets not being spherical but of different shapes i.e. elongated and with apparently different densities (visual observation). Furthermore, scattered mycelia and clumps are observed among the pellets. After 60 h, the pellets slowly disperse. After 79 h, few small pellets and clumps are left and mycelia/hyphae are mostly fractured.

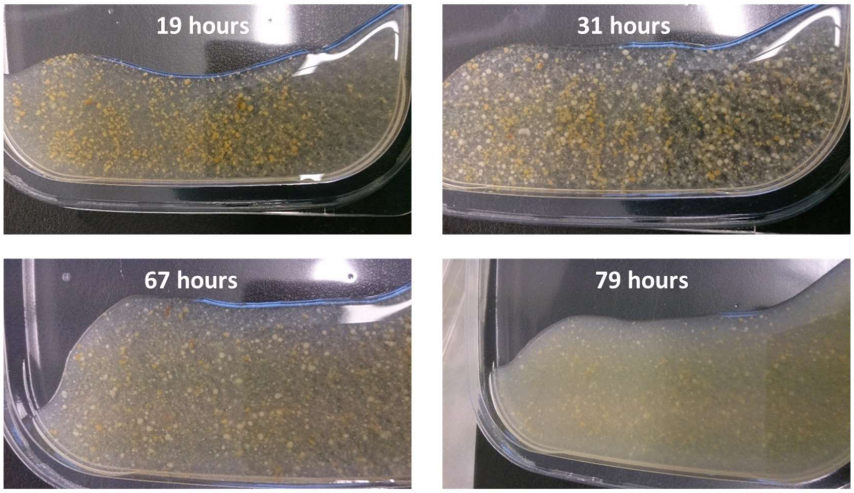

Figure 33: Morphological changes in the production strain at pH 5.5; at first mixed morphology with later defragmentation into mycelial growth after 79 h

6.3.2 Production strain growth at pH 3 and 4

Growth at lower pH than 5.5 is intended to result in freely dispersed mycelia. In fact, it resulted in no growth at all (data not shown). A positive control has been conducted with a shift to pH 5 after which biomass growth was observed with identical morphological traits as depicted for pH 5.5.

6.3.3 Production strain growth at pH 6

Because no growth was observed at pH 3 and 4, pH was moved upwards to achieve a higher repulsion between the conidia as described in section 6.1.4 and Figure 30: The zeta-potential at pH 6 is with 6 mV quite "far" away from 0, similar to pH 3. pH 6 should thus result in less/no pellets. Figure 34 presents several pictures as an illustration of the achieved morphology in this experiment.

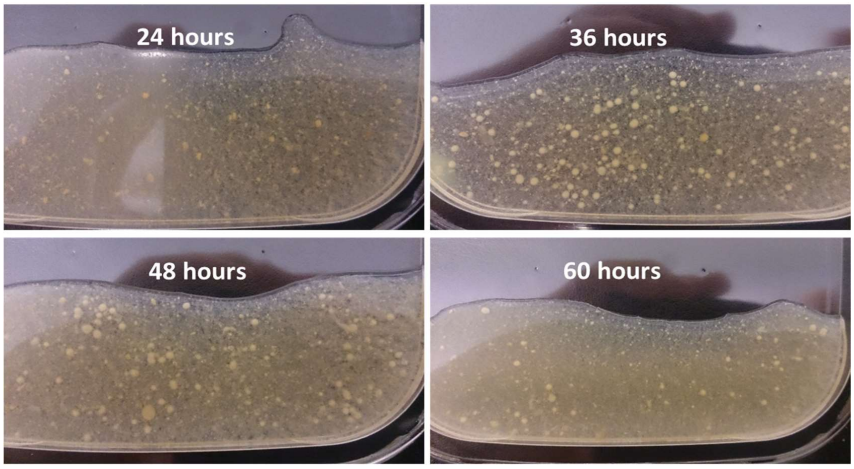

Figure 34: Morphological changes in the production strain at pH 6; against expectations pellets are present in a mixed morphology which disaggregates after 60 h.

The morphology was more aligned with the theory with less pelleted growth and more formation of mycelia. Still, pelleted growth was clearly present during the fermentation, although the pellets were present in lower numbers than at pH 5.5. Also, aggregated mycelia and fluffy biomass clumps were contributing to the overall morphology. An earlier exponential growth was observed by off-gas measurement and by microscopic control. Mycelia and small aggregates were already after 19 h and larger pellets formed later. This could be an indication for a tertiary aggregation type of hyphal interaction.

6.3.4 Production strain with increased initial conidia concentration

As described for the academic strain *Aspergillus niger* AB1.13 and as described by Grimm[25], the initial conidia concentration has an influence on the morphogenesis. Chapter 6.1.1.3 and 6.1.3.2 refer to the experiments with high inoculum concentrations which should promote enhanced mycelial growth. The pH level is chosen according to the findings reported in the previous section. The highest employed inoculum features in $1*10^5$ spores L^{-1} which is very comparable to the starting conditions of the academic strain.

Compared to the standard conditions of the industrial strain, 7 * 10^2 L^{-1} & pH 5.5, the lag phase lasts 10 h which is 9 h shorter. Based on off-gas (CO_2-) analysis, the amount of biomass formed seems to be improved compared to standard conditions (pH 5.5, 7 * 10^2 L^{-1}). In contrast to the AB1.13 strain, the biomass development benefits from increasing the initial conidia concentration.

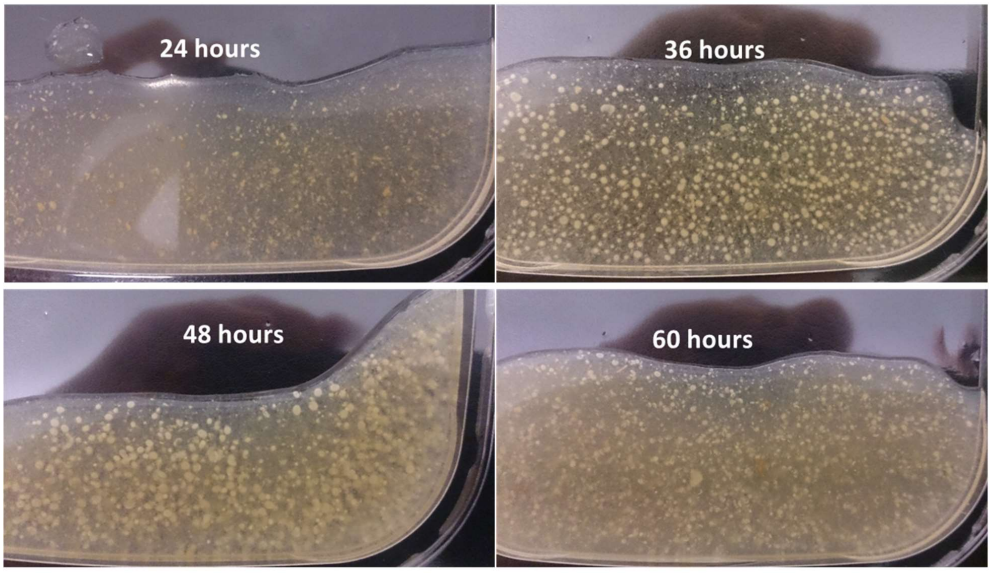

Figure 35: High initial conidia concentration of 10^5 L^{-1} at pH 6 showed more and smaller pellets than with normal initial conidia concentration (according to visual inspection).

The morphology for high initial conidia concentration started with the development of very small pellets only. Morphology example pictures are shown in Figure 35. The pellets were seen to be formed by small aggregates, and from there developed into more distinguished and small pellets. Around 50 – 60 h, the pellets begin to break up which means pellets lasted longer regarding the earlier growth than at standard conditions (depicted in the previous section).

The increase of the inoculum to 10^5 conidia L^{-1} does not result in mycelial growth. Instead, many small pellets develop with a later dispersion.

6.3.5 Production strain in media with high osmolality

Cultivations at pH 5.5 under high osmolality conditions are conducted in order to promote mycelial growth which is reported in the literature[80]. Since it was not possible to measure or monitor the osmolality on site, the hypothesis test was based on a theoretically calculated osmolality (see section 5.2.2.2).

As expected, the germination phase was affected by the high osmolality[80]. It was prolonged to a duration of up to 70 hours compared to an average of ~27 h under normal conditions.

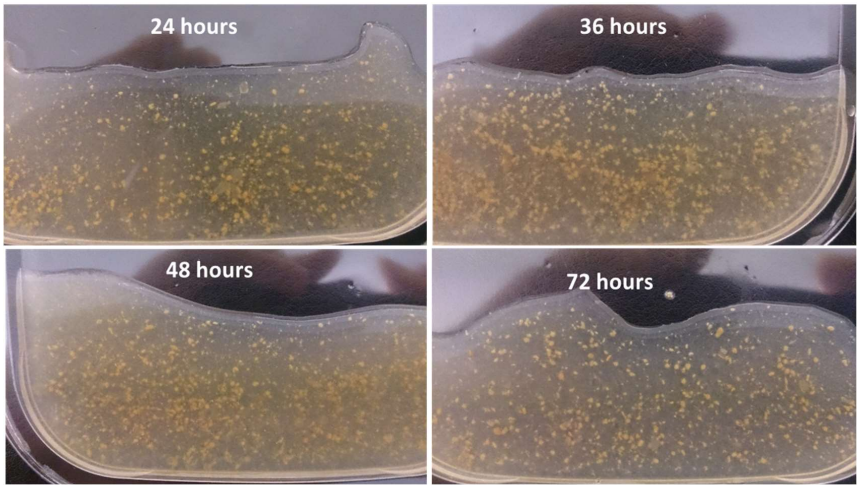

Figure 36: Morphological changes in the production strain at pH 5.5 with high osmolality; pellets present against expectations

It can be concluded that despite an osmolality of 2.4 osmol/kg, small pellets were formed. Still, the amount of pellets seemed lower by visual inspection than experienced with pH 5.5. These results are in contrast to the findings achieved by Wucherpfennig with the AB1.13 strain[80]. A possible cause for the observed results could be the specific fermentation conditions, like the industrially inspired complex media and the theoretically estimated osmolality. However, exceeding the osmolality levels employed in the pursuit of gaining control of the fermentation with respect to achieving mycelial growth can be considered an unrealistic scenario for industrial purposes.

6.4 *Aspergillus niger* BO-1 wildtype

This chapter's scope is the creation of an alternative fermentation strategy to develop distinct pelletised and dispersed growth in submerged cultivation after the "interesting failure" of morphology engineering with the production strain. The approach is based on the impression that the soy particles were the main cause for the observed mixed morphology. Therefore, two major fermentation conditions are developed and referred to as 'basis pelletised growth' and 'basis dispersed growth' conditions (see Table 5, section 5.3.3 "*Aspergillus niger* BO-1 conditions for provoking different morphologies").

The first result was the choice of the cultivation media (compare to chapter 5.2.2.3 BO-1 media): The MLC media contained, just like the media used for the industrial strain cultivations, soy. All the MLC cultivations resulted in a mixed morphology with a score of 3 – 4 on the morphology scale displayed in Figure 14 in section 5.4.5 "BO-1 morphology scale".

Most importantly, the mixed morphology was achieved independently of pH and agitation. Figure 37 displays the morphological outcome after 41 h of cultivation in combination with a MasterSizer 3000 laser diffraction measurement of the volume density distribution. The particle size distribution can be employed as a quantitative indicator for the general state of the morphology where a broader distribution represents the less pelleted morphology.

Negative trials were conducted with Bacto-Soytone, a digested and particle free soy replacement. It resulted in pelleted growth under low agitation condition, though two thirds of the cultivations showed unsatisfyingly low biomass development.

The BO-1 strain, showed the inverse behaviour compared to the findings with the *Aspergillus niger* AB1.13 lab strain that lower pH results in more freely dispersed mycelia in general. The pelleting conditions were found at pH 3.5 while the freely dispersed mycelia grew at 4.2. However, it is concluded that pH is not a major factor for morphological development. Under high agitation speed, the morphology will be fully dispersed (morph. scale: 1).

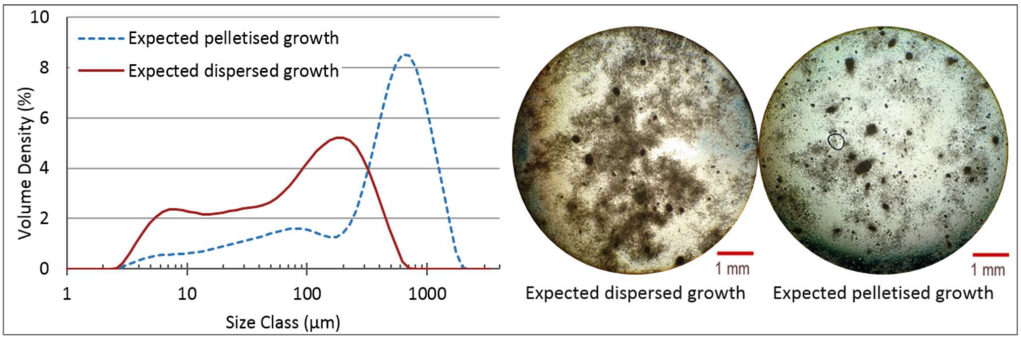

Figure 37: Particle size distribution and microscopy pictures after 41 hours from the two cultivations with MLC medium.

6.4.1 Particle size and morphology

6.4.1.1 A. niger *BO-1 under conditions for freely dispersed mycelia*

Figure 38 consists of two plots and microscopy pictures to compare dispersed growth with and without change of pH. In that figure, A and B represent the particle size distribution over time at pH 4.2 and 3.5, respectively. The cultivation conditions are stated in Table 5. Below the particle size distributions, time series of microscopy pictures for both cultivations are presented.

The figure demonstrates that there were no major differences in morphology by changing pH to 3.5. The development of the particle size distribution was very similar, and was supported by microscopic analysis. At lower cultivation pH, the mycelia elements seemed to grow in a wider size span and with higher average size.

Mycelia in the cultivation with basis pH grew to around 800 µm in maximum average size, whereas the cultivation with the lower pH of 3.5 reached a maximum size of 1200 µm. The overall morphology is mycelial and these big "particles" represented entanglement of flocs (agglomerates). These differences were hence an artefact because no pellets are present.

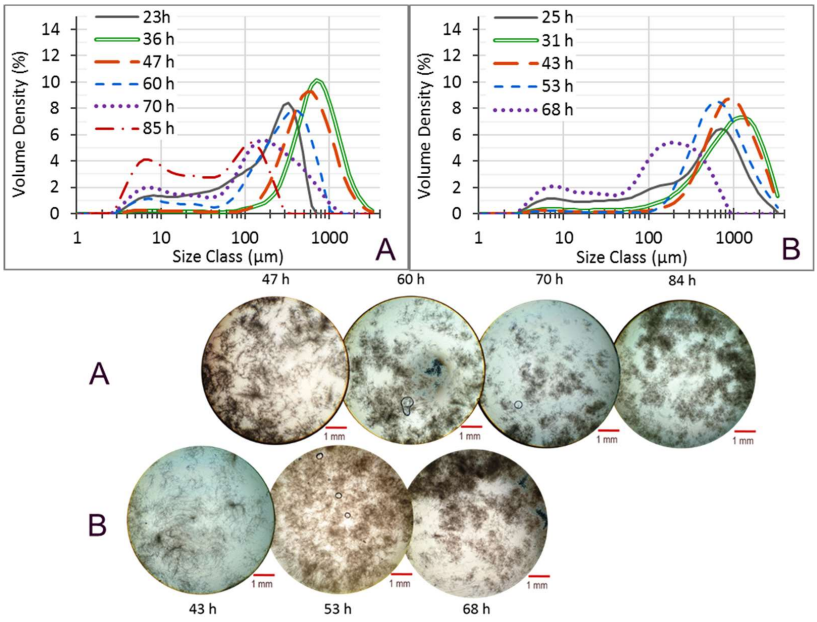

Figure 38: Particle size distribution and microscopy pictures from the two cultivations in reactors with dispersed growth. ***A*** *has the basis condition of dispersed growth defined in Table 5 which is the reproduction of the dispersed growth found in the preliminary study.* ***B*** *has the same cultivation conditions, except that the pH is 3.5.*

The overall patterns of the particle size distribution observed for the two cultivations are similar. Initially, elements of dispersed growing mycelia expanded in size and were measured as large particles by the Mastersizer 3000. With a maximum size of 800-1200 µm around 35 to 45 hours of cultivation, these began to break up into smaller elements. This resembled the behaviour of the industrial strain (see section 6.3).

Analogous to MLC trials, cultivation pH is not a major factor for morphological development of *Aspergillus niger* BO-1 strain in ½MU-1 media. With high agitation speed, the morphology will be fully dispersed (morph. scale: 1).

6.4.1.2 A. niger *BO-1 under pelleting cultivation conditions*

Figure 39 represents particle size distribution for cultivations run with pelletizing conditions of pH 3.5 instead of 4.2 and 150 RPM instead of 600 RPM (Table 5). The achieved pellets developed in size towards an average diameter of around 1000-1100 µm.

Distinct pelletised growth was present for the first two time points as no particles with a diameter smaller than 500 µm could be detected. After around 65 h, the distribution became wider towards the smaller particle sizes as the pellets began to fracture.

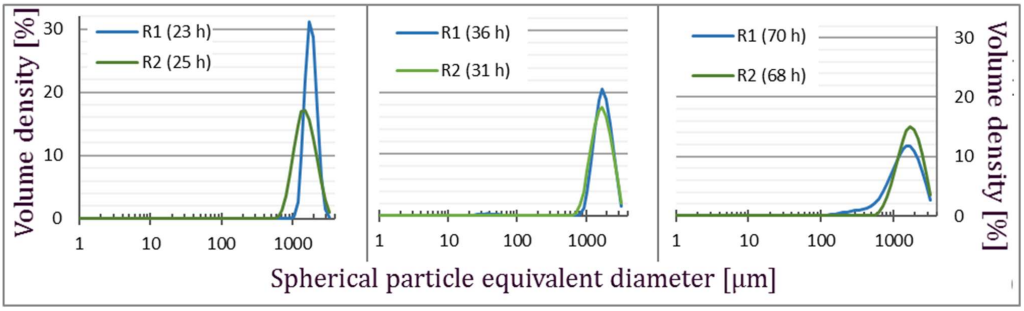

Figure 39: Particle size distribution of two replicates R1 and R2 under pelletizing conditions for three different time points; earliest samples to the left; cultivations not performed in parallel → slight deviation in sampling time (stated in the figure legends).

Figure 40 depicts microscopy pictures from these cultivations. Pellets were very hairy and loose in structure which resembled *A. niger* AB1.13 lab strain pellets developed under low agitation conditions described by Kelly[28]. The fluffy structure presumably indicates susceptibility towards shear stress. With diameters in the range from 800 µm to more than 3000 µm, internal substrate limitation problems might occur.

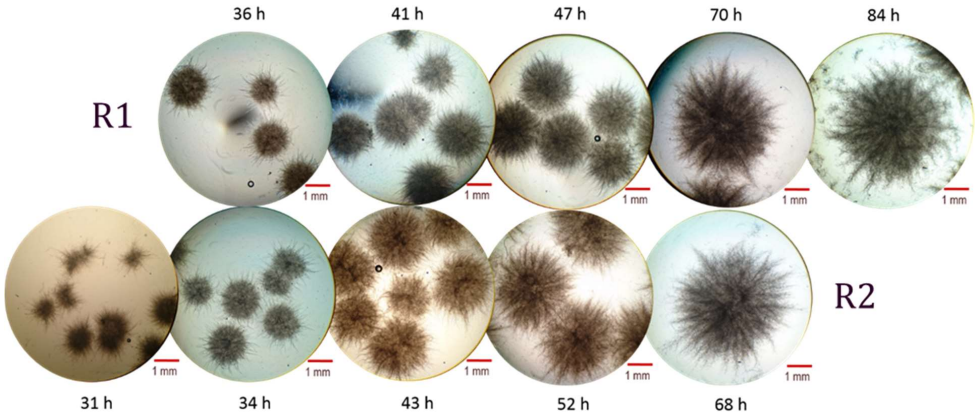

Figure 40: Microscopy pictures from independent duplicates performed under pelletising conditions; each picture in one row is derived from the same cultivation: Reference 1 as R1 at the top and R2 as second reference in the bottom with each cultivation point in time in hours stated above or below the pictures for R1 and R2, respectively.

6.4.1.3 A. niger *BO-1 Initial conidia concentration*

Analogue to the AB1.13 and the industrial strain, the initial conidia concentration was increased to manipulate the particle size[27,83,136]. The conditions were set to promotion of pellet formation with a conidia inoculation concentration increase by a factor 10 to 5 * 10^8 conidia L^{-1} after inoculation.

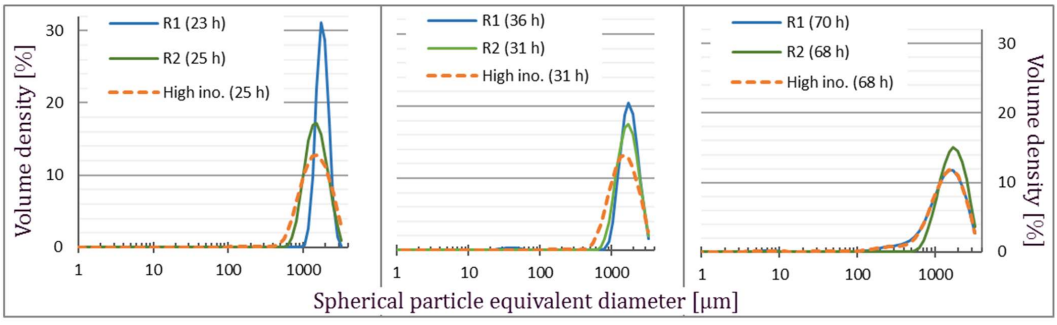

Figure 41: Particle size distribution of the cultivations under pelletising growth conditions called R1 and R2 (from Figure 39), compared with the cultivation with 10 times higher initial spore concentration called High ino. The figure represents the size distribution from samples taken at three different time points, with the earliest samples to the left and the latest to the right. As the cultivations were not performed simultaneously the sample times are different and the exact time of sampling is written in between brackets in the legends of each figure.

Figure 41 represents the particle size distribution for the cultivation with high inoculation concentration along with the pellet references R1 and R2 (from the previous section 6.4.1.2). The average pellet diameter reached around 1000-1100 µm for all three cultivations. The increased inoculum had no major impact on the size of the pellets despite the expectation of smaller pellets[83,136,137].

As expected, the pellet concentration increased with higher inoculum concentration. The increase of the pellet concentration did however not directly correspond with the increased spore concentration: While the initial concentration was increased by a factor 10, the pellet concentration raised just by factor 2 to 5.

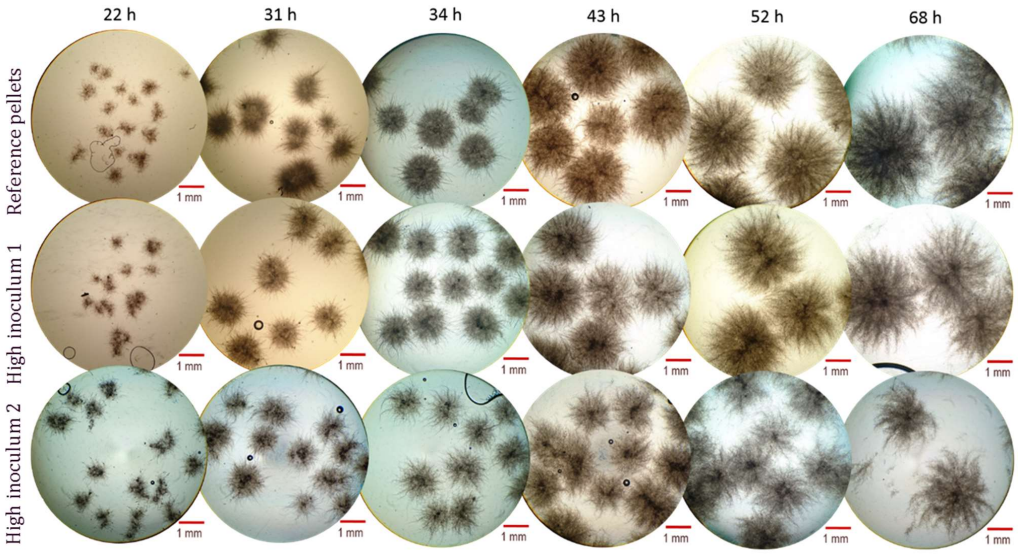

Figure 42: Microscopy pictures from cultivation with pelletising conditions and cultivations with high spore inoculation concentration; rows represent the cultivations, columns the respective different time points where samples were taken.

The method of increasing inoculum concentration is also found inconsistent. Figure 42 represents the microscopic control of three cultivations: the top row corresponds to the

reference pelletised growth conditions and the two bottom rows are from cultivations with 10 times higher spore inoculation concentration. Similarities in morphology can be observed in the two top rows compared to the bottom row meaning that the two higher inoculum cultivations differed more from each other than the difference between the high inoculum 1 cultivation and the pellet reference cultivation. The pellets of high inoculum 2 grew hairier and were more loose in structure. Particle size distributions revealed similarly sized pellets though. This implies that a higher conidia inoculation concentration is not well suited as lever for engineering the particle size.

6.4.1.4 A. niger *BO-1 Power input*

Like for the *A. niger* AB1.13 strain, a shift in power input was evaluated for its potential to influence morphology. In contrast to the lab strain, the aim of the BO-1 trials was to limit the pellet size growth with higher agitation speeds like described by Kelly[28]. Six cultivation setups start with standard pelleting conditions (see Table 5 in section 5.3.3). After formation of pellets, the agitation speed was gradually raised with 100 RPM per 4 hours. Table 7 describes how and when the agitation speed was raised. The resulting morphology after 52 and 68 hours of cultivation was characterised by means of the morphology scale (see Figure 14, section 5.4.5).

Table 7: Overview over experiments initiated with standard pelletizing conditions with gradual increase in agitation speed introduced after pellet formation at different time points; red arrows across table cells mark the time point of the shift.

Name	Agitation speed (RPM)					Morphology	
Time	0-23 h	27 h	31 h	35 h	39-97 h	52 h	68 h
↑850	150 →	600	600 →	850	850	3	1
↑600	150	150	150 →	600	600	3	1
↑250, late	150	150	150 →	250	250	6	4
↑350, late	150	150	150 →	250 →	350	3	2
↑250, early	150 →	250	250	250	250	6	5
↑350, early	150 →	250 →	350	350	350	5	3

Increase of agitation speed to 600 and 850 RPM

For cultivations with agitation speed increase to 850 and 600 RPM, the agitation speed was gradually increased from 150 RPM to 600 RPM over a period of 4 hours. The agitation speed was then further increased to 850 RPM during another 4 hours period for the respective cultivation. The particle size distribution of the two cultivations is provided in Figure 43 which illustrates the development of the morphology throughout the cultivations.

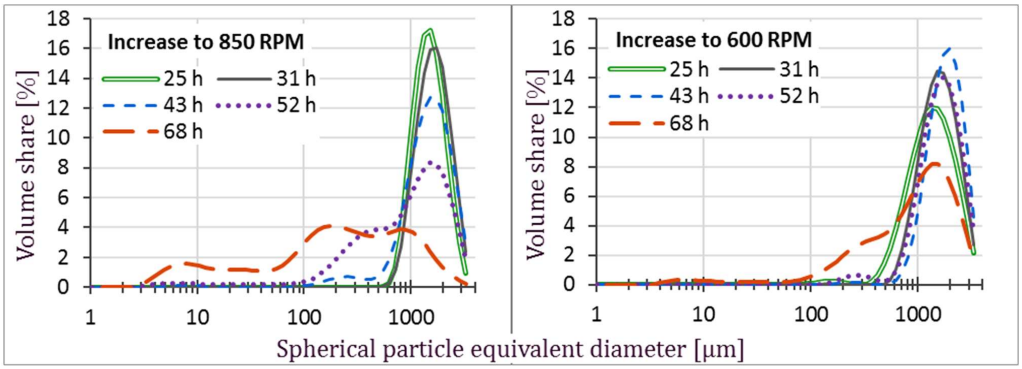

Figure 43: Particle size distribution for cultivations started under pelletising conditions with agitation speed increased from 150 RPM to 850 RPM and 600 RPM after respectively 23 and 31 hours of cultivation.

Pellets continued to grow in particle size after the agitation speed increase. Instead of reduced particle growth, pellets began to fracture leading to a rating of 3-4 on the morphology scale after 43 hours of cultivation.

A comparison with microscopy pictures in Figure 44 confirmed that both cultivation types with raised agitation resulted in combined dispersed and pelletised morphology 8 hours after their respective maximum agitation speed was reached (600 and 850 RPM). After 68 hours, both cultivation types were fully dispersed (morph. scale: 1).

Figure 44 also shows that the pellets lost their spherical shape. Instead, the shape became more elongated with long mycelia threads sticking out. This could be a result of the combination of the loose structure of the pellets and the increased impact of shear.

The loss of spherical shape observed with microscopic analysis also leads to a general questioning of the usefulness of the assessment of particle size with laser diffraction. The basic requirements of the technique (spherical particles being impervious to light) were not matched any longer. Particle size analysis with laser diffraction for this type of morphology should just be employed as an indicator of the development.

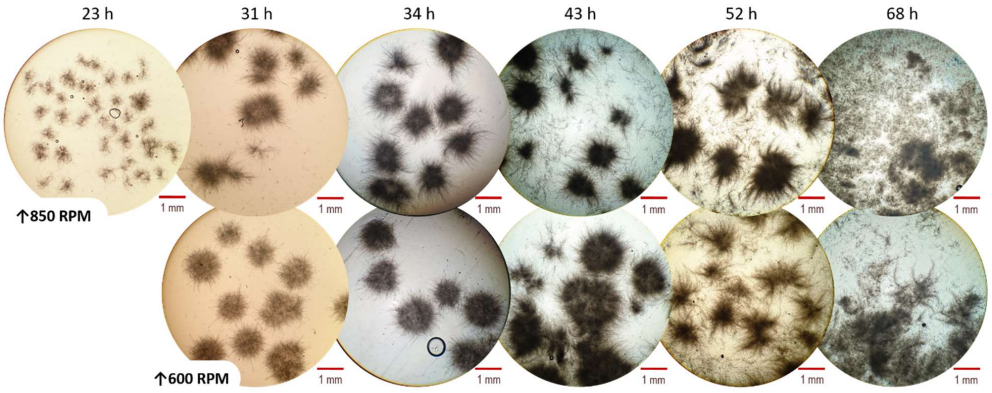

Figure 44: Microscopy pictures for cultivations started under pelletising conditions with agitation speed increased from 150 RPM to 850 RPM and 600 RPM after respectively 23 and 31 hours of cultivation; top row with increased agitation to 850 RPM after 23 hours at different time points; bottom row with increased agitation speed to 600 RPM after 31 h at different time points.

Increase of agitation speed to 250 and 350 RPM

To avoid breaking of the pellets, the agitation speed was increased to "just" 250 and 350 RPM. That was assumed to be a condition that resembles higher agitation speed conditions which should cause the formation of smaller and more compact pellets[28]. At 23 and 31 hours, respectively, the agitation speed was raised gradually with 100 RPM over a period of 4 hours.

While no major morphological difference could be observed between agitation speeds raised to 850 and 600 RPM respectively, the agitation speed increase to 250 and 350 RPM resulted in differences in the observed morphologies. Figure 45 depicts that pelletised growth was maintained after the shift. Cultivations with agitation speed raised to 250 RPM continued to grow pelletised (morph. scale: 6) after 52 h. In contrast, the pellets in cultivations with the agitation speed raised to 350 RPM fractured after 52 hours, scoring only between 3 and 5 on the morphology scale.

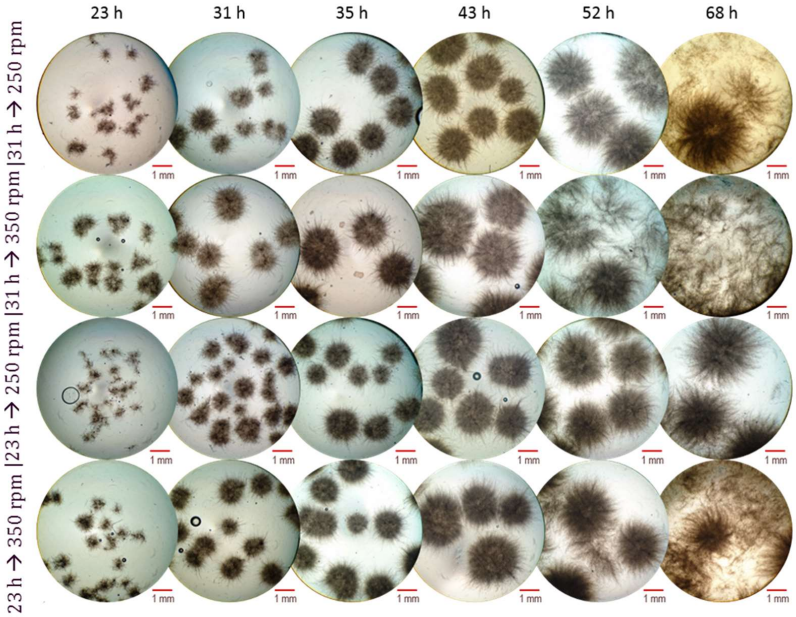

Figure 45: Microscopy pictures for cultivations started under pelletising conditions with agitation speed increased: top row with increased agitation to 250 RPM after 31 hours; second row bottom with increased agitation to 350 RPM after 31 hours, third row with increased agitation to 250 RPM after 23 hours and bottom row with increased agitation speed to 350 RPM after 23 hours.

At 23 hours, large aggregates were in the process of developing into pellets. Eight hours later, spherical pellets were formed with 2-3 times larger diameter than previously. It appears that the

smaller particles adapted to higher agitation (shift after 23 h) while applying higher agitation on larger pellets (shift after 31 h) induced fragmentation.

Visual inspection showed that pellets in cultures with later agitation increase were more hairy than the ones with late agitation increase. Especially in combination, i.e. a pellet with more hairy appearance and larger diameter, the pellet would be expected to be more prone to disintegration due to lower mechanical stability with long threads of mycelia sticking out of pellets. Hyphae could be sheared off and would then develop into dispersed growth. The pellets remaining intact and keeping their larger size could suffer from diffusion limitation and autolysis [76,138].

In consequence, it was not possible to create smaller or more shear resistant pellets of *Aspergillus niger* BO-1 by raising agitation speed after pellets were formed. However, the time point of the increase of agitation speed influenced fracturing of pellets which was not intended. It was expected that industrial production conditions provide a higher power input than the one applied in the experiments described here, meaning that power input as control handle for particle size control is not applicable here.

6.4.1.5 A. niger *BO-1 Added cellulose particles*

The purpose of adding particles into the cultivation is to confirm the impression from the industrial strain that the fungus prefers to attach to solids. Cellulose was chosen as it is indigestible to *A. niger*, in contrast to soy. Cellulose particles were added in concentrations from 0.05 to 50 g L^{-1}.

Figure 46 gives an overview of the differences in morphology achieved with the different cellulose concentrations. With a cellulose concentration of 50 g L^{-1}, mostly dispersed growth with small mycelial aggregates (morph. scale: 2) with a size about 80-90 µm in diameter could be created.

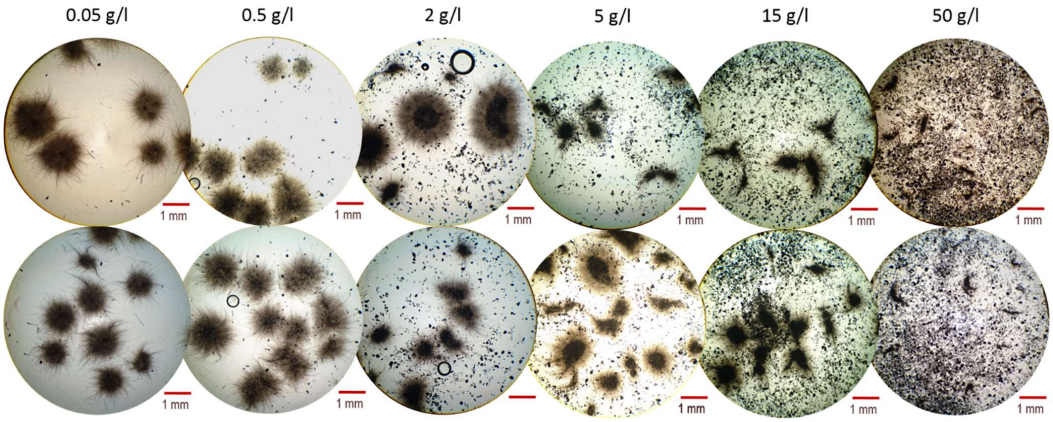

Figure 46: Microscopy pictures from preliminary shake flask cultivations with added cellulose particles to the medium; 2 pictures displayed after 40 hours per setup; the cellulose concentration added is stated above the images.

With a cellulose concentration of 15 g L^{-1} and 5 g L^{-1}, the aggregates became larger. Pellets, in contrast, are not frequently observed (morph. scale: 3-4). With 2 g L^{-1} of cellulose particles, large pellets with a diameter up to 3500 µm are formed along with small aggregates with a size down to 600 µm (morph. scale: 4).

Common for the three cultivations with 15, 5 and 2 g L^{-1} cellulose particles was that dispersed mycelium was rare while aggregates in a size range from respectively 425, 550 and 600 µm and up to above 3500 µm dominated the morphological development.

Cultivations with a cellulose concentration of 0.5 and 0.05 g L^{-1} resulted in distinct pelletised morphology (morph. scale: 6) with pellet diameters in a more limited range from 900 – 3200 µm.

6.4.2 *A. niger* BO-1 Biomass growth, morphology and enzyme activity

Differentiating morphology solely by addition of particles makes it possible to determine how the morphology affects growth and enzyme production. This is without changing parameters which possess high influence on productivity, like agitation and pH.

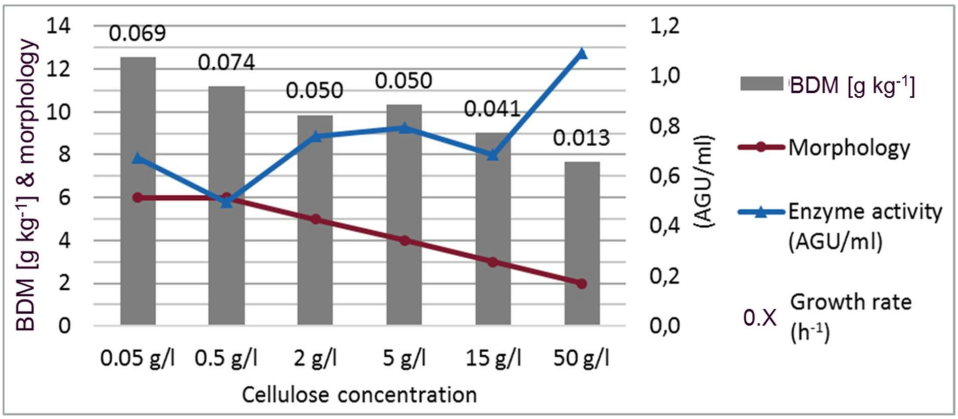

Figure 47: Graphic overview of BDM, morphological outcome per morphology scale, enzyme activity and growth rate. The cultivations experienced the same conditions in each shake flask with ½ MU-1 medium but with addition of different cellulose concentrations. The growth rate is indicated above the grey bars in h^{-1} units.

Figure 47 presents the BDM, enzyme activity and morphological outcome after 88 hours of shake flask cultivation. There was a tendency that growth rate is affected by the particle concentration.

Cultivations with the highest concentration of particles, i.e. dispersed growth, had the lowest bio dry matter concentration. Cultivations with low concentration of cellulose, i.e. pelletised growth, showed the highest growth rate. The enzyme activity was, in contrast to the growth rate, highest in the cultivations with highest particle concentration and lowest in the ones with low particle concentration. The activity difference was 60 %.

The enzyme activity and activity per biomass was proportional to the morphological development. The higher the number of larger pellets and the lower the extent of free mycelia was, the lower was the resulting enzyme activity. Driouch et al.[81] described the same tendency for the AB1.13 strain.

6.4.2.1 Activity development in function of dissolved oxygen tension

Figure 48 depicts the relation between dissolved oxygen tension (DOT) and enzyme activity per quantity of biomass dry matter for a series of cultivations discussed in section 6.4.1.4 . All

cultivation conditions were identical except for agitation speed. Along with the previously discussed cultivations initiated at 150 RPM with a subsequent raise of agitation speed to 250, 350, 600 and 850 RPM, respectively, cultivations were run with constant agitation speed of 150 and 600 RPM as well.

The best results in terms of activity development could be reached with higher agitation rates with the cultivations with constant speed of 600 RPM being superior. The second-best setup were cultivations with agitation speed raised from 150 to 850 RPM at the respective cultivation time points of 49 and 57 hours. In comparison to each other, it is striking that the 600 RPM became oxygen limited 8 h earlier after 49 h than cultivations shifted to 850 RPM. Despite these additional 8 h under oxygen limitation, the enzyme activity per BDM was 40 % higher with the 600 RPM constant agitation speed.

These two different agitation regimes resulted in different morphologies: The constant speed of 600 RPM results in distinct dispersed growth (morph. scale: 1) throughout the whole cultivation. In contrast, the low initial agitation of 150 RPM lead to pelleted growth which subsequently evolved into a mixed morphology between 34 and 43 hours (morph. scale: 6→4) and into dispersed growth between 52 and 68 hours (morph. scale: 3→1). The process of changes in the morphology have been discussed in section 6.4.1.4 and Figure 44 depicts the development.

In consequence, the morphology of the biomass is of greater importance for enzyme production than the DOT. The cultivation with most dispersed growth results in the highest enzyme productivity despite being oxygen limited first.

A similar observation can be made for cultivations with agitation speed raised to 350 RPM after 23 hours and 31 hours, respectively: The later up-shift in agitation speed after 31 h resulted in the occurrence of a DOT limitation that was 5 h earlier than in the experiment with the earlier agitation speed shift (after 23 h). The enzyme activity per BDM is though 34 % higher for the later shift.

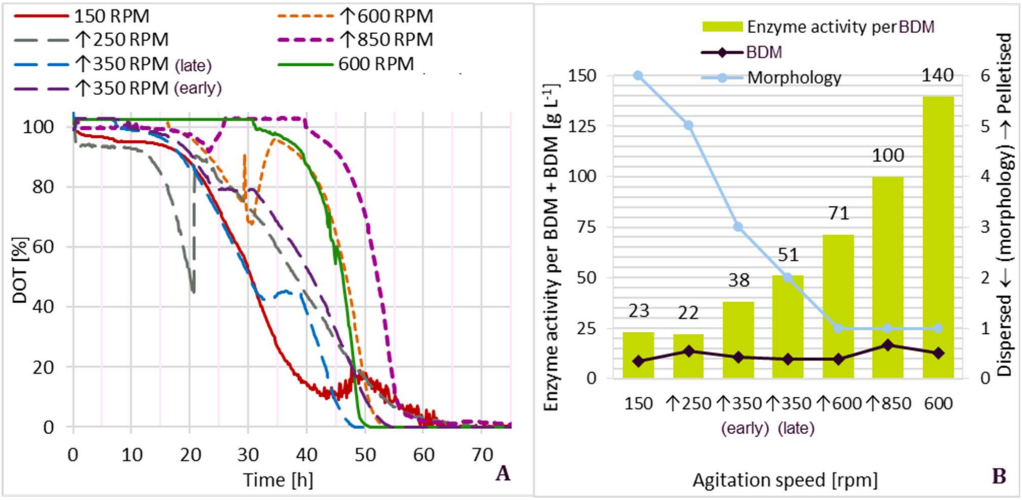

*Figure 48: Data from a series of experiments with identical fermentation conditions except for agitation speed: Constant agitation speed of 150 and 600 RPM, cultivations initiated with 150 RPM with agitation speed raised subsequently are indicated with an arrow (↑); **A** represents dissolved oxygen tension (DOT) as function of cultivation time, **B** represents enzyme activity per BDM and morphology for samples taken after 68 hours of cultivation.*

The only difference between these two cultivations was the point in time at which agitation speed has been raised. The later shift resulted in earlier fracturing of the pellets, and thus the cultivation was operated for a longer time with a more dispersed morphology.

6.4.2.2 Activity development after inoculation with pelleted and mycelial pre-cultures

Morphology appeared to be decisive for amylase production. To conclude on this, identical main cultivations are prepared which are inoculated with dispersed and pellet growing precultures, respectively. For better comparison in terms of DOT, the same setup was carried out at different agitation speeds. An overview over the setup is given in Table 8.

Table 8: Overview of cultivations inoculated with different morphologies; fermentation conditions are presented along with the expected (Exp.) and the observed morphology after 40 hours of cultivation per Figure 14; column 'Setup' indicates pre-cultures were carried out in shake flask (Sh. F.) defined after Table 5.

Pre-culture	Main cultivation			
Morphology of preculture	Agitation (RPM)	pH	Morphology	
			Expect.	Observed
Pelletised	150	4.8	6	6| Pelletised
Pelletised	250	4.8	5	5| Pelletised
Dispersed	150	4.8	2	3| Aggregates
Dispersed	250	4.8	1	2| Dispersed

Precultures were grown in shake flasks under the basis conditions for pelletised and dispersed growth provided in Table 5 with the exception that pH in the cultivation with dispersed growth was lowered to 3.5 for technical reasons. After 31 hours of cultivation, new shake flasks with fresh medium were inoculated with equal amounts of biomass from the precultures.

The top rows of the pictures in Figure 49 and Figure 50 present the morphological development of the pelletised inoculated cultivation. Cultivations inoculated with pelletised biomass maintained their pelletised morphology until 40 hours of cultivation with agitation speed at 250 RPM. Until 65 h, the morphology changed from pellets to dispersed growth (morph. scale: 5→3).

The cultivation with pelletised inoculum and agitation speed at 150 RPM developed large pellets up to 6000 µm in diameter in samples taken after 40 and 65 hours cultivation time. After 65 hours of cultivation, pellets began to fracture. The major part of the biomass remained pelletised (morph. scale: 5→4).

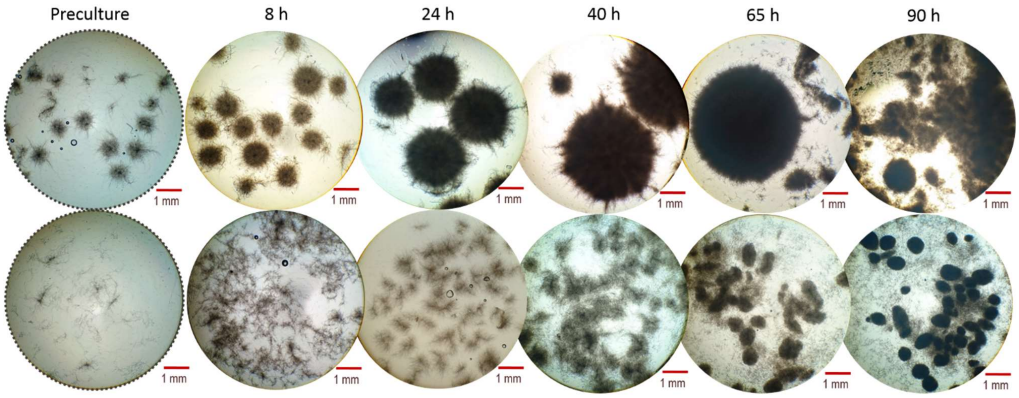

Figure 49: Microscopy pictures from cultivations inoculated with pelletised (top row) and dispersed (bottom row) precultures; pictures taken from samples from different time points as stated above the pictures; shake flask cultivations were running at 150 RPM.

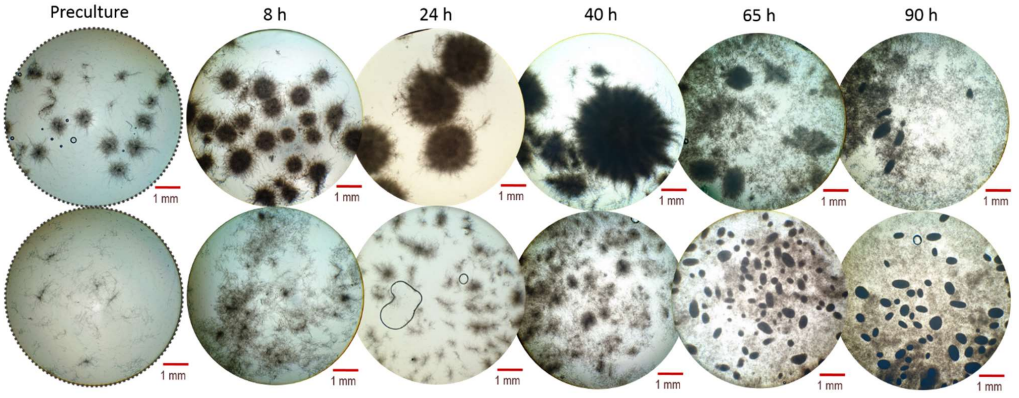

Figure 50: Microscopy pictures from cultivations inoculated with pelletised (top row) and dispersed (bottom row) precultures; pictures taken from samples taken at different time points as stated above the pictures; shake flask cultivations were running at 250 RPM.

The bottom rows of pictures in Figure 49 and Figure 50 present the morphological development of the dispersed inoculated cultivation at the respective agitation speeds of 150 and 250 RPM. After 40 hours, the mycelium in the main cultivations inoculated with dispersed growing preculture clumped together and forms aggregates. After 65 hours, small, dense oval, pellets began to form at both agitation speeds.

Dispersed mycelia were still present at this point (morph. scale: 4). The agitation speed of 250 RPM resulted in smaller and denser clumps: The sizes of the pellets at 150 RPM reach from 200 to 800 µm in diameter compared to 100 to 700 µm at 250 RPM.

Figure 49 and Figure 50 depict that the morphological development resulted in a mixture, dominated by dispersed mycelium with aggregates and/or pellets. The obtained morphology across the trials was not alike.

Figure 51 presents the morphological development, the bio dry matter (BDM) concentration and the enzymatic activity (AGU) during the cultivations inoculated with pelletised and dispersed preculture.

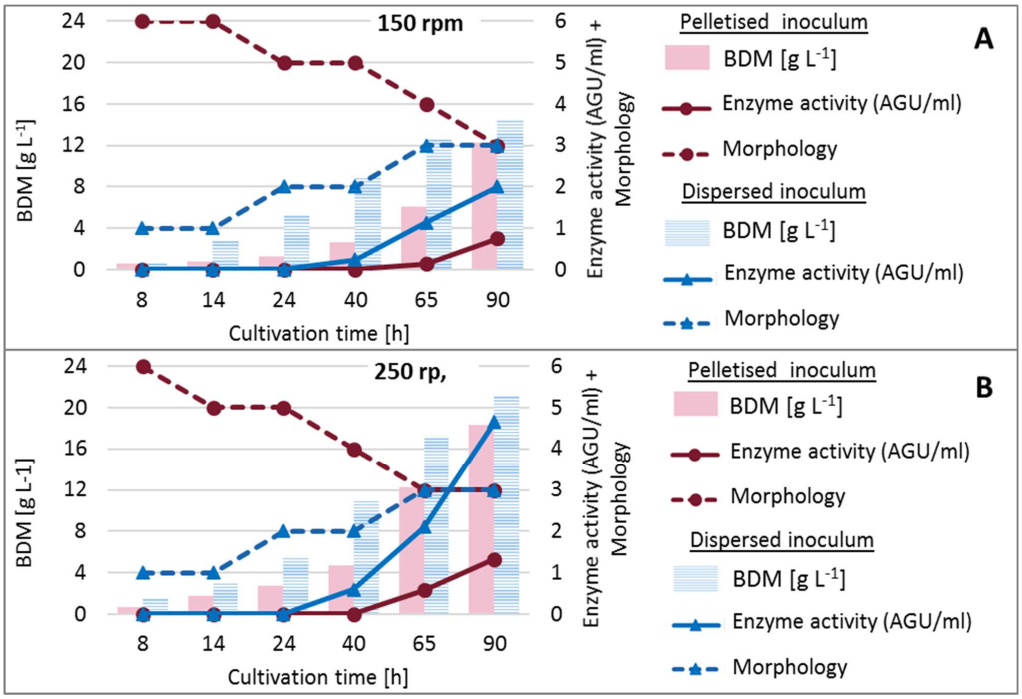

*Figure 51: BDM, enzyme activity and morphology plotted as function of time for the cultivations inoculated with pelletised biomass (red, circle marker) and dispersed biomass (blue, triangle marker); **A** represents an agitation speed of 150 RPM, figure **B** represents cultivations with an agitation speed of 250 RPM.*

According to Figure 51, the BDM concentration after 40 h was 2 to 3-fold higher for cultivations which were inoculated with dispersed mycelium compared to pellets. It was maybe a result of inferior biomass development that activity development has not been initiated at this point in time with the pelletised inoculum.

After 65 hours, the enzyme activity was more than 3.5 times higher in dispersed inoculated cultivations than for pelletised inoculated cultivations run with an agitation speed of 250 RPM.

For cultivations running at 150 RPM, enzyme activity with dispersed inoculum reaches 8 times higher values than for pelletised inoculated cultivations.

Between 40 and 65 h at 250 RPM and between 65 and 90 hours at 150 RPM, the differences in BDM concentration became lower. It could be caused by the higher growth rate of the dispersed inoculated cultures that led to oxygen limitation earlier. The pelletised inoculated cultivation thus got time to "catch up".

In general, the cultivations performed better at 250 RPM. The bio dry matter content was 31 % improved when inoculated with dispersed biomass, and even 50 % for pelleted inoculum. The activity trend followed the general biomass development which was improved to 140 % (dispersed inoculum) and 33 % (pelletised inoculum), respectively.

There is a clear correlation to the power input and it can be argued that the underlying cause is higher OTR achieved with higher agitation. According to literature[139], especially the high viscosity prone disperse cultivation should benefit from better mixing which is confirmed in the experiments.

To emphasize the difference between the different inoculum morphologies, the activity per bio dry matter was calculated as a condensed version of the comparison in Figure 51. The result is given in Figure 52. Cultivations with dispersed inoculum at 250 RPM reached three-fold higher enzyme production per biomass after 90 hours of cultivation than pelleted inoculum. That result was obtained despite the occurrence of oxygen limitation (see section 6.4.2.1).

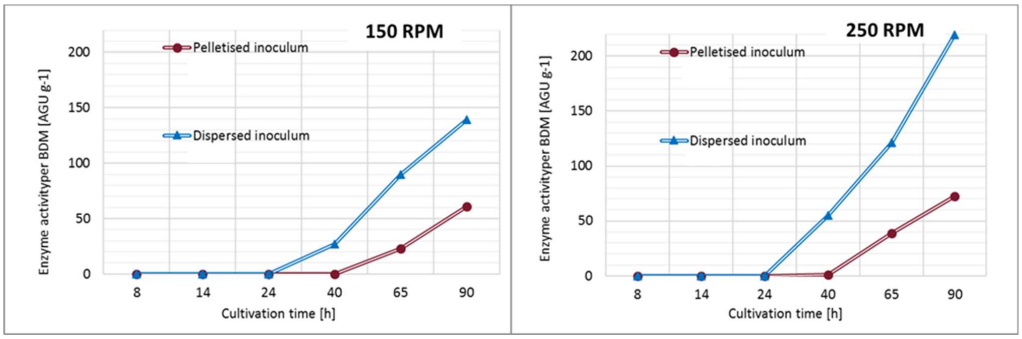

Figure 52: Enzyme activity per BDM plotted as function of time for the cultivations inoculated with pelletised biomass (red, circle marker) and dispersed biomass (blue, triangle marker). The graph to the left represents cultivations with an agitation speed of 150 RPM, the graph to the right represents cultivations with an agitation speed of 250 RPM.

Summarizing both figures (Figure 51 & Figure 52), it can be stated that the level of agitation has impact on the biomass growth rate and enzyme production of *A. niger* BO-1. A more pronounced effect can though be achieved by inoculating with different morphologies.

The impact can be seen in measured enzyme activity (Figure 51). It is even clearer when employing enzyme activity per BDM (Figure 52). Both enzyme activity and enzyme activity per BDM are higher for the dispersed morphology than for the pellets under the respective agitation regimes. Interestingly, the low agitated dispersed cultivation reaches higher values in both enzyme activity and enzyme activity per biomass.

6.5 Overall result

The most striking result across the strain comparison is how much their respective behaviour towards different environments or changes therein varies. After all, all 3 strains tested belong to the same genus, *Aspergillus niger*. Table 9 gives an overview over the strains that were studied, and the respective experiments and results.

In terms of morphology, the strain AB1.13 is the best investigated one with publications from several scientists[e.g. 19,25,29,74,80,81,140]. Strain BO-1, in contrast, is well investigated in terms of its metabolic aspects and production of amylase[e.g.20,103,119,124,141,142]. It must be pointed out that the

focus of this work is on morphological engineering to enforce either freely dispersed growth or formation of pellets with a (application) defined maximum particle diameter and structure.

*Table 9: Overview over all three Aspergillus niger strains, the tested factors and their respective impact on morphology; fields marked with * are tested and described in this report*

Factors	***A. niger* AB1.13**		***A. niger* production**		***A. niger* BO-1**	
	tested	impact	tested	impact	tested	impact
Initial conidia conc.	Yes*,[25,97]	Low on pellet size	Yes*	No	Yes*	Low
pH	Yes*	Major on conidial aggregation	Yes*	Major on growth (does not grow below pH 5)	Yes*	Low on morphology
Power input	Yes*,[25,29]	Major on pellet size development	No	–	No	Major on aggregate formation
Particles	Yes[143]	Major on conidial aggregation	Yes*	Potential reason for mixed morphologies	Yes*	Major to prevent biomass aggregation
Media	No	–	No	–	Yes*	No (most effect of media derives from particles)
Molality/salt content	Yes[80]	Major on pellet size development	Yes*	Slower growth	No	–
productivity	Yes[27,144]	Lower in bigger particles	NA	–	Yes*	Pellets were inferior for amylase production

First after observing the interesting failure of applying the AB1.13 settings to both the industrial strain and the BO-1 wildtype reference, did the question of productivity related preferences of the morphology become more important to answer.

To summarize: *A. niger* AB1.13 grows best at pH 3 with highest biomass formation in a dispersed morphology while pH 5 induces pelleted growth with just 30 % biomass. A shift from pH 3 to 5.5 can be considered the best way to achieve pellets of defined diameter and density.

Other parameters like power input and initial spore concentration are inferior to pH in shaping morphology but could be applied for tuning. The bigger the particles grow, the more influential becomes the effect of power input. Salt content/molality and addition of particles have also been tested but are not included in the conception of morphology engineering in Figure 10.

Applying the achieved AB1.13 knowledge about designed particle size/morphology in general on a production strain couldn't be called successful as the industrial strain did not grow at pH values below 5. ζ– (zeta–) potential measurements showed that pH 6 might feature the same repulsion behaviour between the conidia. An effect could indeed be observed but model conception failed, mainly because the propagated two-staged aggregation[26] did not happen (to the expected degree).

It was concluded that the particles contained in the media could be the course for the resulting mixed morphologies. At least, the trends of getting a higher content of mycelia and pellets, respectively, could be confirmed which includes the findings of high osmolality.

The background of the industrial strain is "classic strain optimisation". It is known that this might result in some different behaviour based on the "out-of-phase" phenomenon[145,146]. The unspecified background nature is shared with AB1.13. Therefore, the known wildtype BO-1 was chosen for a second series of evaluation experiments. Planned as the decisive strain, it responded to changes in its environment in a different way.

Yet again and like the industrial strain, the pH did not play a decisive role for morphogenesis of the strain BO-1. In contradiction to the AB1.13 findings, more pellets were formed at lower pH

values for the BO-1 strain. Most experiments ended in mixed morphology with a tendency towards one of the extreme forms.

It was, however, possible to differentiate the biomass into only dispersed mycelia and only pellets. Pellets could only be achieved with – in industrial terms unrealistically – low agitation[147]. For BO-1, the two-staged aggregation process from the lab strain AB1.13 could not be repeated. Conidial aggregation could though be observed in one cultivation meaning that there is aggregation potential but it does not play a major role for this strain.

Two out of the three tested strains did not show the two-staged aggregation that was described earlier. To put the melanin desorption model (Figure 31, section 6.1.4) in focus: Wargenau et al. did several investigations on the ζ-potential of AB1.13 and calculated the electrical charge[148,149].

The investigation confirmed the melanin desorption model and this study's findings that conidial aggregation could be prevented at a low pH of 2 while pH 5 showed a maximum of this phenomenon. Introducing a ζ-potential dependent degree of ionization in the surface coating (i.e. melanin), the thickness of the layer decreased with increasing pH. Their statement is that aggregation of conidia is more an electrostatic effect than a physiological one. However, melanin desorption and electric repulsion/attraction should be universal and hence detectable for all strains.

Alternatively, instead of the melanin, a structural change of rodlets might be the cause for the observed behaviour. The rodlets of conidia are usually described as self-assembling amphipathic proteins/amyloids which include the hydrophobins[150,151]. The purpose is manifold, but of main interest is their ability as surfactant and their respective feature of hydrophobicity. If the AB1.13 suffers a mutation which increases the latter, it could be a reasonable explanation for the increased aggregation rates observed with AB1.13 compared to the industrial and BO-1 strains.

Addition of indigestible cellulose particles to BO-1 cultivations could be used to enforce a certain morphology. These experiments gave indications that a morphology with dispersed mycelia was the superior morphology in terms of producing glycoamylase. A decisive test with dispersed and

pelleted pre-cultures proved a higher amylase production per bio dry matter when dispersed morphology is applied, even if the cultivation suffers from oxygen limitation.

Chapter 7: Conclusions

7.1 *Aspergillus niger* AB1.13

The introduction of this thesis describes the possibilities of value creation with microbiological and biotechnological processes as well as the challenges related to this approach. Therein, the focus lies in the control of the morphology of the cultures.

Control of the morphology of a culture can be achieved with the help models describing the system. The models incorporate the knowledge of different biomass aggregation mechanisms. This includes the coagulative conidiophores in respect to the fermentation parameters like pH of the culture, the mechanical power input and the initial conidiophore concentration.

Most of the published growth models are limited to the micromorphology like the tip growth[56], avoidance of food spoilages by *Aspergilli*[152] or the description of human infection pathways[153]. Newer papers that cover the macro-morphology that occurs in stirred tank reactors[154] are often based on the work of Grimm[25] and Kelly[29]. The time gap between both models has previously been discussed. Because of the gap, the complete fermentation process is not covered by these models.

The present work closes the time gap in terms of metrology and ideology and matches therefore the requirements posted in the introduction:

Particle size analysis

The method used for measuring particle sizes is laser diffraction analysis. It is well established in inorganic processes (concrete, toner particles). Within biotechnology, this method is rather unknown and means entering a new area of research. It has successfully been shown that microbiological cultures of *A. niger* can be characterized by means of particle size distributions created with laser diffraction.

The sensitivity of the methods is so good that swelling of the spores during the lag phase could be detected. Despite the small size and the usage of the volume distribution, spores could be detected throughout fermentations under the applied settings.

Effects of the pH value on *A. niger* AB1.13 conidiophores and growing biomass could successfully be demonstrated. Furthermore, it is not only possible to record and visualize particle size distribution, but also to track the changes in morphology online. This feature has not yet been reached by any other optical method[20,155].

The further course of the cultivation could also be tracked in terms of particle size information by splitting the bi-modal distribution into modes. This enables to follow the formation of aggregates in dependency of the pH. The comparison of the modes, *conidiophores* and *pellets*, of each experimental set-up can be visualized in easily understandable graphs and is therefore well suited for further trials aiming at detailed characterization of the biomass status inside a bioreactor.

Confirming & extending Grimm's and Kelly's models

Due to the employed analysis methods and the conducted experiments, the previously published findings of Grimm and Kelly could be confirmed. The gap in fermentation time left by their works could be closed.

Furthermore, the question of a hypothetical third aggregation step of the biomass as a hyphae-hyphae interaction could positively be answered by circumstantial evidence. The existing aggregation model for spores of the organism *A. niger* AB1.13 could be extended. Deeper investigation of the primary aggregation in terms of a population balance is not possible though due to that fact that laser diffraction is a counting measurement method.

The now developed model should enable to predict and control the target parameters bio dry matter and particle size of cultivations without introducing substances as aggregation seeds into the process[143], which might otherwise cause issues in downstream processing. An application could, for example, be an improved seed tank for biotechnological production. Optimized

biomass concentrations in the desired morphology could be achieved by using the settings given by the control model.

The underlying idea is that optimal growth in seed tanks would lead to a reduced lag phase of the inoculated main fermenter. This would directly translate into increased productivity as well as optimal use of costly fermentation capacity.

Different cultivation parameters have been evaluated in terms of their impact on the growth of *A. niger* AB1.13 cultivations. The tendencies can be summarized as follows:

- Cultivation pH 3 results in disperse biomass. pH 5.5 results in pelleted biomass. Changing pH from 3 to 5.5 will make biomass aggregate.
- pH 3 for the complete cultivation period leads to non-swollen and non-germinated conidia being detectable with laser diffraction until the end of the cultivation. This confirms the two-staged aggregation model for pH 5.5[30] and its circumvention at pH 3.
- Cultivations with initial pH of 3 result in an up to 3 times higher concentration in biomass even if pH is shifted to pH 5.5 later during the cultivation. This is fundamental for all growth dependent functions of the cell, like for example the production of enzymes in industry.
- With increasing pellet size, further growth is found to be dependent on the mechanical power input. There is a minimum threshold in power input as 25 W m^{-3} (150 min^{-1}) has led to insufficient mixing with less biomass growth.
- Aggregates/pellets with bigger particle size and higher bio dry matter content might pass beyond the particle size recommendations as diffusion limitations inside the pellet might occur[156]. Being more susceptible to mechanical power input, particle size controlled agitation could ensure that pellets with a pre-defined size will grow slowly in diameter[28].
- The melanin desorption is correlated to the pH value of the broth: The AB1.13 spores lose their melanin layer at a pH of 5.5 and an increased aggregation can then be observed consequently.
    - Aggregation of the spores can thus be avoided by starting the fermentation at a pH of 3 and increasing to the desired pH after germination. The shift should take place

before the exponential growth phase as developed biomass requires longer adaptation time.

7.2 Production strain

When the AB1.13 settings are applied to the industrial strain, it followed the same trend like biomass growing as pellets at pH 5.5. It comes as a surprise that this strain does not seem to be able to thrive or even germinate at pH 3.

Employing the results from the AB1.13 ζ-potential measurement (Figure 30), pH 5 or 6 should be similarly suited for dispersed growth of the industrial strain. The respective ζ-potentials are -5.8 and 6 mV, where both values are almost equally far away from 0 mV at pH 5.5. A decrease in pH to 5.0 does not influence morphology while pH 6 successfully shifted the morphology to mostly dispersed.

The main conclusion from the previous two paragraphs is though that the chosen strain does not show "pure" growth as dispersed mycelia or pelleted biomass. Instead, mixed morphology with tendencies in one or the other direction is observed.

A threefold increase in the spore inoculum concentration at pH 6 does not maintain or promote mycelial growth. Instead, larger pellets could be observed which remained throughout the fermentation. Their number and size decreased towards the end when some form of fragmentation happened.

It could be shown that the large pellets do not result in oxygen limitation in the bulk phase, thereby conforming known facts about viscosity and oxygen transfer[62].

A general connection could be made between oxygen limitation and the production of polyols which should be lower in the presence of oxygen[119], and which in turn promotes organic acids production. The latter has been seen for the academic AB1.13 strain while the production strain formed glycerol, probably as overflow metabolite. It could be argued whether this is due to the partly pelleted morphology with particle internal transport limitation or a trait of this particular strain.

The changes made in pH, osmolality and inoculum concentration impact the metabolism and growth profiles of the cells. This cannot be said in relation to morphology. It has not been possible to prevent pellet formation through the applied means. All of this signifies the complexity of submerged fermentations with filamentous fungi in industrial environments where the impacts described in the literature do not necessarily suit, also if the strains belong to the same genus.

7.3 *Aspergillus niger* BO-1

The study of the wild type strain *Aspergillus niger* BO-1 is intended to verify the model built on the lab strain AB1.13 and to avoid discussions about the genetic (unknown) lineage of the production strain. The focus has been on creating small pellets with a diameter below 1000 µm and to double-check if there is a difference in productivity between dispersed growth and pelleted growth in submerged fermentation.

As for the other strains, parameters stated in the model are employed to pursuit the purpose:

- pH screening
- 10 times increase of initial conidia concentration
- Two different media with one containing particles
- Addition of particles in several concentrations in the else particle free medium
- Agitation speed at four different levels
    - Two different points in time with agitation speed increase

The pellets resulting from "normal" pelletised growth conditions turn into a loose and hairy structure and are vulnerable to an agitation speed of 350 RPM or higher in shake flasks. In general, it is rather difficult to achieve the same clear pelletised morphology as for the AB1.13 lab strain. In contrast to the lab strain, the most influencing factor is power input (and not pH).

The ½ MU-1medium employed for this strain contains 130 g L^{-1} maltodextrin which means a 10-fold higher concentration of C-source compared to the lab strain. This is a considerable difference to the reported media (this work's AB1.13 media & [26,27,80,97,143]), but here is should be mentioned

that the C-source has though not been reported as differentiator for morphology. Also, pH effects on morphology are adverse as lower pH of 3.2 resulted in "better" pelleted growth while the higher pH of 4.2 resulted in a higher free mycelial content which is a contradiction of the AB1.13 findings of lower pH being beneficial for mycelial growth by skipping conidial aggregation.

Conidia aggregation could though be observed in a single cultivation with particle free MLC medium (soybactone instead of soy). Here, the two-staged aggregation could be confirmed by microscopic analysis. However, it can be concluded that the BO-1 strain is capable of conidial aggregation under special circumstances that could not be deeper investigated in this study.

This finding though paved the way for pellet-engineering with cellulose particles. As *A. niger* is incapable of digesting cellulose, particles enable investigation of morphological effects on enzyme production without changing parameters affecting productivity. The result is that amylase production is enhanced when the fungus growth is freely dispersed.

Dissolved oxygen tension is crucial to enzyme production[37]. Pelletised growth leads to delayed DOT declination in a cultivation compared to dispersed growth. Still, cultivations with more dispersed growth develop higher AGU activity at the end of the cultivation, even when oxygen limitation set in earlier. Dispersed mycelial growth has a higher positive effect on productivity than the availability of oxygen.

In conclusion, there are two major results from studies with the BO-1 strain:

1. It is not possible to control pellets size in the sense of the model developed with the lab strain *A. niger* AB1.13.
    - Limiting the pellet size below 1 mm (the maximum diameter for avoiding internal substrate limitations) has failed.
    - The initial morphology would not be maintained under production conditions as the pellets fracture quickly under high shear. In contrast, dispersed mycelia also develop some type of (elongated) pellet.

2. Morphology has the major effect on enzyme productivity. It is more pronounced than DOT and agitation. Dispersed mycelia are considerably more productive than fluffy pellets and other aggregates developed in this study.

7.4 Overall conclusion

It is possible to employ laser diffraction as a tool to monitor submerged fungal cultivations: Effects of the pH value on *A. niger* AB1.13 conidiophores and growing biomass could successfully be demonstrated. The sensitivity of the method is so good that swelling of the spores during the lag phase could be detected. Despite their small size and the usage of the volume distribution, conidia could be detected throughout all conducted fermentations with circumvented primary aggregation.

The further course of the cultivation could also be tracked in terms of particle size information by splitting the bi-modal distribution into its modes. This enables to follow the formation of aggregates as a function of pH. The comparison of the modes, *conidiophores* and *pellets*, of each experimental set-up can be visualized in easily understandable graphs and is therefore well suited for further experiments on characterization of the biomass status inside a bioreactor.

A. niger is known to be a spore aggregating species under submerged cultivation and thereby forms coagulating pellets [26,76,81]. Many recently published investigations are based on the AB1.13 strain and its well described aggregating behaviour. The results achieved in this study reveal that two other strains of the same genus, *Aspergillus niger*, one production strain and one wild type strain, do not show this pronounced conidia aggregation behaviour. Consequently, it can be concluded that conclusions reported for the AB1.13 strain cannot be extrapolated to other strains, even if these strains are from the same genus.

Without the conidial aggregation, the onset of pellet formation[26,76,81] is omitted and hence, also in accordance to the morphology control model (Figure 10, section 4.3), more mycelial growth could be observed with a tendency towards formation of mixed morphologies.

The general conclusion in terms of morphology is that strains of the same genus might react differently to changes in the environome and hence the advice for production purposes is to do individual tests. The arguments supporting this conclusion are the rather unspecific effects of classical strain optimization which usually includes random mutagenesis and screening[146], or side effects of genetic manipulations[124].

In terms of productivity, not much recent literature is available[92] which means that there has not been a clear answer on how much morphology matters for enzyme production. The discussion usually is about balancing oxygen mass transfer into the liquid phase which is improved with lower viscosity if the biomass comes in the shape of pellets or if the number of growing tips enhances the production and secretion of enzyme.

The conclusion from the conducted experiments is clear: Dispersed mycelia is the superior morphology for producing enzymes with wildtype *Aspergillus niger*. Moreover, it could be demonstrated that morphology is more important than the dissolved oxygen tension.

Literature

1. van Leewenhoeck, A. & de Graaf, R. A Specimen of Some Observations Made by a Microscope. *Philos. Trans. B* **8,** 10–92 (1673).

2. Pasteur, L. Mémoire sur la fermentation alcoolique. *Ann. Chim. 3e Ser* **58,** 323–426 (1860).

3. Currie, J. N. The citric acid fermentation of *Aspergillus niger*. *J Biol Chem* **31,** 15–37 (1917).

4. Hirche, C. *Weiße Biotechnologie - Chancen für die chemische Industrie*. (2006).

5. Papagianni, M. Advances in citric acid fermentation by *Aspergillus niger*: Biochemical aspects, membrane transport and modeling. *Biotechnol. Adv.* **25,** 244–263 (2007).

6. Papagianni, M. Fungal morphology and metabolite production in submerged mycelial processes. *Biotechnol. Adv.* **22,** 189–259 (2004).

7. Punt, P. J. *et al.* Filamentous fungi as cell factories for heterologous protein production. *Trends Biotechnol.* **20,** 200–206 (2002).

8. Aracil, J., Vicente, M., Martinez, M. & Poulina, M. Biocatalytic processes for the production of fatty acid esters. *J. Biotechnol.* **124,** 213-–223 (2006).

9. Snajdrova, R. *et al.* Nitrile biotransformation by *Aspergillus niger*. *J. Mol. Catal. B Enzym.* **29,** 227–232 (2004).

10. Kardinahl, S., Rabelt, D. & Reschke, M. Biotransformation: Von der Vision zur Technologie! *Chemie Ing. Tech.* **78,** 209–217 (2006).

11. Naundorf, A., Melzer, G., Archelas, A., Furstoss, R. & Wohlgemuth, R. Influence of pH on the expression of a recombinant epoxide hydrolase in *Aspergillus niger*. *Biotechnol. J.* **4,** (2009).

12. Savitha, S., Sadhasivam, S., Swaminathan, K. & Lin, F. H. Fungal protease: Production, purification and compatibility with laundry detergents and their wash performance. *J. Taiwan Inst. Chem. Eng.* (2010).

13. Fang, X., Shen, Y., Zhao, J., Bao, X. & Qu, Y. Status and prospect of lignocellulosic bioethanol production in China. *Bioresour. Technol.* **101,** 4814–4819 (2010).

14. Xu, Q., Li, S., Huang, H. & Wen, J. Key technologies for the industrial production of fumaric acid by fermentation. *Biotechnol. Adv.* **30,** 1685–96 (2012).

15. Wohlgemuth, R. Biocatalysis-key to sustainable industrial chemistry. *Curr. Opin. Biotechnol.* **21,** 713–724 (2010).

16. Choi, J. M., Han, S. S. & Kim, H. S. Industrial applications of enzyme biocatalysis: Current

status and future aspects. *Biotechnol. Adv.* **33,** 1443–1454 (2015).

17. Franssen, M. C. R., Steunenberg, P., Scott, E. L., Zuilhof, H. & Sanders, J. P. M. Immobilised enzymes in biorenewables production. *Chem. Soc. Rev.* **42,** 6491 (2013).

18. Elander, R. P. Industrial production of ß-lactam antibiotics. *Appl. Microbiol. Biotechnol.* **61,** 385–392 (2003).

19. Emmler, M. Freisetzung von Glucoamylase in Kultivierungen mit *Aspergillus niger.* (IBVT-Schriftenreihe, FIT-Verlag, Paderborn, zugl. Dissertation: TU Braunschweig, 2007).

20. Petersen, N., Stocks, S. & Gernaey, K. V. Multivariate Models for Prediction of Rheological Characteristics of Filamentous Fermentation Broth From the Size Distribution. *Biotechnol. Bioeng.* **100,** 61–71 (2008).

21. Quintanilla, D., Hagemann, T., Hansen, K. & Gernaey, K. V. in *Filaments in Bioprocesses* (eds. Krull, R. & Bley, T.) 29–54 (Springer International Publishing, 2015). doi:10.1007/10_2015_309

22. Integration gen- und verfahrenstechnischer Methoden zur Entwicklung biotechnologischer Prozesse 'Vom Gen zum Produkt'. in (Deutsche Forschungsgemeinschaft, 2007).

23. Mattern, I. E. *et al.* Isolation and characterization of mutants of *Aspergillus niger* deficient in extracellular proteases. *Mol. Genet. Genomics* **234,** 332–336 (1992).

24. Grimm, L. H., Kelly, S., Krull, R. & Hempel, D. C. Morphology and productivity of filamentous fungi. *Appl Microbiol Biotechnol* (2005). doi:10.1007/s00253-005-0213-5

25. Grimm, L. H. Sporenaggregationsmodell für die submerse Kultivierung koagulativer Myzelbildner. (Institut für Bioverfahrenstechnik, Technische Universität Carolo Wilhelmina zu Braunschweig, 2006).

26. Grimm, L. H., Kelly, S., Hengstler, J., Göbel, A. & R. Krull, D. C. H. Kinetic Studies on the Aggregation of Aspergillus niger conidia. *Biotechnol. Bioeng.* **87,** 213–218 (2004).

27. Kelly, S. *et al.* Agitation effects on submerged growth and product formation of *Aspergillus niger*. *Bioprocess Biosyst. Eng.* **26,** 315–323 (2004).

28. Kelly, S., Grimm, L. H., Bendig, C., Hempel, D. C. & Krull, R. Effects of fluid dynamic induced shear stress on fungal growth and morphology. *Process Biochem.* 315–323 (2006). doi:10.1016/j.procbio.2006.06.007

29. Kelly, S. Fluiddynamischer Einfluss auf die Morphogenese von Biopellets filamentöser Pilze. (Institut für Bioverfahrenstechnik, Technische Universität Carolo Wilhelmina zu Braunschweig, 2006).

30. Grimm, L. H., Kelly, S., Völkerding, I. I., Krull, R. & Hempel, D. C. Influence of Mechanical Stress and Surface Interaction on the Aggregation of *Aspergillus niger* Conidia. *Biotechnol. Bioeng.* **VOL. 92,** 879–888 (2005).

31. Lin, P. J., Scholz, A. & Krull, R. Effect of volumetric power input by aeration and agitation on pellet morphology and product formation of A*spergillus niger*. *Biochem. Eng. J.* **49,** 213–220 (2010).

32. Bentz, D. P., Garboczi, E. J., Haecker, C. J. & Jensen, O. M. Effects of cement particle size distribution on performance properties of Portland cement-based materials. *Cem. Concr. Res.* **29,** 1663–1671 (1999).

33. Concessio, N. M., Van Oort, M. M., Knowles, M. R. & Hickey, A. J. Pharmaceutical Dry Powder Aerosols: Correlation of Powder Properties with Dose Delivery and Implications for Pharmacodynamic Effect. *Pharm. Res.* **16,** 828–834 (1999).

34. Hofmann, M. P. Physikalische Charakterisierung von Calciumphosphat-Pulvern zur Einstellung von Prozessparametern für die Herstellung von Knochenzement. (Julius-Maximilian-Universität Würzburg, 2003).

35. Lartiges, B. S. *et al.* Composition, structure and size distribution of suspended particulates from the Rhine River. *Water Res.* **35,** 808–816 (2001).

36. Hagemann, T., Ringel, A. K., Lin, P.-J., Hempel, D. C. & Krull, R. Tagungsband zur VAAM-Jahrestagung 2007: Osnabrück, 1. - 4.April 2007 ; program and abstracts. in *Changes in* Aspergillus niger *morphology towards shifted pH values* (Spektrum, 2007).

37. Ghobadi, N., Ogino, C., Yamabe, K. & Ohmura, N. Characterizations of the submerged fermentation of *Aspergillus oryzae* using a Fullzone impeller in a stirred tank bioreactor. *J. Biosci. Bioeng.* **123,** 101–108 (2017).

38. Farrán, A. *et al.* Green Solvents in Carbohydrate Chemistry: From Raw Materials to Fine Chemicals. *Chem. Rev.* **115,** 6811–6853 (2015).

39. Dobrev, G. *et al.* Lipase biosynthesis by *Aspergillus carbonarius* in a nutrient medium containing products and byproducts from the oleochemical industry. *Biocatal. Agric. Biotechnol.* **4,** 77–82 (2015).

40. Kocsubé, S. & Varga, J. in *Mycotoxigenic Fungi: Methods and Protocols* (eds. Moretti, A. & Susca, A.) 131–140 (Springer New York, 2017). doi:10.1007/978-1-4939-6707-0_7

41. Munk, K. & Eikmanns, M. *Mikrobiologie*. (Spektrum, Akad. Verl., 2001).

42. Samson, R. A., Hong, S. B. & Frisvad, J. C. Old and new concepts of species differentiation in Aspergillus. *Med. Mycol.* **44,** 133–148 (2006).

43. Norvell, L. L. Fungal nomenclature 1. Melbourne approves a new Code. *Mycotaxon* **116,** 481–490 (2011).

44. Samson, R. A. *et al.* Studies in Mycology. *Stud. Mycol.* **78,** 141–173 (2014).

45. Kocsubé, S. *et al. Aspergillus* is monophyletic: Evidence from multiple gene phylogenies and extrolites profiles. *Stud. Mycol.* **85,** 199–213 (2016).

46. Houbraken, J. & Samson, R. A. Current taxonomy and identification of foodborne fungi. *Curr. Opin. Food Sci.* **17,** 84–88 (2017).

47. Schoch, C. L. *et al.* Nuclear ribosomal internal transcribed spacer (ITS) region as a universal DNA barcode marker for Fungi. *Proc. Natl. Acad. Sci.* **109,** 6241–6246 (2012).

48. Visagie, C. M. *et al.* Identification and nomenclature of the genus *Penicillium*. *Stud. Mycol.* **78,** 343–371 (2014).

49. Abarca, M. L., Accensi, F., Cano, J. & Cabañes, F. J. Taxonomy and significance of black aspergilli. *Antonie Van Leeuwenhoek* **86,** 33–49 (2004).

50. Atoui, A. & Khoury, A. El. in *Mycotoxigenic Fungi: Methods and Protocols* **1542,** (2017).

51. Znidarsic, P. & Pavko, A. The Morphology of Filamentous Fungi in Submerged Cultivations as a Bioprocess Parameter. *Food Technol. Biotechnol.* **39,** 237–252 (2001).

52. Bennett, J. W. Mycotoxins, mycotoxicoses, mycotoxicology and Mycopathologia. *Mycopathologia* **100,** 3–5 (1987).

53. Blumenthal, C. Z. Production of toxic metabolites in *Aspergillus niger*, *Aspergillus oryzae*, and *Trichoderma reesei*: justification of mycotoxin testing in food grade enzyme preparations derived from the three fungi. *Regul. Toxicol. Pharmacol.* **39,** 214–228 (2004).

54. Belaish, R. *et al.* The *Aspergillus* nidulans cetA and calA genes are involved in conidial germination and cell wall morphogenesis. *Fungal Genet. Biol.* **45,** 232–242 (2008).

55. Fischer, R., Zekert, N. & Takeshita, N. Polarized growth in fungi - interplay between the cytoskeleton, positional markers and membrane domains. *Mol. Microbiol.* **68,** 813–826 (2008).

56. Taheri-Talesh, N. *et al.* The tip growth apparatus of *Aspergillus nidulans*. *Mol. Biol. Cell* **19,** 1439 (2008).

57. Adams, T. H., Wieser, J. K. & Yu, J.--H. Asexual Sporulation in *Aspergillus nidulans*. *Microbiol. Mol. Biol. Rev.* **62,** 35 (1998).

58. Mims, C. W., Richardson, E. A. & Timberlake, W. E. Ultrastructural analysis of conidiophore development in the fungus *Aspergillus nidulans* using freeze-substitution. *Protoplasma* **144,** 132–141 (1988).

59. Katz, D., Goldstein, D. & Rosenberger, R. F. Model for branch initiation in *Aspergillus nidulans* based on measurements of growth parameters. *J. Bacteriol.* **109,** 1097 (1972).

60. Agger, T., Spohr, A. B., Carlsen, M. & Nielsen, J. Growth and product formation of *Aspergillus oryzae* during submerged cultivations: Verification of a morphologically structured model using fluorescent probes. *Biotechnol. Bioeng.* **57,** 321–329 (1998).

61. Cox, P. W., Paul, G. C. & Thomas, C. R. Image analysis of the morphology of filamentous micro-organisms. 817–827 (2017).

62. Metz, B., Kossen, N. W. F. & van Suijdam, J. C. The rheology of mould suspensions. *Adv Biochem Eng* **11,** 103–156 (1979).

63. Li, Z. J. *et al.* Estimation of hyphal tensile strength in production-scale *Aspergillus oryzae* fungal fermentations. *Biotechnol. Bioeng.* **77,** 601–613 (2002).

64. Spohr, A., Carlsen, M., Nielsen, J. & Villadsen, J. Morphological characterization of recombinant strains of *Aspergillus oryzae* producing alpha-amylase during batch cultivations. *Biotechnol. Lett.* **19,** 257–261 (1997).

65. Casas López, J. L., Sánchez Pérez, J. A., Fernández Sevilla, J. M., Rodríguez Porcel, E. M. & Chisti, Y. Pellet morphology, culture rheology and lovastatin production in cultures of *Aspergillus terreus*. *J. Biotechnol.* **116 (2005),** 61–77 (2005).

66. Hille, A., Neu, T. R., Hempel, D. C. & Horn, H. Oxygen profiles and biomass distribution in biopellets of *Aspergillus niger*. *Biotechnol. Bioeng.* **92,** 614–623 (2005).

67. Dai, Z., Mao, X., Magnuson, J. K. & Lasure, L. L. Identification of Genes Associated with Morphology in *Aspergillus niger* by Using Suppression Subtractive Hybridization. *Appl. Environ. Microbiol.* **70,** 2474–2485 (2004).

68. Hille, A., Neu, T. R., Hempel, D. C. & Horn, H. Einfluss der Morphologie auf Stofftransport und-umsatz in *Aspergillus niger*-Pellets. *Chemie Ing. Tech.* **78,** 627 (2006).

69. Rinas, U. *et al.* Model-based prediction of substrate conversion and protein synthesis and excretion in recombinant *Aspergillus niger* biopellets. *Chem. Eng. Sci.* **60,** 2729–2739 (2005).

70. Barry, D. J. & Williams, G. a. Microscopic characterisation of filamentous microbes: Towards fully automated morphological quantification through image analysis. *J. Microsc.* **244,** 1–20 (2011).

71. Deo, Y. M. & Gaucher, G. M. Semicontinuous and continuous production of penicillin-G by *Penicillium chrysogenum* cells immobilized in k-carrageenan beads. *Biotechnol. Bioeng.* **26,** 285–295 (1984).

72. Magnuson, J. K. & Lasure, L. L. Organic Acid Production by Filamentous Fungi. *Adv. Fungal Biotechnol. Ind. Agric. Med.* 307–339 (2004).

73. Bai, Z., Harvey, L. M. & McNeil, B. Oxidative stress in submerged cultures of fungi. *Crit. Rev. Biotechnol.* **23,** 267–302 (2003).

74. Kiep, K. A. Einfluss von Kultivierungsparametern auf die Morphologie und Produktbildung von *Aspergillus niger*. (Institute of Biochemical Engineering, Technische Universität Braunschweig, 2011).

75. Emerson, S. The Growth Phase in *Neurospora* Corresponding to the logarithmic Phase in Unicellular Organisms. *J. Bacteriol.* **60,** 221–223 (1950).

76. Metz, B. & Kossen, N. W. F. The growth of molds in the form of pellets–a literature review. *Biotechnol. Bioeng.* **19,** 781–799 (1977).

77. Pera, L. M., Baigor, M. D. & Callieri, D. Influence of Environmental Conditions on Hyphal Morphology in Pellets of *Aspergillus niger*: Role of beta-N-Acetyl--D-Glucosaminidase. *Curr. Microbiol.* **39,** 65–67 (1999).

78. Tresner, H. D. & Hayes, J. A. Sodium chloride tolerance of terrestrial fungi. *Appl. Microbiol.* **22,** 210–213 (1971).

79. Fiedurek, J. Effect of osmotic stress on glucose oxidase production and secretion by Aspergillus niger. *J. Basic Microbiol.* **38,** 107–112 (1998).

80. Wucherpfennig, T., Hestler, T. & Krull, R. Morphology engineering - Osmolality and its effect on *Aspergillus niger* morphology and productivity. *Microb. Cell Fact.* **10,** 58 (2011).

81. Driouch, H., Sommer, B. & Wittmann, C. Morphology engineering of *Aspergillus niger* for improved enzyme production. *Biotechnol. Bioeng.* **105,** 1058–1068 (2009).

82. Kaup, B. A., Ehrich, K., Pescheck, M. & Schrader, J. Microparticle-enhanced cultivation of filamentous microorganisms: Increased chloroperoxidase formation by *Caldariomyces fumago* as an example. *Biotechnol. Bioeng.* **99,** 491–498 (2008).

83. Paul, G. C., Priede, M. A. & Thomas, C. R. Relationship between morphology and citric acid production in submerged *Aspergillus niger* fermentations. *Biochem. Eng. J.* **3,** 121–129 (1999).

84. Washington, C. *Particle Size Analysis in Pharmaceutics and Other Industries: Theory and Practice*. (Ellis Horwood Ltd, 1992).

85. Nichols, G. *et al.* A review of the terms agglomerate and aggregate with a recommendation for nomenclature used in powder and particle characterization. *J. Pharm. Sci.* **91,** 2103–2109 (2002).

86. *The Oxford English Dictionary*. (Clarendon Press, 1989).

87. Nichols, G. *et al.* A Review of the Terms Agglomerate and Aggregate with a Recommendation for Nomenclature Used in Powder and Particle Characterization. *J. Pharm. Sci.* **91,** 2103–2109 (2002).

88. Witt, W., Köhler, U. & Stübinger, T. Laserbeugung zur Partikelgrössenanalyse mit absoluter Präzision. *Chemie Ing. Tech.* **81,** 1179 (2009).

89. de Boer, G. B. J., de Weerd, C., Thoenes, D. & Goossens, H. W. J. Laser Diffraction Spectrometry: Fraunhofer Diffraction Versus Mie Scattering. *Part. Part. Syst. Charact.* **4,** 14–19 (1987).

90. Information, S. Malvern mastersizer 2000. (2008).

91. Jones, R. M. Particle size analysis by laser diffraction: ISO 13320, standard operating procedures, and Mie theory. *Am. Lab.* **35,** 44–47 (2003).

92. Quintanilla, D., Hagemann, T., Hansen, K. & Gernaey, K. V. Fungal Morphology in Industrial Enzyme Production—Modelling and Monitoring. 29–54 (2015). doi:10.1007/10_2015_309

93. Kossen, N. W. in *Advances in Biochemical Engineering/biotechnology* **69,** 1–33 (2000).

94. Malvern Instruments Ltd. Mastersizer 3000 user manual. 208 (2015).

95. Malvern. Mastersizer 3000. 182 (2013).

96. Wulkow, M. Brochure_Parsival_LQ.pdf.

97. Lin, P. J., Grimm, L. H., Wulkow, M., Hempel, D. C. & Krull, R. Population balance modeling of the conidial aggregation of *Aspergillus niger*. *Biotechnol. Bioeng.* **99,** (2008).

98. Loeb, A. L., Overbeek, J. T. G. & Wiersema, P. H. The electrical double layer around a spherical colloid particle. *J. Electrochem. Soc.* **108,** 269C (1961).

99. Pollack, J. K., Li, Z. J. & Marten, M. R. Fungal mycelia show lag time before re-growth on endogenous carbon. *Biotechnol. Bioeng.* **100,** 458–465 (2008).

100. Cronenberg, C. C. H. *et al.* Influence of age and structure of Pencillium chrysogenum pellets on the internal concentration profiles. *Bioprocess Biosyst. Eng.* **10,** 209–216 (1994).

101. van Hartingsveldt, W., Mattern, I. E., van Zeijl, C. M. J., Pouwels, P. H. & van den Hondel, C. A. M. J. J. Development of a homologous transformation system for *Aspergillus niger* based on the pyrG gene. *Mol. Genet. Genomics* **206,** 71–75 (1987).

102. Pedersen, H., Beyer, M. & Nielsen, J. Glucoamylase production in batch, chemostat and fed-batch cultivations by an industrial strain of *Aspergillus niger*. *Appl. Microbiol. Biotechnol.* **53,** 272–277 (2000).

103. Aalbaek, T., Reeslev, M., Jensen, B. & Eriksen, S. H. Acid protease and formation of multiple forms of glucoamylase in batch and continuous cultures of *Aspergillus niger*. *Enzyme Microb. Technol.* **30,** 410–415 (2002).

104. Vongsangnak, W., Hansen, K. & Nielsen, J. Integrated analysis of the global transcriptional response to α-amylase over-production by *Aspergillus oryzae*. *Biotechnol. Bioeng.* **108,** 1130–1139 (2011).

105. Banaszkiewicz, T. *Nutritional Value of Soybean Meal*. *Agricultural and Biological Sciences Grain Legumes* (InTech, 2011). doi:10.5772/711

106. Malvern Instruments Ltd. Mastersizer software - v.3.50.

107. Lin, D.-Q., Brixius, P. J., Hubbuch, J. J., Thömmes, J. & Kula, M.-R. Biomass/adsorbent electrostatic interactions in expanded bed adsorption: a zeta potential study. *Biotechnol. Bioeng.* **83,** 149–157 (2003).

108. Vankuyk, P. A. *et al. Aspergillus niger* mstA encodes a high-affinity sugar/H+ symporter which is regulated in response to extracellular pH. *Biochem. J.* **379,** 375–383 (2004).

109. Ramachandran, S., Fontanille, P., Pandey, A. & Larroche, C. Gluconic acid: Properties, applications and microbial production. *Food Technol. Biotechnol.* **44,** 185–195 (2006).

110. Carlsen, M. & Nielsen, J. Influence of carbon source on alpha-amylase production by *Aspergillus oryzae*. *Appl. Microbiol. Biotechnol.* **57,** 346–349 (2001).

111. Müller, C., Spohr, A. B. & Nielsen, J. Role of Substrate Concentration in Mitosis and Hyphal Extension of *Aspergillus*. *Biotechnol. Bioeng.* **67,** 390–397 (2000).

112. Karaffa, L. & Kubicek, C. P. *Aspergillus niger* citric acid accumulation: do we understand this well working black box? *Appl. Microbiol. Biotechnol.* **61,** 189–196 (2003).

113. Andersen, M. R., Nielsen, M. L. & Nielsen, J. Metabolic model integration of the bibliome, genome, metabolome and reactome of *Aspergillus niger*. *Mol. Syst. Biol.* **4,** 1–13 (2008).

114. Li, Z. J. *et al.* Effects of Increased Impeller Power in a Production-Scale *Aspergillus oryzae* Fermentation. *Biotechnol. Prog.* **18,** 437–444 (2002).

115. Klich, M. A. & voor Schimmelcultures, C. *Identification of Common* Aspergillus *Species*. (Centraalbureau voor Schimmelcultures, 2002).

116. Witteveen, C. F. B. *et al.* Induction of glucose oxidase, catalase, and lactonase in *Aspergillus niger*. *Curr. Genet.* **24,** 408–416 (1993).

117. Schlegel, H. G. *Allgemeine Mikrobiologie, 7. überarbeitete Auflage*. (Georg Thieme Verlag Stuttgart, New York, 1992).

118. Dowdells, C. *et al.* Gluconic acid production by *Aspergillus terreus*. *Lett. Appl. Microbiol.* **51,** 252–257 (2010).

119. Diano, A., Bekker-Jensen, S., Dynesen, J. & Nielsen, J. Polyol synthesis in *Aspergillus niger*: Influence of oxygen availability, carbon and nitrogen sources on the metabolism. *Biotechnol. Bioeng.* **94,** 899 (2006).

120. Feng, K. C., Rou, T. M., Liu, B. L., Tzeng, Y. M. & Chang, Y. N. Effect of fungal pellet size on the high yield production of destruxin B by *Metarhizium anisopliae*. *Enzyme Microb. Technol.* **34,** 22–25 (2004).

121. Sitanggang, A. B., Wu, H. S., Wang, S. S. & Ho, Y. C. Effect of pellet size and stimulating factor on the glucosamine production using *Aspergillus* sp. BCRC 31742. *Bioresour. Technol.* **101,** 3595–3601 (2010).

122. Swift, R. J. *et al.* The Effect of Organic Nitrogen Sources on Recombinant Glucoamylase Production by *Aspergillus niger* in Chemostat Culture. *Fungal Genet. Biol.* **31,** 125–133 (2000).

123. Shafique, S. & Bajwa, R. Mutagenesis and genetic characterisation of amylolytic *Aspergillus niger*. *Nat. Prod. Res.* **24,** 1104–1114 (2010).

124. Hofmann, G., Diano, A. & Nielsen, J. Recombinant bacterial hemoglobin alters metabolism of *Aspergillus niger*. *Metab. Eng.* (2008).

125. Wargenau, A. & Kwade, A. Determination of Adhesion between Single *Aspergillus niger* Spores in Aqueous Solutions Using an Atomic Force Microscope. *Langmuir* (2010).

126. Yanagita, T. Biochemical aspects on the germination of conidiospores of *Aspergillus niger*. *Arch. Microbiol.* **26,** 329–344 (1957).

127. d'Enfert, C. Fungal Spore Germination: Insights from the Molecular Genetics of *Aspergillus nidulans* and *Neurospora crassa*. *Fungal Genet. Biol.* **21,** 163–172 (1997).

128. Appel, C. Numerische Simulation der Strömung in Bioreaktoren. (TU Braunschweig, Institut für Bioverfahrenstechnik, 2009).

129. Hogan, D. A. Talking to Themselves: Autoregulation and Quorum Sensing in Fungi. *Eukaryot. Cell* **5,** 613–619 (2006).

130. Hinze, F., Ripperger, S. & Stintz, M. Praxisrelevante Zetapotentialmessung mit unterschiedlichen Meßtechniken. *Chemie Ing. Tech.* **71,** 338–347 (1999).

131. Singaravelan, N. *et al.* Adaptive Melanin Response of the Soil Fungus *Aspergillus niger* to UV Radiation Stress at "Evolution Canyon", Mount Carmel, Israel. *PLoS One* **3,** (2008).

132. Mason, H. S. The Chemistry of Melanin III. Mechanism of the Oxidation of Dihydroxyphenylalanine by Tyrosinase. *J. Biol. Chem.* **172,** 83–99 (1948).

133. Riley, P. A. Melanin. *Int. J. Biochem. Cell Biol.* **29,** 1235–1239 (1997).

134. Dynesen, J. & Nielsen, J. Surface Hydrophobicity of *Aspergillus nidulans* Conidiospores and Its Role in Pellet Formation. *Biotechnol. Prog.* **19,** 1049–1052 (2003).

135. Wargenau, A., Kampen, I. & Kwade, A. P25- *Aspergillus niger* Spore Interactions in Submerged Fermentation.

136. Xu, J., Wang, L., Ridgway, D., Gu, T. & Moo-Young, M. Increased heterologous protein production in *Aspergillus niger* fermentation through extracellular proteases inhibition by pelleted growth. *Biotechnol. Prog.* **16,** 222–227 (2000).

137. Whitaker, A. & Long, P. A. Fungal pelleting. *Process Biochem.* **8,** 27–31 (1973).

138. Clark, D. S. Submerged citric acid fermentation of ferrocyanide-treated beet molasses: morphology of pellets of *Aspergillus niger*. *Can.J.Microbiol.* **8,** 133–136 (1962).

139. Albaek, M. O. Evaluation of the efficiency of alternative enzyme production technologies. (2012).

140. Bohle, K. Morphologie- und produktbildungsrelevante Gen- und Proteinexpression in submersen Kultivierungen von *Aspergillus niger*. (Institut für Bioverfahrenstechnik, 2009).

141. Andersen, M. R. & Nielsen, J. Current status of systems biology in *Aspergilli*. *Fungal Genet. Biol.* **46,** 180–190 (2009).

142. Pedersen, L., Hansen, K., Nielsen, J., Lantz, A. E. & Thykaer, J. Industrial glucoamylase fed-batch benefits from oxygen limitation and high osmolarity. *Biotechnol. Bioeng.* **109,** 116–124 (2012).

143. Driouch, H., Sommer, B. & Wittmann, C. Morphology engineering of *Aspergillus niger* for improved enzyme production. *Biotechnol. Bioeng.* **105,** 1058–1068 (2010).

144. Emmler, M. *et al.* Apparent delay of product secretion by product adsorption in *Aspergillus niger*. *Eng. life Sci.* **6,** 488–491 (2006).

145. Büchs, J., Maier, U., Milbradt, C. & Zoels, B. Power Consumption in Shaking Flasks on Rotary Shaking Machines: I. Power Consumption Measurement in Unbaffled Flasks at Low Liquid Viscosity. *Biotechnol. Bioeng.* **68,** 589–593 (2000).

146. Peter, C. P., Lotter, S., Maier, U. & Büchs, J. Impact of out-of-phase conditions on screening results in shaking flask experiments. *Biochem. Eng. J.* **17,** 205–215 (2004).

147. Formenti, L. R. *et al.* Challenges in industrial fermentation technology research. *Biotechnol. J.* **9,** 727–38 (2014).

148. Wargenau, A. *et al.* On the origin of the electrostatic surface potential of *Aspergillus niger spores in acidic environments. Res. Microbiol. **162,** 1011–1017 (2011).*

149. Wargenau, A., Kampen, I. & Kwade, A. Linking aggregation of *Aspergillus niger* spores to surface electrostatics: a theoretical approach. *Biointerphases* **8,** 7 (2013).

150. Shewmaker, F., McGlinchey, R. P. & Wickner, R. B. Structural insights into functional and pathological amyloid. *J. Biol. Chem.* **286,** 16533–16540 (2011).

151. Ren, Q., Kwan, A. H. & Sunde, M. Two forms and two faces, multiple states and multiple uses: Properties and applications of the self-assembling fungal hydrophobins. *Biopolymers* **100,** 601–612 (2013).

152. Samapundo, S. *et al.* Modelling of the individual and combined effects of water activity and temperature on the radial growth of *Aspergillus flavus* and *Aspergillus parasiticus* on corn. *Food Microbiol.* **24,** 517–529 (2007).

153. Pinchai, N. *et al. Aspergillus fumigatus* calcipressin CbpA is involved in hyphal growth and calcium homeostasis. *Eukaryot. Cell* **8,** 511 (2009).

154. Krull, R. *et al.* Morphology of Filamentous Fungi: Linking Cellular Biology to Process Engineering Aspergillus niger. *[Without Title]* 1–21 (2010).

155. Kim, Y. J., Choi, Y. G. & Chung, T. H. A simple image analysis algorithm for evaluation of extended filaments length based on the enhanced digitized image. *J. Environ. Sci. Heal. Part A* **43,** 1489–1494 (2008).

156. Hille, A., Neu, T. R., Hempel, D. C. & Horn, H. Effective diffusivities and mass fluxes in fungal biopellets. *Biotechnol. Bioeng.* (2009).

List of figures

Process and Systems Engineering Centre (PROSYS)
Department of Chemical and Biochemical Engineering
Technical University of Denmark
Søltofts Plads, Building 229
DK - 2800 Kgs. Lyngby
Denmark

Phone: +45 45 25 28 00
Web: www.kt.dtu.dk/forskning/prosys